

# **Thermophysical behaviour and applications of *N*- isopropylacrylamide-based Ionogels**

Simon Gallagher (B.Sc.)

Thesis submitted in partial fulfilment of the requirements

for the degree of

**Doctor of Philosophy**

**June 2014**

Supervisor: Prof. Dermot Diamond

Co-Supervisor: Dr. Kevin J. Fraser

National Centre for Sensor Research / School of

Chemical Sciences

Dublin City University

# General Declaration

I hereby certify that this material, which I now submit for assessment on the programme of study leading to the award of Doctor of Philosophy is entirely my own work, and that I have exercised reasonable care to ensure that the work is original, and does not, to the best of my knowledge, breach any law of copyright, and has not been taken from the work of others save and to the extent that such work has been cited and acknowledged within the text of my work.

Signed: \_\_\_\_\_

Date: \_\_\_\_\_

(Simon Gallagher, ID: 5528354)

# Acknowledgements

First of all I would like to thank Prof. Dermot Diamond for giving me the opportunity to work in his group and for his contribution, patience, support and sense of humour during my Ph.D. Since I first worked with him on my 4<sup>th</sup> year project many years ago, I have progressed personally and professionally under his tutelage and I feel there is simply no other supervisor that would have steered me to who and where I am today. Thanks should also go to Dr. Robert Byrne for initially choosing myself for this project.

I would like to thank Kevin and Andrew for contributing their knowledge and experience to my project. Their scientific support throughout my Ph.D. was essential for finding my feet as a researcher and was invaluable at times when I needed guidance. Most of their time spent on my project was of their own generosity and I can never thank them enough.

I am also grateful to thank Prof. Doug MacFarlane of Monash University for his sharing of facilities and knowledge towards my work. A big thanks to Mega and Ted for their welcoming attitude, which made a visit to Australia feel like a trip down the road.

Thanks to all the members of the Adaptive Sensor Group; Michele, Monika, Vincenzo and especially Bartosz and Larisa for helping me get over the finish line. One of Prof. Diamond's great attributes is hiring not only competent researchers but also exceptional people. So I would like to take everybody that I worked with, past and present, in Clarity and the NCSR – Deirdre, Damien, Fiachra, John C, Simon, Guisy, Dylan, Tom, Conor, Eoghan, Wayne, Aishling, Alex and Jen. Working with

these people day-to-day really does make the daunting task of completing my Ph.D. a lot more pleasant experience.

Thanks to all of my friends for their support, in spite of their confusion as to what it is I actually do everyday. And finally, I would like to thank my family – Mam, Mike, Michael, Matthew, Marie, Alison and little Harry and Jack. Their patience and support are the main reasons I decided to further my education and my main goal has, and always will be, to make them proud. Thank you.

# List of Publications

## Journal Publications

1. Simon Gallagher, Larisa Florea, Eoin Fox, Kevin J. Fraser and Dermot Diamond, *Synthesis and Characterisation of 1-Vinylimidazolium Alkyl Sulphate Polymeric Ionic Liquid* – Macromolecular Chemistry and Physics, 2014, **Accepted**.
2. Simon Gallagher, Larisa Florea, Kevin J. Fraser and Dermot Diamond, *Swelling and Shrinking Properties of Thermo-responsive Polymeric Ionic Liquid Hydrogels with Embedded Linear pNIPAAm*. – International Journal of Molecular Sciences, 5337-5349, 15, 2014, DOI:10.3390/ijms15045337.
3. Simon Gallagher, Andrew Kavanagh, Larisa Florea, Bartosz Ziolkowski, Douglas R. MacFarlane, Kevin J. Fraser and Dermot Diamond, *Ionic Liquid modulation of swelling and LCST behaviour of N-isopropylacrylamide polymer gels*, Physical Chemistry Chemical Physics, 3610-3616, 16, 2014, DOI: 10.1039/C3CP53397B.
4. Simon Gallagher, Andrew Kavanagh, Larisa Florea, Bartosz Ziolkowski, Robert Byrne, Douglas R. MacFarlane, Kevin J. Fraser and Dermot Diamond, *Temperature & pH triggered water / fluorescein release characteristics 1-ethyl-3-methylimidazolium ethylsulphate – based ionogels*. - Chemical Communications, 4613, 49, 2013, DOI: 10.1039/c3cc41272e.

## Oral Presentations

1. Simon Gallagher, Andrew Kavanagh, Larisa Florea, Doug MacFarlane, Kevin J. Fraser, Dermot Diamond, "*Temperature and pH triggered release characteristics of water/Fluorescein from [C<sub>2</sub>mIm][EtSO<sub>4</sub>]-based ionogels.*" April 21-25<sup>th</sup>, 2013, COIL5 - 5th International Congress on Ionic Liquids, Algarve, Portugal.
2. Simon Gallagher, Robert Byrne, Kevin J. Fraser, Dermot Diamond, "*Physico-chemical Properties of Ionic-Liquid Water Mixtures*", February 15th-17th 2012, International Electromaterials Science Symposium, Melbourne, Australia.

## Poster Presentations

1. Simon Gallagher, Andrew Kavanagh, Larisa Florea, Katya Izgorodina, Kevin J. Fraser, Douglas MacFarlane, Dermot Diamond, "*Exploring the Behaviour of in-situ Polymerised Ionogel Thermal Actuators*", 2nd International Symposium on Functional Nanomaterials 2012, 6-7th September, Dublin City University, Dublin, Ireland.
2. Simon Gallagher, Andrew Kavanagh, Larisa Florea, Katya Izgorodina, Kevin J. Fraser, Douglas MacFarlane, Dermot Diamond, "*Exploring the Behaviour of in-situ Polymerised Ionogel Thermal Actuators*", EUCHEM: Molten Salts and Ionic Liquids XXIV, Celtic Manor, Newport, Wales, 5-6th August 2012.

3. Simon Gallagher, Jason Rigby, Ekaterina Izgorodina, Kevin J. Fraser, Dermot Diamond and Doug MacFarlane, "*Thermophysical properties of pure and water-saturated Ionic Liquids*", 64th Irish Universities Chemistry Research Colloquium 2012, June 14-15, 2012, Dublin, Ireland.
  
4. Simon Gallagher, Robert Byrne, Kevin J. Fraser, Dermot Diamond, "*Physico-chemical Properties of Ionic-Liquid Water Mixtures*" COIL4 - 4th International Congress on Ionic Liquids, June 15-18, 2011, Arlington, Virginia, USA.

# Aim of the Thesis

The aim of this thesis is to investigate and develop thermo-responsive ionic liquid-based polymer gels suitable for stimuli responsive applications, in particular the polymer, *N*-isopropylacrylamide (pNIPAAm). This thermo-responsive polymer is found to swell and shrink in the presence of aqueous medium as a function of temperature. It is known to have weak mechanical stability and poor reproducibility. In this thesis, we investigate the influence of Ionic liquids (ILs) on the properties of pNIPAAm-based gels, and to also understand the underlying physicochemical interactions that may occur between them. In particular this thesis focuses on:

1. The influence of certain ILs on the mechanical and actuation properties of pNIPAAm-based gels.
2. The incorporation of a biomedical dye into a pNIPAAm-based ionogel, and the ILs subsequent effect on the release properties of this dye, as a function of pH/temperature.
3. The synthesis and characterization of thermo-responsive polymeric ionic liquid interpenetrating networks
4. The synthesis and characterization of 1-vinylimidazolium alkyl sulphate polymeric ILs.

## Author Contribution to Publications

This thesis includes three original manuscripts with a core theme involving thermo-responsive polymers. The ideas, development and writing up of all manuscripts in this thesis were the principle responsibility of myself, the candidate, working within the School of Chemical Sciences under the supervision of Prof. Dermot Diamond and Dr. Kevin J. Fraser. The inclusion of co-authors reflects the fact that part of the work came from active collaborations between researchers and acknowledges input into team-based research. In the case of chapters 2 to 5 my contribution to the work involved the following:

Thesis Chapter	Publication Title	Publication Status	Nature and extent of candidate's contribution
2	<i>Ionic Liquid modulation of swelling and LCST behaviour of N-isopropylacrylamide polymer gels</i>	Published, Physical Chemistry Chemical Physics, 3610-3616, <b>16</b> , 2014. DOI: 10.1039/C3CP53397B	First author, key ideas, data collection and analysis, manuscript development and writing up.
3	<i>Temperature &amp; pH triggered water / fluorescein release characteristics 1-ethyl-3-</i>	Published, Chemical Communications, 4613, <b>49</b> , 2013.	First author, key ideas, data collection and analysis, manuscript

	<i>methylimidazolium ethylsulphate – based ionogels</i>	DOI: 10.1039/C3CC41272E	development and writing up.
4	<i>Swelling and Shrinking Properties of Thermo-responsive Polymeric Ionic Liquid Hydrogels with Embedded Linear pNIPAAm</i>	International Journal of Molecular Sciences, 5337-5349, <b>15</b> , 2014. DOI:10.3390/ijms15045337.	First author, key ideas, data collection and analysis, manuscript development and writing up.
5	<i>Synthesis and Characterisation of 1-Vinylimidazolium Alkyl Sulphate Polymeric Ionic Liquids</i>	Accepted, Macromolecular Chemistry and Physics, 2014	First author, key ideas, data collection and analysis, manuscript development and writing up.

Signed: \_\_\_\_\_

Date: \_\_\_\_\_

Simon Gallagher

Signed: \_\_\_\_\_

Date: \_\_\_\_\_

Prof. Dermot Diamond

Signed: \_\_\_\_\_

Date: \_\_\_\_\_

Dr. Kevin J. Fraser

# Thesis Outline

An overview summary of each chapter is given below:

## Chapter 1

This chapter reviews important topics relevant in this thesis and sets the following chapters in the context of the existing literature. These topics include ionic liquids, stimuli responsive materials, stimuli responsive ionogels and potential applications. These subjects are discussed in order to inform the reader on the concepts that will underpin the subsequent experimental chapters (Chapter 2 to 5). Furthermore, this chapter presents the context in which the experimental chapters contribute to the scientific advancement of the research area.

## Chapter 2

This chapter presents the physicochemical properties of imidazolium- and phosphonium-based ILs and their influence on characteristics of thermo-responsive pNIPAAm gels generated. Varying swelling and shrinking behaviour of the “ionogels” are described as well as their effect on the pNIPAAm Lower Critical Solution Temperature (LCST). Also presented are Scanning Electron Microscopy images of the resultant ionogels that reveal distinct morphological changes across different ionogels, for example; highly porous, nodule type morphology, and efficiently pre-disposed surfaces for water uptake.

## Chapter 3

In this chapter, an ionogel is presented displaying improved transmittance properties, enhanced water/uptake release, greater thermal actuation behaviour and

distinct solvatomorphology over its hydrogel equivalent. It is also found that the rate of release of fluorescein, a biomedical dye, pre-loaded into membranes was considerably greater for ionogels compared to the equivalent hydrogel, and release characteristics could be controlled through changes in pH and temperature.

## Chapter 4

In this chapter, semi-interpenetrating polymer networks are prepared using a crosslinked thermo-responsive polymeric ionic liquid with varying concentrations of linear pNIPAAm incorporated in the hydrogel. Due to the presence of linear pNIPAAm, the semi-IPNs show improvement in mechanical, shrinking and reswelling properties compared to the conventional hydrogel.

## Chapter 5

In this chapter, three ionic monomers based on a 1-vinylimidazolium cation are synthesized and characterised. The ionic liquid monomers are prepared using a halide-free route by a quaternization reaction with alkyl sulphates. Through free-radical polymerization, solid, free-standing linear polymeric ionic liquid (PILs) gels were obtained and were also characterized by thermal and rheology methods. The films displayed high thermal and mechanical stability.

## Chapter 6

This chapter presents the conclusions of this thesis, summarises the work carried and outlines the challenges and opportunities lying ahead.

# Thesis Contents

<b>General Declaration.....</b>	<b>ii</b>
<b>Acknowledgements .....</b>	<b>iii</b>
<b>List of Publications .....</b>	<b>v</b>
<b>Aim of the Thesis .....</b>	<b>viii</b>
<b>Author Contribution to Publications .....</b>	<b>ix</b>
<b>Thesis Outline .....</b>	<b>xi</b>
<b>Abstract .....</b>	<b>1</b>
<b>List of Abbreviations .....</b>	<b>4</b>
<b>Chapter 1: Introduction.....</b>	<b>8</b>
1.1 Ionic Liquids .....	9
1.1.1 Ionic Liquid Synthesis.....	10
1.1.2 Ionic Liquid Properties.....	13
1.2 Ionogels.....	16
1.2.1 Organic Ionogels .....	16
1.2.2 Inorganic Ionogels .....	17
1.2.3 Stimuli-responsive Ionogels and their applications.....	19
1.3 Polymeric Ionic Liquids.....	22
1.3.1 Overview .....	23
1.3.2 Structures and Synthesis.....	24
1.3.3 Applications .....	27
1.4 Temperature Responsive Materials .....	30
1.4.1 Manipulation of the pNIPAAm LCST .....	32
1.4.2 Mechanical Properties of pNIPAAm .....	33
1.4.3 Applications .....	34
1.5 References .....	36
<b>Chapter 2: Ionic Liquid modulation of swelling and LCST behaviour of <i>N</i>-isopropylacrylamide polymer gels.....</b>	<b>45</b>
2.1 Introduction .....	47
2.2 Experimental .....	49

2.2.1 Chemical and Materials .....	49
2.2.2 Preparation of Crosslinked Ionogels.....	50
2.2.3 Preparation of Linear Homopolymers.....	51
2.3 Results and Discussion.....	52
2.3.1 Swelling and Shrinking Properties .....	52
2.4 Ionogels based on the [DCA] <sup>-</sup> anion .....	57
2.5 Enhanced Viscoelastic Ionogels .....	61
2.6 Conclusion.....	65
Acknowledgements.....	66
2.7 References .....	66
<b>Chapter 2: Supporting Information.....</b>	<b>69</b>
<b>Chapter 3: Temperature &amp; pH triggered release characteristics of water/fluorescein from 1-ethyl-3-methylimidazolium ethylsulphate based ionogels. ....</b>	<b>80</b>
Abstract .....	81
3.1 Introduction .....	82
3.2 Results & Discussion .....	84
Acknowledgements.....	92
3.3 References .....	92
<b>Chapter 3: Supporting Information.....</b>	<b>94</b>
<b>Chapter 4: Swelling and Shrinking Properties of Thermo-responsive Polymeric Ionic Liquid Hydrogels with Embedded Linear pNIPAAm .....</b>	<b>114</b>
Abstract .....	115
4.1 Introduction .....	116
4.2 Results and Discussion.....	118
4.2.1 Morphological Properties of Hydrogels .....	118
4.2.2 Thermal Behaviour of Hydrogels .....	121
4.2.3 Shrinking Behaviour of Hydrogels.....	122
4.2.4 Reswelling Behaviour of Hydrogels.....	125
4.3 Experimental Section .....	127
4.3.1 Chemicals and Materials.....	127
4.3.2 Synthesis of pNIPAAm .....	128
4.3.3 Synthesis of Tributyl-hexyl phosphonium 3-sulfopropylacrylate (P-SPA).....	128
4.3.4 Preparation of Semi-IPN hydrogel. ....	129

4.3.5 Thermobehaviour of Semi-IPN Hydrogels.....	129
4.3.6 Measurement of Shrinking of Semi-IPN Hydrogels .....	130
4.3.7 Measurement of Reswelling of Semi-IPN Hydrogels.....	131
4.4 Conclusions .....	<b>131</b>
Acknowledgments.....	<b>132</b>
4.5 References .....	<b>132</b>
<b>Chapter 4: Supporting Information.....</b>	<b>135</b>
<b>Chapter 5: Synthesis and Characterisation of 1-Vinylimidazolium-based Polymeric Alkyl Sulphate Ionic Liquids .....</b>	<b>139</b>
Abstract .....	<b>140</b>
5.1 Introduction .....	<b>141</b>
5.2 Experimental Section .....	<b>143</b>
5.2.1 Chemicals and Materials.....	143
5.2.2 Characterization.....	143
5.3 Experimental Section .....	<b>145</b>
5.3.1 1-vinyl-3-methylimidazolium methyl sulphate (ILM 1).....	145
5.3.2 1-vinyl-3-ethylimidazolium ethyl sulphate (ILM 2) .....	146
5.3.3 1-vinyl-3-propylimidazolium propyl sulphate (ILM 3).....	146
5.3.4 Free radical polymerization of ILMs.....	147
5.4 Results and Discussions.....	<b>148</b>
5.4.1 Synthesis .....	148
5.4.2 Physicochemical properties of ILMs.....	149
5.4.3 Polymerization properties of the ILMs.....	150
5.4.4 Physicochemical properties of PILs.....	153
5.5 Conclusions .....	<b>156</b>
Acknowledgments.....	<b>157</b>
5.6 References .....	<b>158</b>
<b>Chapter 5: Supporting Information.....</b>	<b>160</b>
<b>Chapter 6: Summary, conclusions and future perspectives .....</b>	<b>171</b>
6.1 Overall summary and conclusions.....	<b>172</b>
6.2 Possible future applications and limitations .....	<b>174</b>
6.3 References .....	<b>180</b>

# Abstract

This thesis is focused on ways to control the characteristics of a thermo-responsive polymer called poly(*N*-isopropylacrylamide) (pNIPAAm). The thermal behaviour of pNIPAAm displays an inverse solubility upon heating above what is known as its Lower Critical Solution Temperature (LCST). Experimentally, it converts from a hydrophilic to a hydrophobic structure when placed in aqueous media between the temperatures 30-35 °C.

This phenomenon places pNIPAAm as a potential candidate for use as a soft polymer actuator, and we are specifically interested in exploiting this behaviour for potential applications in microfluidic valves and drug delivery. However, there are some drawbacks associated with this thermo-responsive polymer. Generally, the polymerization medium used for the synthesis of pNIPAAm is an organic solvent. This is a limitation for pNIPAAm-based hydrogels used in open atmosphere and in a wide range of temperatures, as the liquid phase of the gel can be prone to freezing or evaporation due to its volatility. Its poor mechanical properties, especially in its swollen state, are detrimental to its role as a vessel for drug delivery. Because of its non-biodegradable nature, surgical removal after drug release may be required. If the device were too soft and easily broken during handling, it would be difficult to be completely removed through traditional surgical procedures. Also, weak mechanical properties are not desirable for microfluidic valves which can be exposed to harsh chemicals and high solvent pressures. The main focus of this thesis is to address these limitations and further optimize the pNIPAAm hydrogel for application.

The main theme of my work was the replacement of the common organic solvent with Ionic Liquids (ILs) as a polymerization medium for pNIPAAm, in order to create a series of *ionogels*. ILs are molten salts that consist of a cation and anion held together via weak electrostatic interactions, which reduce the lattice energy of the salt. This chemical environment contributes to factors such as negligible vapour pressure and general high thermal stability. The tailoring of the anion or cation can also lead to a variation of properties.

The first chapter of my work described the physicochemical properties of free-standing crosslinked pNIPAAm gels generated in the presence of varying ILs. The resulting *ionogels* were found to exhibit LCST values different to that of pNIPAAm and improved swelling/shrinking behaviour compared with that of the conventional pNIPAAm hydrogel. Most interestingly, the pNIPAAm shrinking behaviour was completely eliminated with use of dicyanamide as the IL anion.

The ionogel from this report with the most desirable shrinking/swelling behaviour was then studied in terms of drug release. This ionogel was found to have greater water uptake, and better mechanical stability than the conventional hydrogel. When pre-loaded with a dye acting as a drug mimic it was also found to have greater release capabilities.

Following this, varying concentrations of pNIPAAm were integrated into a cross-linked thermo-responsive Polymeric Ionic Liquid (PIL), producing an interpenetrating network (IPN). This novel material is characterized as a function of the concentration of pNIPAAm within the gel. The IPN with the highest concentration of pNIPAAm was found to display the most favourable swelling/shrinking properties.

Lastly, progressions from this area also led to the synthesis of 1-vinylimidazolium alkyl sulphate polymeric ionic liquids (PILs). These PILs were synthesized using a halide-free method and were found to possess sufficient thermal stability of up to 340 °C and mechanical stability with a storage moduli value as high as  $4.64 \times 10^6$  Pa.

# List of Abbreviations

ATR	Attenuated Total Reflectance
DMPA	Dimethoxy-2-phenylacetophenone
DSC	Differential Scanning Calorimeter
[C <sub>2</sub> mIm][DCA]	1-Ethyl-3-imidazolium Dicyanamide
C-DCA	Linear 1-Ethyl-3-imidazolium Dicyanamide based Poly( <i>N</i> -isopropylacrylamide) gel
[C <sub>2</sub> mIm][EtSO <sub>4</sub> ]	1-Ethyl-3-imidazolium Ethylsulphate
C-EtSO <sub>4</sub>	Linear 1-Ethyl-3-imidazolium Ethylsulphate based Poly( <i>N</i> -isopropylacrylamide) gel
[C <sub>2</sub> mIm][NTf <sub>2</sub> ]	1-Ethyl-3-imidazolium <i>bis</i> (trifluoromethylsulfonyl)imide
C-NTf <sub>2</sub>	Linear 1-Ethyl-3-imidazolium <i>bis</i> (trifluoromethylsulfonyl)imide based Poly( <i>N</i> -isopropylacrylamide) gel
HMPP	2-hydroxy-2-methylpropiophenone
GPC	Gel Permeation Chromatography
IL	Ionic Liquid
ILM	Ionic Liquid Monomer
ILM 1	1-vinyl-3-methylimidazolium methyl sulphate ionic liquid monomer

ILM 2	1-vinyl-3-ethylimidazolium ethyl sulphate ionic liquid monomer
ILM 3	1-vinyl-3-propylimidazolium propyl sulphate ionic liquid monomer
IPN 1	Crosslinked Tributylhexylphosphonium 3-sulfopropylacrylate containing 30 % mol equivalent linear <i>N</i> -isopropylacrylamide
IPN 2	Crosslinked Tributylhexylphosphonium 3-sulfopropylacrylate containing 60 % mol equivalent linear <i>N</i> -isopropylacrylamide
IPN 3	Crosslinked Tributyl-hexyl phosphonium 3-sulfopropylacrylate containing 100 % mol equivalent linear <i>N</i> -isopropylacrylamide
IPN 4	Crosslinked Tributyl-hexyl phosphonium 3-sulfopropylacrylate containing 120 % mol equivalent linear <i>N</i> -isopropylacrylamide
IR	Infra-red
KBr	Potassium Bromide
LCST	Lower Critical Solution Temperature
MBIS	<i>N,N'</i> -methylenebisacrylamide
NIPAAM	<i>N</i> -isopropylacrylamide
NMR	Nuclear Magnetic Resonance
[P <sub>6,6,6,14</sub> ][DCA]	Trihexyltetradecylphosphonium dicyanamide
P-DCA	Linear Trihexyltetradecylphosphonium dicyanamide based Poly( <i>N</i> -isopropylacrylamide) gel

PDMS	Polydimethylsiloxane
PIL	Polymeric Ionic Liquid
PIL 1	Polymerized 1-vinyl-3-methylimidazolium methyl sulphate ionic liquid
PIL 2	Polymerized 1-vinyl-3-ethylimidazolium ethyl sulphate ionic liquid
PIL 3	Polymerized 1-vinyl-3-propylimidazolium propyl sulphate ionic liquid
pNIPAAm	Poly( <i>N</i> -isopropylacrylamide)
PPO 800	Poly(propylene glycol) diacrylate
P-SPA	Tributylhexylphosphonium 3-sulfopropylacrylate
SEM	Scanning Electron Microscopy
$T_g$	Glass Transition Temperature
$T_m$	Melting Point Temperature
$T_{cry}$	Crystallization Temperature
UV-Vis	Ultraviolet Visible
xC-DCA	Crosslinked 1-Ethyl-3-imidazolium Dicyanamide based Poly( <i>N</i> -isopropylacrylamide) gel
xC-EtSO <sub>4</sub>	Crosslinked 1-Ethyl-3-imidazolium Ethylsulphate based Poly( <i>N</i> -

isopropylacrylamide) gel

xC-NTf<sub>2</sub>

Crosslinked

1-Ethyl-3-imidazolium

*bis*(trifluoromethylsulfonyl)imide

based

Poly(*N*-

isopropylacrylamide) gel

xP-DCA

Crosslinked Trihexyltetradecylphosphonium dicyanamide based

Poly(*N*-isopropylacrylamide) gel

# **Chapter 1: Introduction**

# 1.1 Ionic Liquids

Ionic liquids (ILs) are compounds composed entirely of ions, that have a melting point below 100 °C<sup>1</sup>. A sub-class of ILs known as room-temperature ionic liquids (RTILs) possess a melting point below room temperature, and these have attracted particular interest in the scientific community. Typically they consist of an asymmetric organic cation and a small inorganic/ organic anion (Figure 1.1) held together via weak electrostatic interactions, which reduce the lattice energy of the salt, thereby contributing to attractive properties such as negligible vapour pressures, electronic and ionic conductivity, low melting points, and low flammability<sup>2-4</sup>.

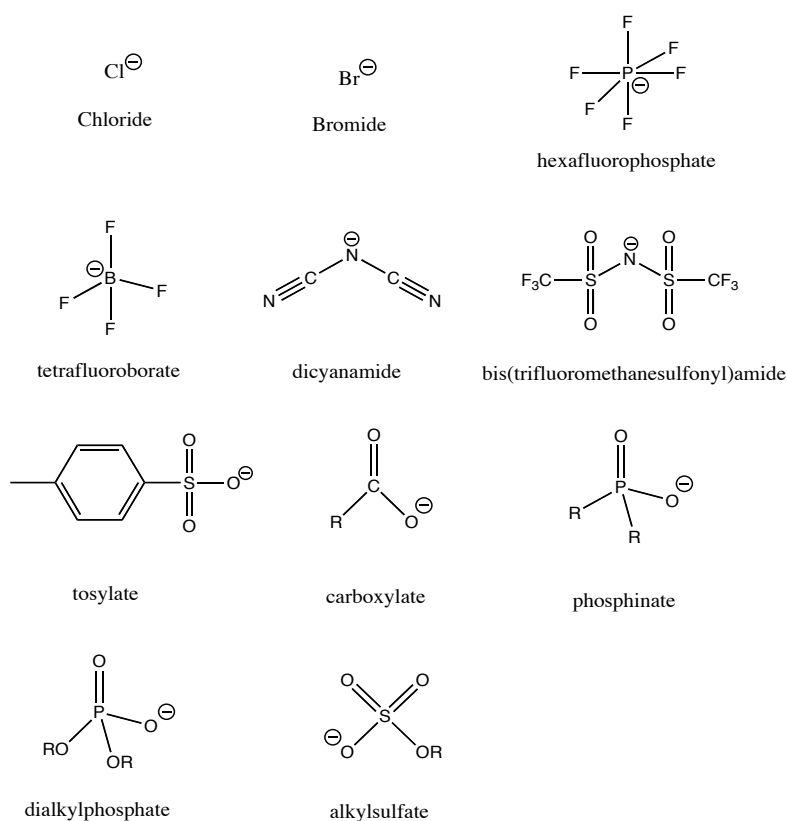


**Figure 1.1.** Examples of anions that can be paired with tetraalkylphosphonium and alkylimidazolium cations to produce ionic liquids.

One property that RTILs have been found to possess is a high solvation capability<sup>4</sup>, which enables compounds to be dissolved, e.g.; monomers (NIPAAM) and crosslinkers (*N,N'*-methylenebisacrylamide) that are difficult to solubilise with conventional molecular solvents<sup>5</sup>.

These favourable physicochemical factors and the number of potential anion-cation combinations available<sup>1</sup> provides a tailorability that has led to many research interests in ILs as benign solvents for diverse applications in scientific research / industry. These include; organic synthesis<sup>1,6</sup>, solid and liquid phase extraction<sup>7,8</sup>, actuators<sup>9-11</sup>, and electrochemically stable electrolytes<sup>12-14</sup>.

A large percentage of studies concerning the physicochemical properties of ILs and their potential applications have focused mainly on alkylimidazolium based ILs<sup>7,8,13,15-17</sup>. These ILs exhibit extensive hydrogen bonding resulting from the delocalized heterocycle of the cation, while branched alkyl chains can be manipulated to vary its hydrophobicity<sup>18</sup>. Another series of ILs that have been thoroughly studied are those based on the tetraalkylphosphonium ion<sup>5,7,19-21</sup>. Fraser *et al.* presented a review showing the advantages of phosphonium ILs over tetra-alkylammonium based ILs such as phase separation and extraction properties<sup>22</sup>, higher thermal stability, generally lower viscosities<sup>23</sup>, and higher stability in strongly basic or reducing conditions<sup>24</sup>.

### 1.1.1 Ionic Liquid Synthesis

One of the most common synthetic routes used in production of ILs is the quaternization reaction. In this reaction, one of the stable reacting products undergoes an S<sub>N</sub>2 nucleophilic addition with an alkyl halide. Some of the more common cations used in IL synthesis are summarized below in Figure 1.2.

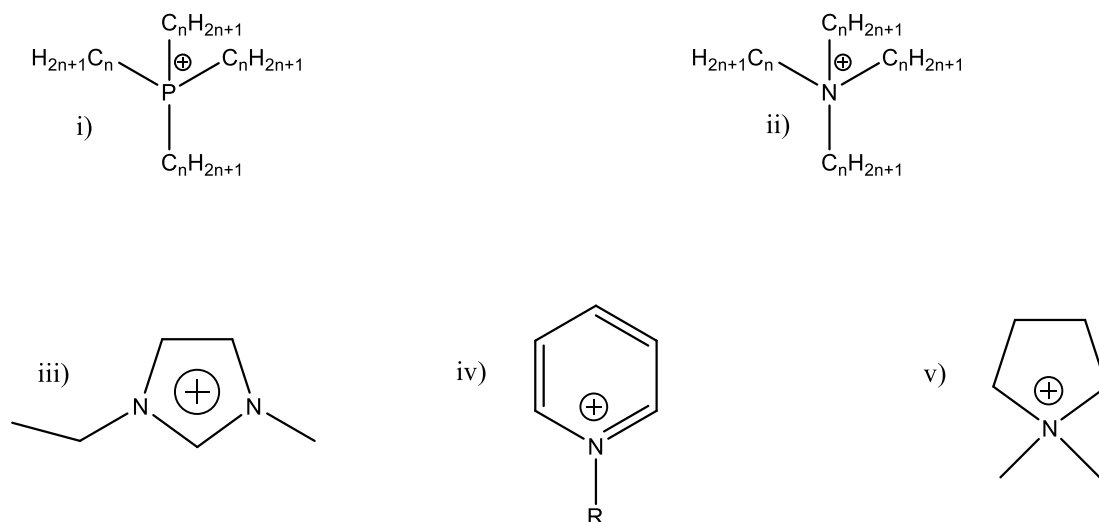


**Figure 1.2.** A selection of some of the common cations used in IL syntheses; i) tetraalkylphosphonium, ii) tetraalkylammonium, iii) 1-ethyl-3-methylimidazolium, iv) pyridinium and v) pyrrolidinium.

As previously described by Bradaric <sup>25</sup> and Ermolaev <sup>26</sup> *et al.*, Figure 1.3 displays a quaternization reaction of a tertiary phosphine/amine with a haloalkane. As both the reactants and products are air and moisture sensitive, the reaction is carried out in an inert atmosphere. The reaction is also performed at elevated temperatures to facilitate both the leaving halide (X) group and the addition of the corresponding alkane. Bradaric *et al.* concluded that even though phosphines exhibit a lower  $pK_a$  (i.e less stable) than their corresponding amines, the kinetics of a phosphonium salt formation are favoured over other cations, such as amines, due to their large radii and more polarizable lone pair.

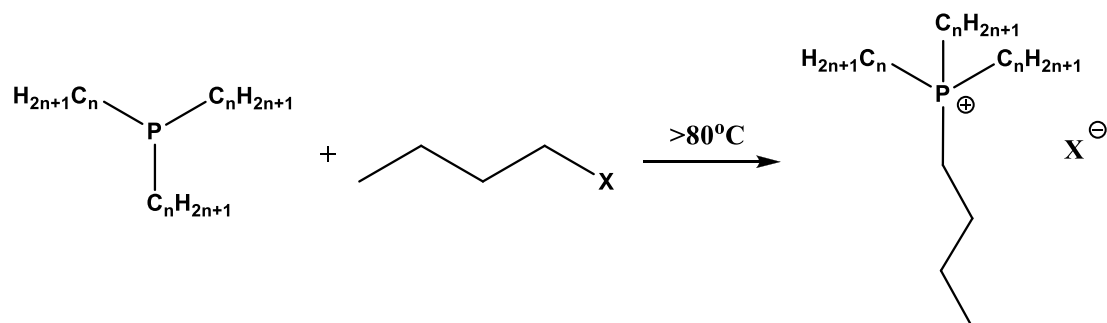


**Figure 1.3.** Direct nucleophilic addition of a tertiary phosphine by an alkyl halide.

The degree of temperature at which the reaction is performed is dependent on the nature of the halide leaving group; which can be summarized in the following order;  $I > Br > Cl > F$ . Therefore, for example, a reaction involving a chloroalkane is performed at slightly elevated temperature compared to their bromo derivatives. Once the reaction is complete, excess haloalkane is usually vacuum dried to remove any volatile components.

Regarding synthesis of imidazole-based ILs, as described by Wilkes *et al.*, the nucleophilic centre of 1-methylimidazole is attacked with a corresponding haloalkane resulting in the formation of the desired cation (Figure 1.4) <sup>27</sup>. This is a common synthetic route used to produce ILs containing a nitrogen-based heterocycle cation.

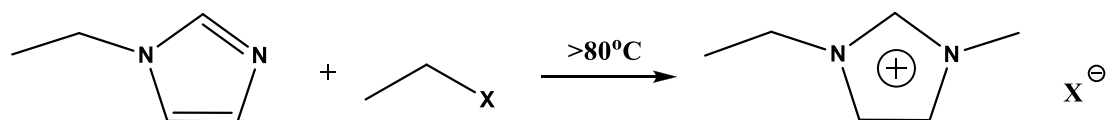


**Figure 1.4.** Direct nucleophilic attack of 1-methylimidazole with an alkyl halide.

The reaction generally requires no solvent, as both reactants are liquid below 20 °C, and is allowed to reflux where the salt forms as a precipitate. The halide anion of the formed IL can be exchanged via an ion-exchange metathesis reaction in order to alter

the properties of the IL. This process generally involves the interchange of the halide salt with an anion originating from a strong Lewis acid<sup>28</sup>, and it can therefore readily disassociate in solution. As the anion is generally a group one salt, the expected by-product of the reaction is a classical alkali-halide compound. The choice of medium with which the reaction is carried out in must serve to keep the new IL solvated, and promote the precipitation of the unwanted by-product. A volatile solvent is generally preferred, as the IL product can be easily isolated by vacuum drying.

### 1.1.2 Ionic Liquid Properties

The interactions between the cation and anion components of an IL are exclusively electrostatic, which are weaker than any kind of hydrogen or covalent bonding. Along with the steric hinderance of bulky ions, ILs fail to form a solid lattice. The ability to alter physical IL properties to suit a particular application is a function of the extensive variation of IL combinations available, with a number reputedly equating to one trillion ( $10^{12}$ )<sup>29</sup>.

As is commonly known, densities are related to the molar masses of the ions and ILs containing heavy ions such as  $[\text{NTf}_2]^-$  are in general denser when compared with ILs with smaller  $[\text{DCA}]^-$  ions. ILs are generally found to be denser than either organic solvents<sup>30</sup> and due to impurities, a detailed quantitative analysis on both density and viscosity of ILs can be difficult to make. A review on the effect of impurities on the measured physicochemical properties of ILs was put forward by Marsh *et al.*<sup>31</sup>, while Seddon *et al.*<sup>32</sup>, who put forward an exhaustive study of this problem with a focus on the influence of chloride and water affecting viscosity of ILs.

Viscosity is described as the internal resistance in a fluid to shear stress, which is dependent on intermolecular forces such as coulombic, hydrogen and dispersive

interactions. ILs are well known for their high viscosity compared with other more common molecular solvents. The anion of ILs is known to have a strong influence on the viscosity, with the lowest viscosity ILs formed from small anions that have a diffuse negative charge, resulting in depleted hydrogen bonding<sup>33</sup>. However, variation in IL viscosity can be manipulated by changing the cation. Fraser *et al.* details a series of viscosities obtained for a group of quaternary phosphonium/ammonium ILs based on the [NTf<sub>2</sub>] anion (Table 1.1)<sup>5</sup>.

<b>Ionic Liquid</b>	<b>Viscosity at 25 °C (mPa.s)</b>
[P <sub>2,2,2,12</sub> ][NTf <sub>2</sub> ]	180
[N <sub>2,2,2,12</sub> ][NTf <sub>2</sub> ]	316
[P <sub>2,2,2,8</sub> ][NTf <sub>2</sub> ]	129
[N <sub>2,2,2,8</sub> ][NTf <sub>2</sub> ]	217
[P <sub>2,2,2,5</sub> ][NTf <sub>2</sub> ]	88
[N <sub>2,2,2,5</sub> ][NTf <sub>2</sub> ]	172

**Table 1.1.** Variation of viscosity of phosphonium and nitrogen ILs containing a [NTf<sub>2</sub>] anion<sup>5</sup>.

Keeping the anion constant and incrementally varying the alkyl constituents of the cation can help understand its effect on the IL viscosity. The table shows that the viscosity of the corresponding phosphonium salts are consistently lower than their ammonium counterparts. This could again be attributed to the larger atomic radii of phosphorous compared with nitrogen, meaning it is more polarisable, which in turn lowers the electrostatic forces with the accompanying anion.

Given their charged nature, one would assume the majority of ILs to be miscible with water. This is not the case however, as ILs can be described as *amphiphilic*; meaning they can exhibit both hydrophobic and hydrophilic traits. Several attempts have been made to quantify the relative polarity of a given IL. This has been achieved primarily by the use of solvatochromic dyes whose optical properties change depending on their immediate solvation microenvironment<sup>34-36</sup>. Phosphonium based ILs are generally immiscible in water; primarily as a function of the extended alkyl chains. Whilst it is charged at its core; the high degree of alkylation of these ILs means they are only miscible with molecular solvents. When paired with a water soluble anion, imidazolium-based ILs tend to be completely miscible with water. This can be explained by the intense charge delocalisation across both the cation and anion, which leads to association with water molecules.

Due to their inherent charged nature, ILs have been exhaustively researched as aqueous electrolytes. They possess major advantages over common ionic solutions; most notably their thermal stability at high temperatures and wide electrochemical window<sup>30</sup>. Imidazolium-based ILs are generally found to display higher conductivity than phosphonium-based ILs. This is due to the extensive  $\pi$ -bonding of the heterocycle exhibiting large delocalization<sup>37</sup>. Compare this to their phosphonium-based counterparts, whose cationic charge can be largely alkyl shielded, and the difference in conductivity can be accounted for<sup>12</sup>. The selection of anion of the IL, when measuring ionic conductivity is also very important. It is also commonly known that ionic conductivity of ILs can be related to the size of the ions involved. For example, by keeping the imidazolium cation constant, Vila *et al.* showed that relatively small anions, such as chloride [Cl]<sup>-</sup>, can exhibit larger conductivity values, compared to larger anions such as ethylsulphate [EtSO<sub>4</sub>]<sup>-</sup><sup>37</sup>.

## 1.2 Ionogels

Due to these favourable characteristics, such as negligible vapour pressure and relatively high ionic conductivity, there has been a challenging need for immobilizing ILs in solid-state devices while keeping their unique properties. One method of retention of these features has been the formation of a three-dimensional network, such as a polymer, which percolates throughout the IL creating what is now commonly known as an *ionogel*. These ionogels are regarded as a new class of hybrid material, which can be classified as either organic or inorganic in nature<sup>38</sup>. A number of review articles on ionogels are available<sup>10, 39-42</sup>, most notably from Bideau *et al.*<sup>39</sup>.

### 1.2.1 Organic Ionogels

Organic ionogels can be polymerized by *in situ* polymerization of a monomer that is dissolved within the liquid<sup>9, 14, 43-45</sup>. Ueki *et al.* have demonstrated the polymerization of vinyl and acrylate monomers in common ILs by free radical polymerization creating solid, conductive ionogel membranes (Figure 1.5)<sup>10</sup>.

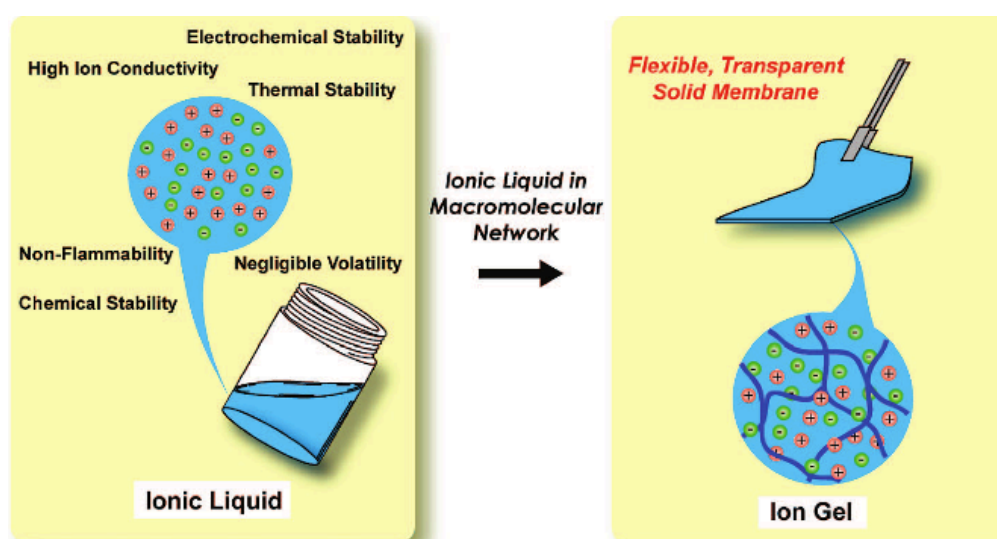


**Figure 1.5.** Compatible binary systems between polymer networks and ionic liquids<sup>10</sup>.

Bai *et al.* have described the formation of polymers prepared via a simple and spontaneous migration of poly(butadiene-*b*-ethylene oxide) block copolymer from a hydrophobic IL, 1-ethyl-3-methylimidazolium *bis*(trifluoromethylsulfonyl)imide, [C<sub>2</sub>mIm][NTf<sub>2</sub>], to water at room temperature. These IL “vesicles” are able to migrate across a liquid-liquid interface with their IL interiors intact <sup>43</sup>.

Lodge *et al.* have reported a new method for developing an ionogel, triggered by micro-phase separation of triblock polymers. The self-assembly of polystyrene-*b*-PEO-*b*-polystyrene triblock polymers in 1-butyl-3-methylimidazolium hexafluorophosphate, [C<sub>4</sub>mIm][PF<sub>6</sub>], was found to yield high ion-conductive polymer electrolyte membranes. Physical gelation of the triblock copolymers in the IL can be achieved by the addition of a small amount of the block copolymer, as low as 5 wt. %, and this gelation is due to the microphase separation of hydrophobic styrene segments at the ends of each copolymer <sup>44</sup>.

## 1.2.2 Inorganic Ionogels

Inorganic ionogels can be based on carbon nanotubes or more commonly, silicon <sup>46-49</sup>. The sol-gel approach is currently the most popular method of synthesizing inorganic ionogels. In classical sol-gel, after condensation, the liquid phase is removed, with the targeted material being the porous solid obtained after drying. However, the use of ionic liquids, endowed with their negligible vapour pressure, permits to regard the gel itself as a material. Most sol-gel derived materials are electronic insulators with low charge-transfer efficiency and substrate diffusion <sup>50</sup>. Ionogels that combine the chemical versatility of ILs with the shaping versatility of sol-gel like organic polymers, offer a new way to design conducting materials for electrochemical devices, such as batteries or fuel cells.

Vioux *et al.* prepared ionogels containing a non-water soluble IL, 1-butyl-3-methylimidazolium *bis*(trifluoromethylsulfonyl)imide [C<sub>2</sub>mIm][NTf<sub>2</sub>], by modifying a silica matrix with hydrophobic organic methyl groups<sup>48</sup>. The modification improved the thermal stability of the ionogels and they exhibited conduction performances similar to those of neat ILs despite the nanoscale level of confinement (Figure 1.6).

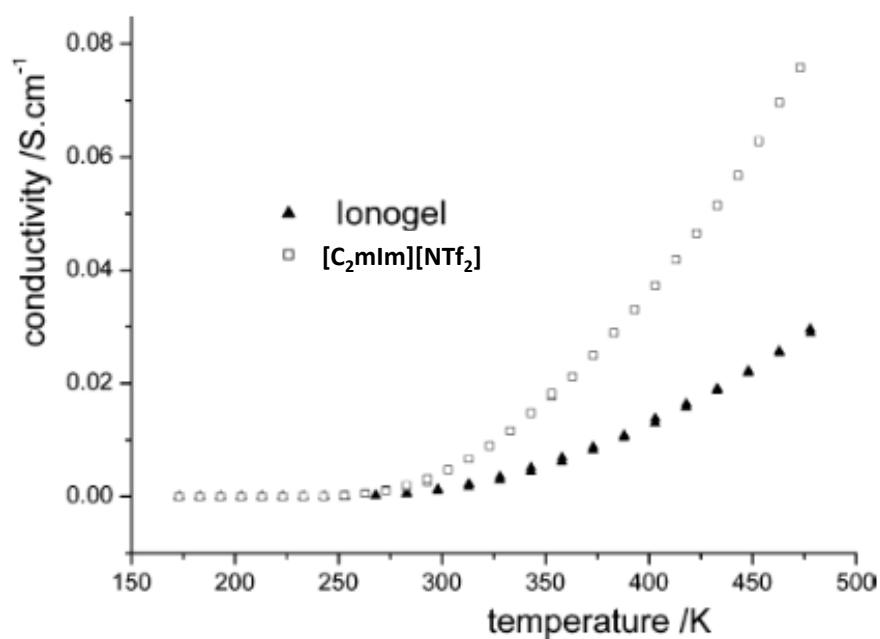


**Figure 1.6.** Conductivity vs. Temperature for the neat IL and a silica-based ionogel<sup>48</sup>.

In the field of drug delivery, silica materials are seen as potential candidates due to their uniform porous structure, high surface area and good biocompatibility. Using a one-step sol-gel synthesis, Vioux *et al.* developed an ionogel containing imidazolium ibuprofenate. The ibuprofen release was governed by the inner and the outer surface of the ionogel, as well as the chemical nature of the surface<sup>51</sup>. These studies have found that the properties of ionogels derive from both those of the IL and those of the polymer forming the solid-like network<sup>9, 10, 12, 48</sup>.

### 1.2.3 Stimuli-responsive Ionogels and their applications

Swann *et al.* have shown that hydrogels can directly convert chemical energy into mechanical work<sup>52</sup>, which can eliminate the requirement of an external power source. The recent introduction of ionogels into hydrogel research has provided a range of diverse new materials. Xie *et al.* used an iron-containing IL, 1-butyl-3-methylimidazolium tetrachloroferrate(III) [BmIm][FeCl<sub>4</sub>], as a building block in the synthesis of paramagnetic PMMA-based ionogels. The material showed strong conductivity temperature dependence with increasing IL weight fractions, as well as retaining the ILs magnetic properties<sup>53</sup>.

Lunstroot *et al.* doped imidazolium-based ILs with lanthanide and incorporated them into a silica network. The coordination sphere of the lanthanide ion was found not to be significantly changed when confined within the matrix of the ionogel. As a result, the ionogels displayed strong photoluminescence when irradiated with ultra-violet light (Figure 1.7)<sup>54</sup>.

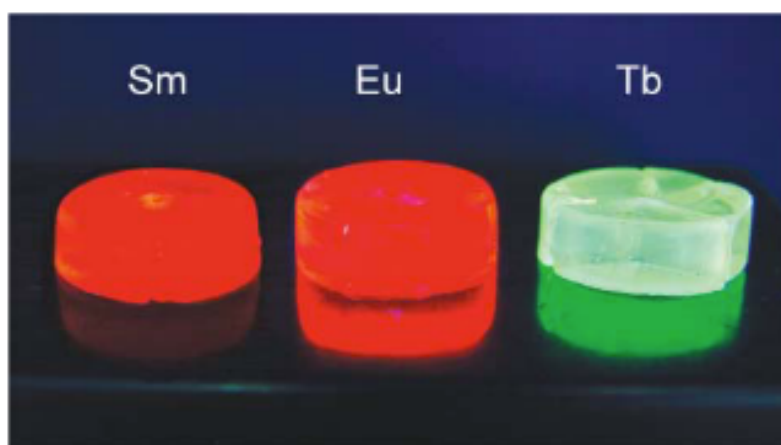


**Figure 1.7.** Lanthanide-doped ionogels produced by Lunstroot<sup>54</sup>.

Ueki *et al.* produced an ionogel containing a pendent azobenzene based on poly(benzylmethacrylate), using 1-ethyl-3-methylimidazolium

*bis*(trifluoromethylsulfonyl)imide [C<sub>2</sub>mIm][NTf<sub>2</sub>] as the polymerization medium <sup>55</sup>.

These materials were found to shrink and swell when exposed to light. This was attributed to the well-known *cis/trans*-azobenzene photo-induced switching phenomenon, along with the LCST behaviour of the polymer (Figure 1.9).

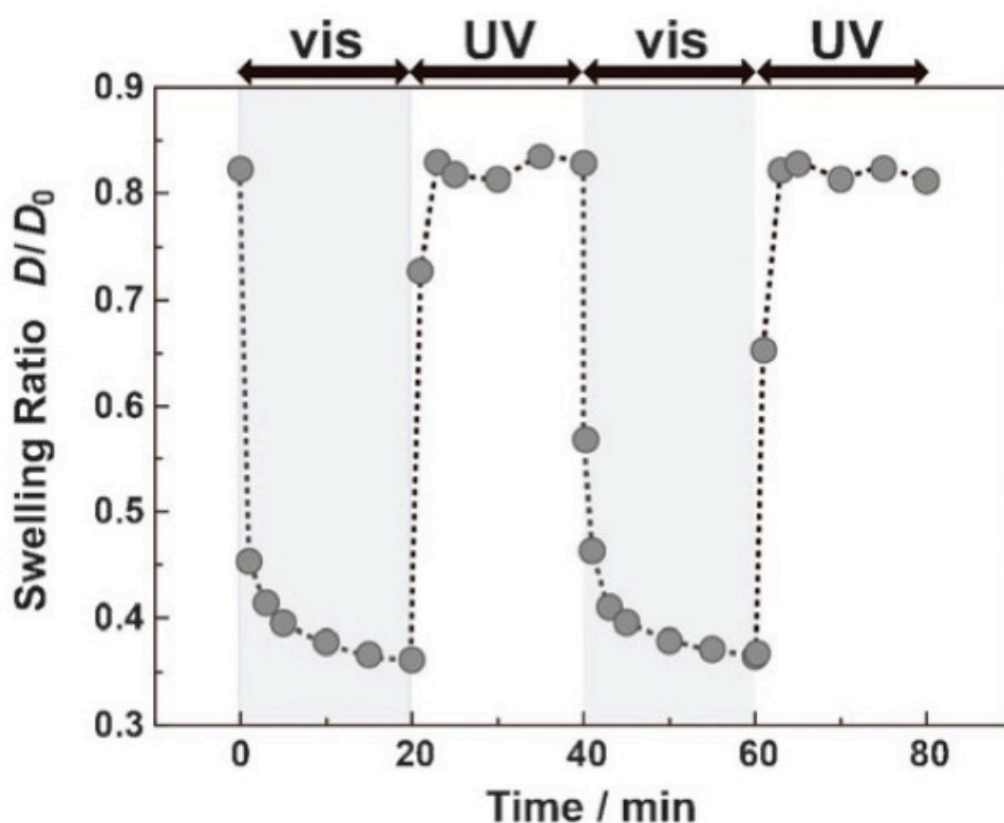


**Figure 1.9.** Photoinduced volume phase transition of poly(azobenzenemethacrylate-co-benzenemethacrylate) gel in [C<sub>2</sub>mim][NTf<sub>2</sub>] at 83 °C. The plots show a change in swelling ratios under visible light (437 nm) irradiation and UV light (366 nm) irradiation <sup>55</sup>.

Lopez *et al.* fabricated photo-responsive ionogels based on varying phosphonium-based ILs by incorporating spiropyran units into poly(methyl methacrylate) networks. Through the photo-responsive co-monomer and variation of the IL, the ionogels rendered different response rates when irradiated with white light (430-760 nm) LEDs <sup>9</sup> (Figure 1.9).

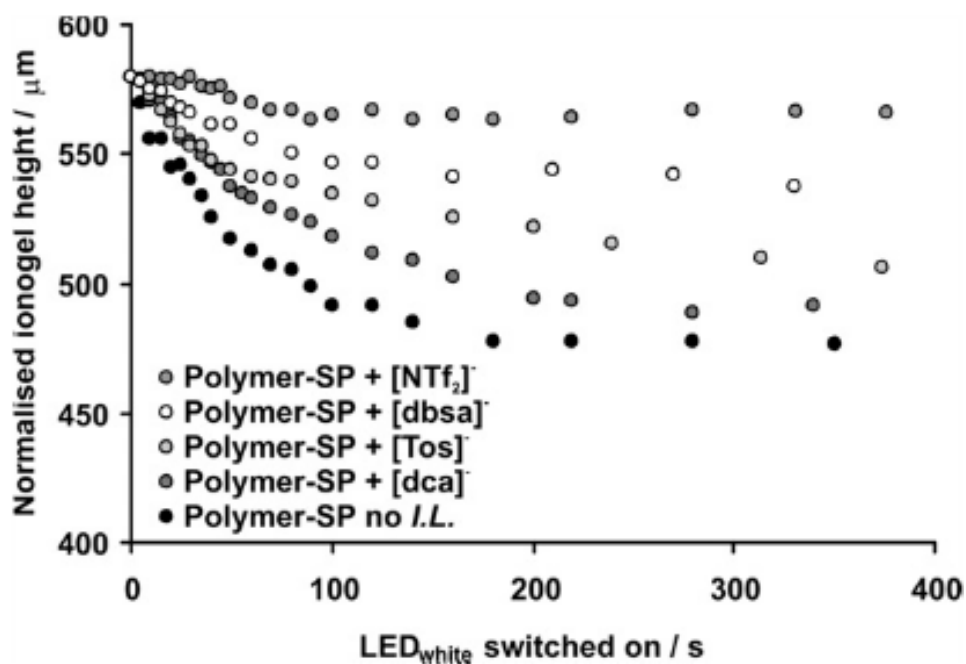


**Figure 1.9.** Different kinetic response rates of phosphonium-based ionogels incorporated with spiropyran when irradiated with visible light <sup>9</sup>.

This showcased the role of these materials as photo-responsive soft-polymer valves, in micro-fluidic channels. The valves were actuated by applying white light irradiation, meaning that no physical contact between the external stimulus and valve is required. However, the fabrication of hydrogels in micro-fluidics with precise control of position and composition is challenging <sup>56</sup>. Lopez *et al.* concept of actuation without physical contact offers improvements in versatility during manifold fabrication, and control of actuation <sup>9</sup>.

This work conducted by Lopez *et al.* <sup>9</sup> has opened an avenue for the use of thermo-responsive ionogels as microfluidic valves, as variation of the IL can facilitate the tailoring valve properties including actuation temperature, response rate, swelling/contracting properties and mechanical stability.

Ionogels have been found to display gradual leaching <sup>39</sup>, however drug release involves the delivery of the hydrogel loading, which may include both the IL and drug.

As previously described, ILs can solubilise compounds which are insoluble in organic solvents, including compounds having pharmaceutical activity such as gelatin<sup>57</sup> and cellulose<sup>58</sup>. Fukumoto *et al.* have made efforts to produce biodegradable ILs based on 1-alkyl-3-methylimidazolium-based ILs using 20 different amino acids as the anions<sup>59</sup>. They found the amino acid ILs to be miscible with organic solvents and could dissolve native amino acids.

While the use of ionogels for biomedical applications has been very limited to-date, the tremendous degree of variation offered by ILs to produce a wide range of responsive polymer gels tailored for specific delivery purposes presents a really exciting opportunity.

## 1.3 Polymeric Ionic Liquids

A progression in recent years from utilizing ILs as the liquid phase of a polymer has been the development of Polymeric Ionic Liquids (PILs) (Figure 1.10). Through simple design of the cationic and/or anionic structures, PILs offer a great opportunity for the regulation of their polymer properties and provide a complementary role towards the amplification of the functions of ILs, with reviews of first-generation PILs available<sup>60-64</sup>. There is currently no clear and widely accepted definition regarding PILs, however the basic concept of PILs is simply based on how they are generated, i.e. by the polymerization of the IL monomer. The physical properties of PILs and ILs are sometimes closely but not necessarily related to each other.

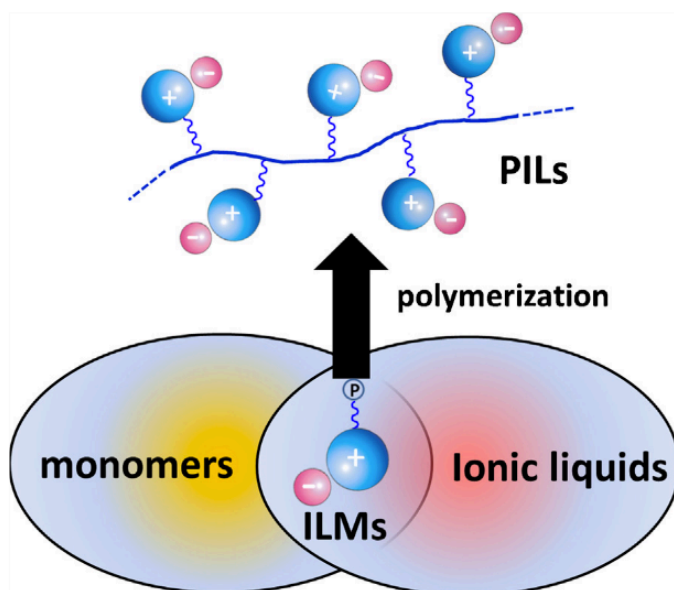


**Figure 1.10.** Illustration of the relationship between ILs and PILs. ILMs: ionic liquid monomers. “P”: polymerizable group <sup>63</sup>.

### 1.3.1 Overview

Due to the solvent-independent ionization state of the IL species, PILs are permanent and strong polyelectrolytes <sup>60</sup>. Based on the general concept of PILs, their physical state is a coupling of the monomer properties of the IL and the polymer character. Most PILs reported to date are solids, and they are commonly reported to have rather broad glass transition temperature ranges from  $-63$  to  $99$  °C <sup>65</sup>, despite their high charge density <sup>65-67</sup>. In addition, they are known to be soluble in many types of organic solvents, from polar to less polar, which depend on the chemical nature of the PIL <sup>67,68</sup>. Like ILs, PILs can undergo structural variation by ion metathesis by anion or cation exchange. Anions play a significant role in governing the solubility of PILs. Maintaining the same cation structure, PILs are often soluble in different solvents, which is decided by the anionic species. Even with the same number of IL monomer units, a PIL can be designed using a variety architectures, such as linear <sup>69, 70</sup> or

crosslinked<sup>65, 71</sup>. Moreover, a PIL can be covalently bonded to other types of polymers to form a PIL block copolymer<sup>45, 72, 73</sup>.

### 1.3.2 Structures and Synthesis

Salamone *et al.* first published several vinylimidazolium-based ILs in the 1970s<sup>74, 75</sup>. However, this did not receive much attention at the time. Since the end of the 1990s, Ohno and co-workers pioneered the polymerization of numerous types of IL monomers in pursuit of solid ion conductor materials<sup>66, 76, 77</sup>, producing imidazolium-based flexible polymers that exhibited ionic conductivity of up to  $1.88 \times 10^{-4} \text{ Scm}^{-1}$  at 30 °C<sup>77</sup>.

As illustrated in Figure 1.11, there are generally two approaches for synthesizing vinylimidazolium type polymers. Similar to the synthesis of ILs, the metathesis approach was reported by Ohno *et al.*, which consisted of anion exchange of the halide anion in water driven by the liquid/liquid phase separation of the formed hydrophobic IL. This group synthesized a variety of IL monomers by anion exchange reaction of a cationic 1-vinyl-3-alkylimidazolium halide type monomer with different counterions<sup>78</sup>. This then followed by direct polymerization of each different IL monomer. Alternatively, the second strategy consists of polymerizing the imidazolium monomer first and then carrying out the anion exchange directly into a polyelectrolyte precursor, such as poly(1-vinyl-3-alkylimidazolium) chloride. Marcilla *et al.* have reported this method, by obtaining different PILs by precipitation in water of the solid PIL synthesized after anion exchange of the halide anion by a more hydrophobic counter anion<sup>68</sup>.

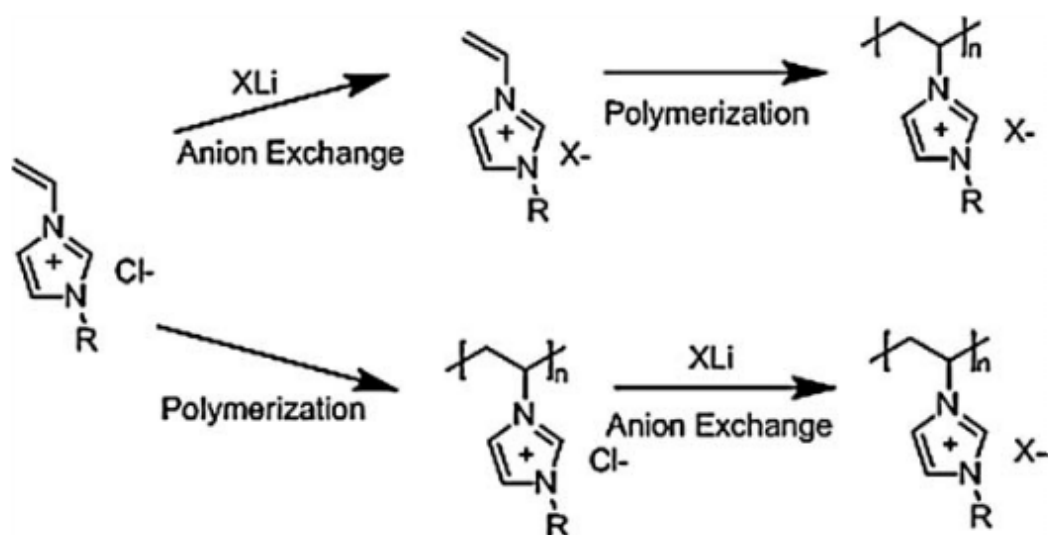


**Figure 1.11.** General synthetic routes of polymeric ionic liquids <sup>79</sup>. (Top) Method involving metathesis reaction with IL monomers <sup>78</sup>. (Bottom) Polymerizing the imidazolium monomer first and then carrying out the anion exchange directly into a polyelectrolyte precursor <sup>68</sup>.

Both methods can present some advantages and disadvantages. The route reported by Ohno *et al.* involving the polymerization of IL monomers enables the preparation of homopolymers as well as copolymers. However, this method involves a number of synthesis and purification steps at the monomer level as well as the need of controlling the polymerization conditions of each individual monomer. The other method is less complicated as it involves only one type of monomer purification and polymerization step, but is limited when more complicated polymer structures are desired.

Polymerization techniques other than radical ones have been employed for the synthesis of PILs. Buchmeiser *et al.* described the synthesis of poly(norbornene) PILs with pendent imidazolium moieties, with three different counter anions of *bis*(trifluoromethylsulfonyl)imide ( $\text{NTf}_2^-$ ), tetrafluoroborate ( $\text{BF}_4^-$ ) and hexafluorophosphate ( $\text{PF}_6^-$ ), via ring opening metathesis polymerization of norbornyl-based IL monomers <sup>80</sup>. The limited solubility of the formed poly(norbenene) PILs in

common organic solvents provided high yields during the polymerization. As expected, measurements of ionic conductivity and thermal stability suggested that the properties of the new PILs were found to be mainly dependent on the nature of the anions chosen.

From the viewpoint of synthetic techniques, highly efficient coupling reactions, so-called click chemistry, have also been introduced in the synthesis of PILs. Drockenmuller *et al.* applied a copper-catalyzed azide-alkane cycloaddition reaction towards the preparation of 1,2,3 triazolium-based main-chain PILs<sup>81</sup>. In the synthetic route, the  $\alpha$ -azide- $\omega$ -alkyne monomer undergoes polyaddition via a click chemistry route. The formed linear polymer with a triazole ring in each repeating unit is converted to the corresponding PIL via a single-step quaternization reaction with methyl iodide, producing a triazolium-based PIL.

For some anions, such as nitrate and dicyanamide, silver salts can assist the anion exchange process. However, the complete removal of the by-product (silver halide) can be problematic. In pursuit of a direct synthesis of halide-free *N*-vinylimidazolium-based IL monomers, attempts have been performed. In an example demonstrated by Ohno *et al.*, a neutralization reaction of *N*-vinylimidazolium with a corresponding acid was carried out to synthesize IL monomers in a single step<sup>82</sup>. An IL monomer with tetrafluoroborate acid was prepared by reacting *N*-vinylimidazolium with tetrafluoroboric acid in a mixture of water and ethanol. In this case, a non-halide is incorporated in the *N*-vinylimidazolium-based IL monomer simultaneously with the formation of an IL monomer without the aid of silver salts.

### 1.3.3 Applications

Ion conductivity is a fundamental physical property of PILs. PILs as solid-state polymeric electrolytes are of significant interest in the field of electrochemistry because they avoid some disadvantages of liquid electrolytes, such as leakage and flammability, in the application of areas of batteries and fuel cells<sup>83,84</sup>. In addition, the polymer nature of the PIL potentially permits production of ion-conductive materials with defined size, shape and geometry, being able to form coatings, gels, films and membranes. These properties have led to applications such as lithium batteries<sup>83</sup>, solar cells<sup>85</sup>, and electrochromic devices<sup>86</sup>.

Ohno *et al.* have systematically studied the structure-related ionic conductivity of *N*-vinylimidazolium PILs<sup>66,76,77</sup>. They found that the polymerization of IL monomers in general causes lower ionic conductivity due to the considerable elevation of glass transition temperature and reduced number of mobile ions after covalent bonding of the polymerizable ions. The structural parameters of PILs that influence the ion conductivity of IL monomers include; cations<sup>66</sup>, anions<sup>87</sup>, the spacer between the polymerizable group and the cation<sup>65</sup>, and the alkyl chain on the imidazolium ring (for *N*-vinylimidazolium-based IL monomers)<sup>88</sup>.

The low ionic conductivity following polymerization of ionic liquid monomers can render them insufficient for practical use. This has led to the designing of polymer electrolytes composed of polymer matrices and ILs. To avoid leakage and bad mechanical properties, PILs are ideally suited to develop tailor-made polymer electrolytes due to their similar chemical structure to ILs. Marcilla *et al.* reported mixing of the PIL poly(1-vinyl-3-ethylimidazolium)

*bis*(trifluoromethylsulfonyl)imide with the IL, 1-butyl-3-methylimidazolium *bis*(trifluoromethylsulfonyl)imide [C<sub>2</sub>mIm][NTf<sub>2</sub>]<sup>89</sup>. As shown in Figure 1.12, the specific ionic conductivity for each mixture usually behaves based on the blends of PIL and IL. At elevated IL concentrations, the ionic conductivity reached to the values of the IL, however the mechanical stability is compromised. As expected, the conductivity decreased and mechanical stability increased, with increasing polymer content.

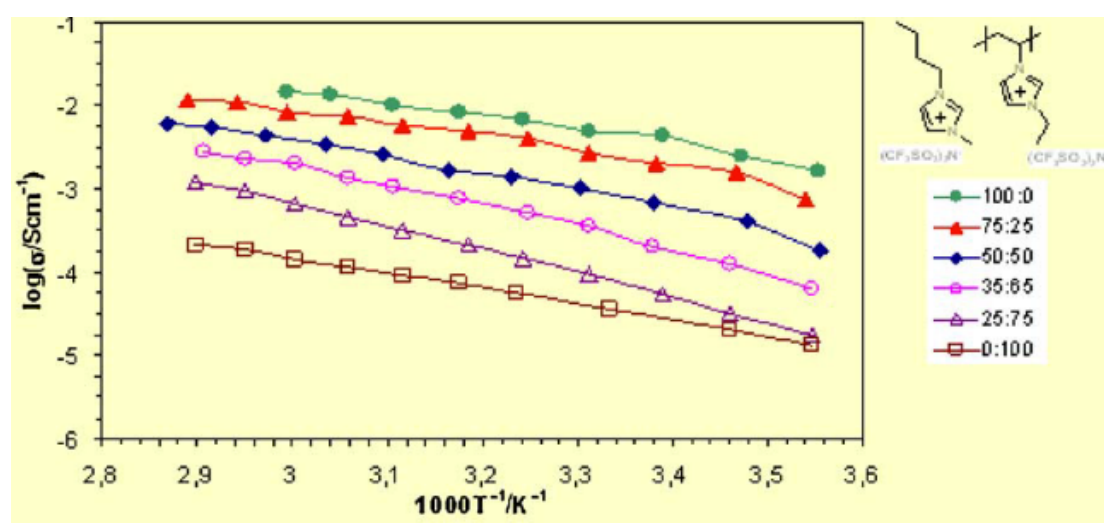


**Figure 1.12.** Temperature dependence of the ionic conductivity for polymer electrolyte blends with different ratios of IL and PIL<sup>89</sup>.

PIL gels prepared from the polymerization of cross-linkable IL monomers, can often show poor ion conductivity due to lack of both mobile cations and anions. However, recent studies by Tarascon *et al.* have shown the addition of the cross-linker poly(ethyleneglycol)dimethacrylate (PEGDM) to increase the degrees of freedom through a “dangling chain effect” which in turn leads to an increase in conductivity<sup>66</sup>,

84.

In the field of separation science, PILs have been examined for use in solid phase extraction. Hsieh *et al.* have recently constructed stationary phases based upon imidazolium-derived PILs for use in gas chromatography, showing good reliability

and structural selectivity <sup>90</sup>. These properties were attributed to the ordered arrangement of the octylimidazolium side chains. González-Álvarez *et al.* designed a total of seven new PIL-based stationary phases in gas chromatography <sup>91</sup>. The coated columns were characterized using Abraham's solvation parameter model and exhibited good thermal stabilities and very high efficiencies.

Recently, a new class of PILs displaying thermo-responsive behaviour has been reported <sup>70, 92-94</sup> (Figure 1.13). The development of these PILs creates new possibilities for applications such as selective extraction of water-soluble proteins <sup>92, 94, 95</sup>. Kohno *et al.* reported the first thermo-responsive PIL to display phase separation at elevated temperatures, or a LCST (Lower Critical Solution Temperature), which consisted of a combination of a phosphonium cation and styrene sulfonate anion <sup>96</sup>. This PIL was dissolved in water and then when heated, precipitated above the LCST, and then re-dissolved when cooled below the LCST, much like the thermo-responsive polymer *N*-isopropylacrylamide (pNIPAAm) <sup>97</sup>. Following this report, thermo-responsive PILs have been based on variations of phosphonium cations, such as tetrabutyl or tributyl-hexyl, combined with anion derivatives based on benzenesulfonic acid <sup>69, 70, 92, 94</sup>.

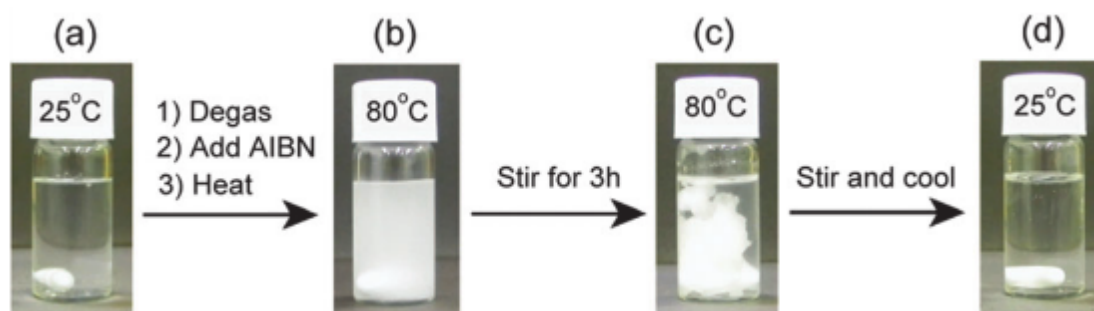


**Figure 1.13.** Suspension of thermo-responsive PIL tributylhexylphosphonium 3-sulfopropylmethacrylate in water. The mixture is initially clear at 25 °C; (a) AIBN is added to mixture which is heated to 80 °C, giving rise to suspension (b). During polymerization the suspension (b) is changed to (c), where the PIL precipitates from the mixture. (d) This polymer reverts back to transparency upon cooling and stirring at 25 °C <sup>70</sup>.

Ziolkowski *et al.* recently reported the polymerization of thermo-responsive monomeric ILs and subsequent formation of thermo-responsive PIL hydrogels <sup>71</sup>. They established suitable cross-linkers and investigated interesting endothermic transition behaviour. The cross-linked PILs were found to display a significant broadening of the temperature range over which the LCST behaviour occurs. This discovery opens up an opportunity of research for PILs in applications such as microfluidics and delivery materials.

## 1.4 Temperature Responsive Materials

Stimuli-responsive gels can undergo controlled and reversible shape changes in response to an applied stimulus <sup>42, 98</sup>. The stimulus or external field applied may include thermal <sup>99, 100</sup>, electrical <sup>101, 102</sup>, magnetic <sup>103</sup>, pH <sup>104-106</sup>, UV/visible light <sup>9, 107</sup> or combinations thereof <sup>104, 106</sup>. These attributes have led to important applications for “smart materials” including drug delivery <sup>104, 108, 109</sup>, microfluidics <sup>9</sup>, polymer actuators <sup>110</sup>, and biomimetic systems <sup>111, 112</sup>.

Examples of temperature responsive polymers include; poly(methylmethacrylate) (PMMA)<sup>53</sup> and poly(N,N'-diethylacrylamide) (PDEAAm)<sup>113</sup>. Another well-studied thermally responsive polymer platform is poly(*N*-isopropylacrylamide) (pNIPAAm)<sup>97</sup> and will be the focus for the rest of this review.

This polymer has been reported thoroughly due to its biocompatibility<sup>114, 115</sup>, controlled actuation<sup>9</sup> and fast response rate<sup>116</sup>. In the presence of water, pNIPAAm displays inverse solubility properties upon heating above and below what is known as its Lower Critical Solution Temperature (LCST)<sup>10, 97</sup>. Experimentally, below the LCST, pNIPAAm is first swollen with water through hydration of the polymerised aliphatic chain and hydrogen bonding interactions with its amide moiety, generating a gel network (Figure 1.15)<sup>117</sup>. Whilst above the LCST, the gel collapses along the polymer backbone before water molecules are expelled<sup>8, 118, 119</sup>.

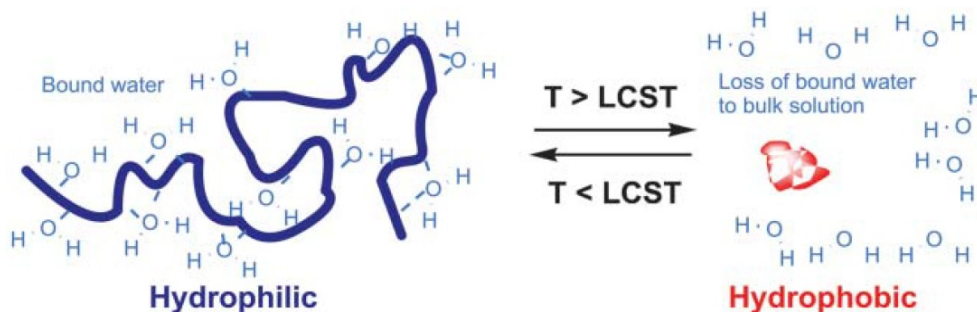


**Figure 1.14.** Schematic of “smart” polymer response with temperature<sup>120</sup>.

Many papers have described the mechanism of the pNIPAAm phase transition<sup>97, 116-118, 121, 122</sup>. A detailed and clear explanation is provided by Ahmed *et al.*<sup>118</sup>. Utilizing UV Raman Resonance measurements, they explain the molecular mechanism of pNIPAAm’s hydrophobic collapse. It is proposed that the hydrophobic collapse is driven by changes in the polymer-water interactions. In the swollen state, the exposed amide bonds provide three hydrogen-bonding sites where water molecules localize

and serve as nucleating sites for formation of large water clusters, i.e., a hydration shell. The energy between the hydrogen binding of these water clusters is highly cooperative. By providing a nucleation site, the amide bond lowers the free energy barrier to formation of large water clusters. This free energy gained via the formation of large water clusters stabilizes the well-hydrated extended pNIPAAm conformation.

As the temperature increases, an increasing entropic “penalty” occurs for the energy binding the water molecules situated at the surface of the hydrophobic surface of the isopropyl groups. A cooperative transition occurs where a hydrophobic collapse minimizes the exposed hydrophobic surface area allowing the water entropy to increase. This polymer structural change results in the loss of a semi-continuous hydrophilic surface due to exposure of the pNIPAAm amide groups. This same hydrophilic face at low temperatures stabilizes the large water clusters. However, upon the hydrophobic collapse, the amide carbonyl and N-H are forced to fold inwards and the water clusters cease to be stabilized. This results in an abrupt cooperative dehydration of the pNIPAAm polymer network.

### 1.4.1 Manipulation of the pNIPAAm LCST

Studies into the control of the lower critical solution temperature (LCST) phase transition of pNIPAAm often involve chemical modification of the polymer backbone or co-polymerization<sup>123-129</sup>. Mi *et al.* have induced a hydrophobic negative shift of the phase transition by synthesis of a pNIPAAm smart thermo-responsive copolymer, poly(*N*-isopropylacrylamide)-*co*-(benzo-15-crown-acrylamide), that can selectively respond to certain alkali metal ions<sup>124</sup>. Hydrophobic modifications, however, have been found to weaken and sometimes eliminate the thermal sensitivity of pNIPAAm-

based hydrogels due to the introduction of the non-thermosensitive moiety <sup>127</sup>.

In the search for a more bio-inspired structure, hydrophilic alterations have been reported which have increased the LCST of pNIPAAm <sup>126, 128, 129</sup>. Teng *et al.* incorporated pNIPAAm and acrylic acid to copolymerise with acrylamide-2-deoxyglucose, to produce a glucosamine carrying microgel <sup>128</sup>, while Choi *et al.* proposed a new possibility for the controlling of intracellular events such as protein and gene expression by copolymerising pNIPAAm with acrylic acid in the presence of a crosslinker <sup>129</sup>.

There have also been studies on the influence of a number of salts on the LCST transition, showing that they decrease phase transition temperature, incurring a “salting out effect”, the degree of which depends on the size and valence of the anions <sup>100</sup>. This has also improved the response rate, assisting water diffusion above the LCST. Most notably, however, Reddy *et al.* reported modification of the LCST phase transition of a pNIPAAm aqueous solution in the presence of an Ionic Liquid, inducing a negative shift as low as 26 °C with increasing concentration <sup>8</sup>.

## 1.4.2 Mechanical Properties of pNIPAAm

Gong *et al.* previously reported a detailed study of the mechanical properties of hydrogels <sup>130</sup>. Several attempts have been made to increase the mechanical stability of pNIPAAm hydrogels and it has been demonstrated that increasing cross-linking density can dramatically improve the mechanical strength of hydrogels <sup>130, 131</sup>. However, in these cases the ductility of the hydrogels was lost. Furthermore, it has been reported that increasing of cross-linking density often leads to structural

inhomogeneities recognizable by a turbid appearance of the gels<sup>132</sup>. Satisfactory mechanical properties have been found by trapping pNIPAAm in the hydrogel network to form a semi-interpenetrating network known as semi-IPNs<sup>114, 133, 134</sup>. Semi-IPNs are composed of two or more chemically identical distinct networks where one of the components is cross-linked and the other is in its linear form. These semi-IPNs hydrogels, entangled in a polyacrylamide network, are mechanically stable while their response to temperature is preserved<sup>133</sup>.

### 1.4.3 Applications

Hydrogels are well known as good candidates for the controlled release of drug formulations for pharmaceutical applications due to their high biocompatibility<sup>114</sup>. In recent years, these polymeric carriers have been extensively considered as sustained and controlled release devices for the delivery of water-soluble drugs<sup>104</sup>. pNIPAAm-based hydrogels have attracted increasing interest in this regard due to the LCST being close to body temperature, 31 – 34 °C<sup>97</sup>.

Copolymers of pNIPAAm have been previously studied for the oral delivery of formulations in the stomach. Serres *et al.* synthesized pNIPAAm copolymers for the delivery of calcitonin<sup>108</sup>, while Kim *et al.* investigated the delivery of insulin<sup>109</sup>. In the case of calcitonin, this method involved immobilizing the hormone in polymeric beads. They remain stable while passing through the stomach; the beads then disintegrate in the upper intestine due to pH and the drug is released. Molecular dyes have been widely used as model drugs to monitor the release and uptake behaviour of pNIPAAm hydrogels. Orange II was used by Guilherme<sup>114</sup> to investigate phase transitions of co-polymers in water. Also, Tasdelen *et al.* have used pH sensitive

hydrogels to monitor the delivery rate of methylene blue in response to dual stimuli<sup>106</sup>, while Asoh performed a similar study using the same dye but with semi-IPNs<sup>135</sup>.

Ionic liquids have been introduced as reaction media for the synthesis of pNIPAAm platforms in order to produce ionogels as discussed in *Section 1.2*. Hao *et al.* successfully grafted pNIPAAm onto microcrystalline cellulose by x-ray irradiation in a 1-butyl-3-methylimidazolium chloride [C<sub>4</sub>mIm][Cl]. Due to the presence of the IL, the grafting of pNIPAAm improved the thermal stability of regenerated cellulose after radiation<sup>136</sup>. Watanabe *et al.* produced azobenzene-containing copolymers containing pNIPAAm and 4-phenylazophenyl methacrylate that displayed an upper critical solution temperature in 1-ethyl-3-methylimidazolium bis(trifluoromethylsulfonyl)imide [C<sub>2</sub>mIm][NTf<sub>2</sub>]<sup>137</sup>. This photoinduced contactless reversible stimuli-responsive phase transition of pNIPAAm in a thermally, non-volatile IL, is another unique way to produce smart materials.

Another application for pNIPAAm-based hydrogel is microfluidics<sup>9,110</sup>. Suzuki *et al.* presented a schematic for employing pNIPAAm gels as microfluidic actuators<sup>110</sup>. The temperature responsive material is used as a “sponge” to absorb the oncoming solution in the valve. As described earlier, pNIPAAm in solution swells below what is known as its LCST, and is found to shrink above this temperature. Suzuki *et al.* proposed that the gel in its collapsed state absorbs the solution from the flow channel, which then causes the flow channel to move (Figure 1.16). The gel can be then heated externally above the LCST and cause the solution in the channel to flow again. Unfortunately, in pNIPAAm, the swelling rate is found to be far slower than that of the shrinking rate, however this microfluidic design could be a promising concept for a disposable (single use) system.

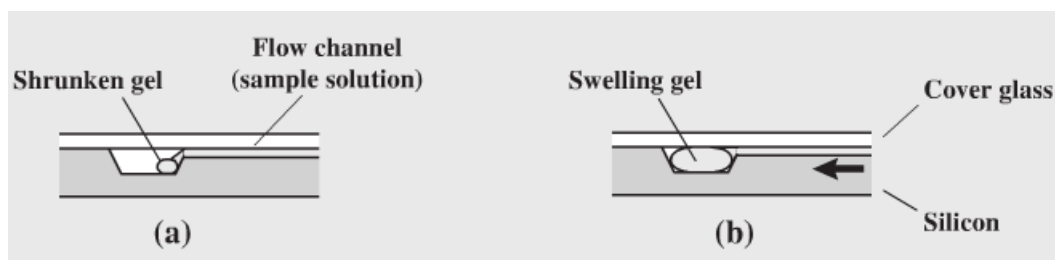


**Figure 1.15.** Structure and function of the sampling mechanism proposed by Suzuki *et al*<sup>110</sup>.

In terms of microfluidic applications, the current position is that thermo-responsive hydrogels such as pNIPAAm, have not fulfilled their potential when organic solvents are employed as the liquid phase. Such organic solvent-based gels are prone to instability at high and low temperatures in an open atmosphere (evaporation, freezing etc.)<sup>138</sup>, that can lead to weak mechanical stability. This presence of a volatile liquid phase is also a considerable drawback for smart materials in terms of reproducibility. The introduction of ILs as the liquid phase, with its own unique properties, including negligible vapour pressure, renders ionogels as a suitable replacement for conventional organic solvent-based hydrogels.

## 1.5 References

1. P. Wasserscheid and T. Welton, *Wiley Online Library*, 2003, **1**.
2. M. J. Earle, J. M. S. S. Esperança, M. A. Gilea, J. N. Canongia Lopes, L. P. N. Rebelo, J. W. Magee, K. R. Seddon and J. A. Widegren, *Nature*, 2006, **439**, 831-834.
3. W. Xu, E. I. Cooper and C. A. Angell, *The Journal of Physical Chemistry B*, 2003, **107**.
4. K. R. Seddon, A. Stark and M.-J. Torres, *Pure Applied Chemistry*, 2000, **72**, 2275-2287.
5. K. J. Fraser and D. R. MacFarlane, *Australian Journal of Chemistry*, 2009, **62**, 309-321.

6. L. Li, J. Wang, T. Wu and R. Wang, *Chemistry (Weinheim an der Bergstrasse, Germany)*, 2012.
7. L. Vidal, M.-L. Riekkola and A. Canals, *Analytica Chimica Acta*, 2012, **715**, 19-60.
8. P. Reddy and P. Venkatesu, *The Journal of Physical Chemistry*, 2011, **115**, 4752-4759.
9. F. Benito-Lopez, R. Byrne, A. M. Raduta, N. Vrana, G. McGuinness and D. Diamond, *Lab on a Chip*, 2010, **10**, 195-396.
10. T. Ueki and M. Watanabe, *Macromolecules*, 2008, **41**, 11.
11. B. Ziólkowski, Z. Ates, S. Gallagher, K. Fraser, A. Heise, R. Byrne and D. Diamond, *Macromolecular Chemistry and Physics*, 2013, **7**, 787-796.
12. A. Kavanagh, R. Copperwhite, M. Oubaha, J. Owens, C. McDonagh, D. Diamond and R. Byrne, *Journal of Materials Chemistry*, 2011, **21**, 8687.
13. M. W. Jan Leys, Chirukandath Preethy Menon, Ravindran Rajesh, and a. C. G. Jan Thoen, *The Journal of Chemical Physics* 2008, **128**, 064509.
14. D. Khodagholya, V. F. Curto, K. J. Fraser, M. Gurfinkel, R. Byrne, D. Diamond, G. G. Malliaras, F. Benito-Lopez and R. M. Owens, *Journal of Materials Chemistry*, 2012, **22**, 4440-4443.
15. M. Ali, P. Dutta and S. Pandey, *The Journal of Physical Chemistry B*, 2010, **114**, 15042-15051.
16. M. Freire, P. Carvalho, R. Gardas, I. Marrucho, L. Santos and J. Coutinho, *The Journal of Physical Chemistry B*, 2008, **112**, 1604-1614.
17. T. Regueira, L. Santos and F. J., *Journal of Chemical & Engineering Data*, 2010, **55**, 645-652.
18. S. Ventura, A. M. Goncalves, T. Sintra, J. Pereira, F. Goncalves and J. Coutinho, *Ecotoxicology (London, England)*, 2013, **22**, 1-12.
19. S. Coleman, S. Gallagher, R. Byrne and D. Diamond, *Physical Chemistry Chemical Physics*, 2010, **12**, 1895-1904.
20. M. G. Freire, P. J. Carvalho, R. L. Gardas, L. M. Santos, I. M. Marrucho and J. A. P. Coutinho, *Journal of Chemical & Engineering Data*, 2008, **53**, 2378-4760.
21. C. Neves, P. J. Carvalho, M. G. Freire and J. A. P. Coutinho, *The Journal of Chemical Thermodynamics*, 2011, **43**, 948-957.

22. J. McNulty, A. Capretta, J. Wilson, J. Dyck, G. Adjabeng and A. Robertson, *Chemical Communications* 2002, 1986-1987.
23. T. Katsuhiko, K. Atsuko, M. Masahiko, K. Shun, E. Ryuichi, S. Masashi and K. Yoshihito, *Electrochemistry Communications*, 2011, **13**.
24. T. Ramnial, S. Taylor, M. Bender, B. Gorodetsky, P. Lee, D. Dickie, B. McCollum, C. Pye, C. Walsby and J. Clyburne, *The Journal of Organic Chemistry*, 2008, **73**, 801-812.
25. C. J. Bradaric, A. Downard, C. Kennedy, A. J. Robertson and Y. H. Zhou, *Green Chemistry*, 2003, **5**, 143-152.
26. V. Ermolaev, V. Miluykov, I. Rizvanov, D. Krivolapov, E. Zvereva, S. Katsyuba, O. Sinyashin and R. Schmutzler, *Dalton Transactions*, 2010, **39**, 5564-5571.
27. J. S. Wilkes, J. A. Levisky, R. A. Wilson and C. L. Hussey, *Inorganic Chemistry*, 1982, **21**, 1263-1264.
28. D. MacFarlane, J. Pringle, K. Johansson, S. Forsyth and M. Forsyth, *Chemical Communications (Cambridge, England)*, 2006, 1905-1917.
29. R. D. Rogers and K. R. Seddon, *Ionic Liquids as Green Solvents: Progress and Prospects; American Chemical Society*, 2003.
30. P. Wasserscheid and T. Welton, *Wiley Online Library*, 2003, **1**, 1-380.
31. K. N. Marsh, J. A. Boxall and R. Lichtenthaler, *Fluid Phase Equilibria*, 2004, **219**, 93-98.
32. K. R. Seddon, A. Stark and M.-J. Torres, *Pure Applied Chemistry*, 2000, **72**, 2275-2287.
33. K. Tsunashima and M. Sugiya, *Electrochemistry Communications*, 2007, **9**, 2353-2358.
34. C. Reichardt, *Green Chemistry*, 2005, **7**, 339-351.
35. R. Byrne, S. Coleman, K. Fraser, A. Raduta, D. MacFarlane and D. Diamond, *Physical Chemistry Chemical Physics*, 2009, **11**, 7286-7291.
36. R. Byrne, S. Coleman, S. Gallagher and D. Diamond, *Physical Chemistry Chemical Physics*, 2010, **12**, 1895-1904.
37. J. Vila, L. Varela and O. Cabeza, *Electrochimica Acta*, 2007, **52**, 7413-7417.
38. J. M. G. Cowie, *Polymers: Chemistry & Physics of Modern Materials Cheltenham*, 1991.

39. J. Le Bideau, L. Viau and A. Vioux, *Chemical Society Reviews*, 2011, **40**, 907-932.
40. A. Kavanagh, R. Byrne, D. Diamond and K. J. Fraser, *Membranes*, 2012, **2**, 16-55.
41. A. Suk-kyun, M. K. Rajeswari, K. Seong-Cheol, S. Nitin and Z. Yuxiang, *Soft Matter*, 2008, **4**.
42. C. Liu, H. Qin and P. T. Mather, *Journal of Materials Chemistry*, 2007, **17**, 1543-1558.
43. Z. Bai and T. Lodge, *Journal of the American Chemical Society*, 2010, **132**, 16265-16270.
44. Y. He, P. Boswell, P. Buhlmann and T. Lodge, *The Journal of Physical Chemistry. B*, 2007, **111**, 4645-4652.
45. E. Karjalainen, N. Chenna, P. Laurinmaki, S. J. Butcher and H. Tenhu, *Polymer Chemistry*, 2013, **4**, 1014.
46. F. Gayet, L. Viau, F. Leroux, F. Mabilille, S. Monge, J.-J. Robin and A. Vioux, *Chemistry of Materials*, 2009, **21**, 5575-5577.
47. S. Shimano, H. Zhou and I. Honma, *Chemistry of Materials*, 2007, **19**, 5216-5521.
48. M.-A. Néouze, J. Le Bideau, P. Gaveau, S. Bellayer and A. Vioux, *Chemistry of Materials*, 2006, **18**, 3931-3936.
49. M.-A. Néouze, J. Le Bideau and A. Vioux, *Progress in Solid State Chemistry*, 2005, **33**, 217-222.
50. V. Andre, V. Lydie, V. Sabrina and B. Jean Le, *Comptes Rendus Chimie*, 2010, **13**, 242-255.
51. L. Viau, C. Tourne-Peteilh, J.-M. Devoisselle and A. Vioux, *Chemical Communications (Cambridge, England)*, 2010, **46**, 228-230.
52. M. G. S. Joshua and J. R. Anthony, *Polymer International*, 2009, **58**, 285-289.
53. X. Zai-Lai, J. Aleksandra, W. Fei-Peng, R. Pierre, F. Alwin, B. Sabine and T. Andreas, *Journal of Materials Chemistry*, 2010, **20**.
54. K. Lunstroot, K. Driesen, P. Nockemann, K. Van Hecke, L. Van Meervelt, C. Görller-Walrand, K. Binnemans, S. Bellayer, J. Le Bideau and A. Vioux, *Chemistry Materials*, 2006, **18**, 5711-5715.
55. T. Ueki, A. Yamaguchi and M. Watanabe, *Chemical Communications*, 2012, **48**, 5133-5135.

56. C. Anindarupa, E. Kenneth, L. Ghanashyam, J. C. Hyoun and Z. Lei, *Colloids and Surfaces A: Physicochemical and Engineering Aspects*, 2009, **333**.
57. P. Vidinha, N. Lourenco, C. Pinheiro, A. Bras, T. Carvalho, T. Santos-Silva, A. Mukhopadhyay, M. Romao, J. Parola, M. Dionisio, J. Cabral, C. Afonso and S. Barreiros, *Chemical Communications*, 2008, 5842-5844.
58. M. Turner, S. Spear, J. Holbrey, D. Daly and R. Rogers, *Biomacromolecules*, 2005, **6**, 2497-2502.
59. K. Fukumoto, M. Yoshizawa and H. Ohno, *Journal of the American Chemical Society*, 2005, **127**, 2398-2399.
60. D. Mecerreyes, *Progress in Polymer Science*, 2011, **36**, 1629-1648.
61. O. Green, S. Grubjesic, S. Lee and M. A. Firestone, *Polymer Reviews*, 2009, **49**, 339-360.
62. J. Lu, F. Yan and J. Texter, *Progress in Polymer Science*, 2009, **34**, 431-438.
63. J. Yuan and M. Antonietti, *Polymer*, 2011, **52**, 1469-1482.
64. M. D. Green and T. E. Long, *Polymer Reviews*, 2009, **49**, 291-314.
65. A. Shaplov, E. I. Lozinskaya, D. O. Ponkratov, I. A. Malyshkina, F. Vidal, P.-H. Aubert, O. g. V. Okatova, G. M. Pavlov, L. I. Komarova, C. Wandrey and Y. S. Vygodskii, *Electrochimica Acta*, 2011, **57**, 74-90.
66. H. Ohno, *Macromolecular Symposia*, 2007, **249-250**, 551-556.
67. A. S. Shaplov, P. S. Vlasov, M. Armand, E. I. Lozinskaya, D. O. Ponkratov, I. A. Malyshkina, F. Vidal, O. V. Okatova, G. M. Pavlov, C. Wandrey, I. A. Godovikov and Y. S. Vygodskii, *Polymer Chemistry*, 2011, **2**, 2609.
68. R. Marcilla, J. A. Blazquez, J. Rodriguez, J. Pomposo, A. and D. Mecerreyes, *Journal of Polymer Science Part A: Polymer Chemistry*, 2004, **42**.
69. Y. Men, H. Schlaad and J. Yuan, *ACS Macro Letters*, 2013, **2**.
70. Y. Kohno, Y. Deguchi and H. Ohno, *Chemical Communications*, 2012, **48**, 11883-11885.
71. B. Ziółkowski and D. Diamond, *Chemical Communications*, 2013, **49**, 10308.
72. C. Plesse, F. Vidal, H. Randriamahazaka, D. Teyssie and C. Chevrot, *Polymer*, 2005, **46**, 7771-7778.
73. H. Mori, M. Yahagi and T. Endo, *Macromolecules*, 2009, **42**, 8082-8092.
74. J. Salamone, S. Israel, P. Taylor and B. Snider, *Journal of Polymer Science Polymer Symposium*, 1974, **45**, 65-73.

75. J. Salamone, S. Israel, P. Taylor and B. Snider, *Polymer*, 1973, **12**, 639-644.
76. H. Ohno, *Electrochimica Acta*, 2001, **46**, 1407-1411.
77. H. Ohno and K. Ito, *Chemistry Letters*, 1998, **27**, 751-752.
78. K. Ito, N. Nishina and H. Ohno, *Electrochim Acta* 2000, **45**, 1295–1298.
79. D. Mecerreyes, *Progress in Polymer Science*, 2011, **36**, 1629-1648.
80. Y. Vygodskii, A. Shaplov, E. Lozinskaya, K. Lyssenko, D. Golovanov, I. Malyshkina, N. Gavrilova and M. Buchmeiser, *Macromolecular Chemistry Physics*, 2008, **209**, 40-51.
81. P. Dimitrov-Raytchev, S. Beghdadi, A. Serghei and E. Drockenmuller, *Journal of Polymer Science Part A: Polymer Chemistry*, 2013, **51**.
82. M. Hirao, K. Ito and H. Ohno, *Electrochimica Acta*, 2000, **45**, 1291-1294.
83. A.-L. Pont, R. Marcilla, I. De Meazza, H. Grande and D. Mecerreyes, *Power Sources*, 2009, **188**, 558.
84. J. Tarascon and M. Armand, *Nature*, 2001, **414**, 359-367.
85. K. Suzuki, M. Yamaguchi, S. Hotta, N. Tanabe and S. Yanagida, *Journal of Photochemistry and Photobiology A: Chemistry*, 2004, **164**, 81-85.
86. M. Kijima, K. Setoh and H. Shirakawa, *Chemistry Letters*, 2000, **29**, 936.
87. Y. Vygodskii, S. , O. Mel'nik, A., E. Lozinskaya, I. , A. Shaplov, S. , I. Malyshkina, A. , N. Gavrilova, D. , K. Lyssenko, A., M. Y. Antipin, D. Golovanov, G. , A. Korlyukov, A. , N. Ignat'ev and U. Welz-Biermann, *Polymers for Advanced Technologies*, 2007, **18**, 50-63.
88. A. S. Shaplov, D. O. Ponkratov, P. S. Vlasov, E. I. Lozinskaya, L. I. Komarova, I. A. Malyshkina, F. Vidal, G. T. M. Nguyen, M. Armand, C. Wandrey and S. V. Ya, *Polymer Science Series B*, 2013, **55**, 122-128.
89. R. Marcilla, F. Alcaide, H. Sardon, J. Pomposo, C. Pozo-Gonzalo and D. Mecerreyes, *Chemical Communications*, 2006, **9**, 482-488.
90. Y.-N. Hsieh, C.-H. Kuei, Y.-K. Chou, C.-C. Liu, K.-L. Leu, T.-H. Yang, M.-Y. Wang and W.-Y. Ho, *Tetrahedron Letters*, 2010, **51**, 3666-3669.
91. J. Gonzalez-Alvarez, D. Blanco-Gomis, P. Arias-Abrodo, D. Diaz-Llorente, N. Rios-Lombardia, E. Busto, V. Gotor-Fernandez and M. Gutierrez-Alvarez, *Analytica chimica acta*, 2012, **721**, 173-181.
92. Y. Kohno and H. Ohno, *Physical Chemistry Chemical Physics*, 2012, **14**, 5063-5070.

93. Y. Fukaya, K. Sekikawa, K. Murata, N. Nakamura and H. Ohno, *Chemical Communications (Cambridge, England)*, 2007, 3089-3091.
94. Y. Kohno and H. Ohno, *Chemical Communications (Cambridge, England)*, 2012, **48**, 7119-7130.
95. K. Fujita, D. MacFarlane, M. Forsyth, M. Yoshizawa-Fujita, K. Murata, N. Nakamura and H. Ohno, *Biomacromolecules*, 2007, **8**, 2080-2086.
96. Y. Kohno and H. Ohno, *Australian Journal of Chemistry*, 2011, **65**, 91-94.
97. H. G. Schild, *Progressive Polymer Science*, 1992, **17**, 163-249.
98. T. Tanaka, *Physical Review Letters*, 1978, **40**, 820-824.
99. M. R. Guilherme, R. d. Silva, A. F. Rubira, G. Geuskens and E. C. Muniz, *Reactive and Functional Polymers*, 2004, **61**.
100. X.-Z. Zhang, X.-D. Xu, S.-X. Cheng and R.-X. Zhuo, *Soft Matter*, 2008, **4**.
101. J. Foroughi, G. M. Spinks and G. G. Wallace, *Sensors and Actuators B*, 2011, **155**, 278-284.
102. G. Rupali and D. Amitabha, *Journal of Materials Chemistry*, 2002, **12**.
103. B. Ziólkowski, K. Bleek, B. Twamley, K. J. Fraser, R. Byrne, D. Diamond and A. Taubert, *European Journal of Inorganic Chemistry*, 2012, 5245-5251.
104. D. Schmaljohann, *Advanced Drug Delivery Reviews*, 2006, **58**, 1655-1670.
105. N. Murthy, J. Campbell, N. Fausto, A. Hoffman and P. Stayton, *Bioconjugate Chemistry*, 2003, **14**, 412-419.
106. B. Tasdelen, N. Kayaman-Apohan, O. Guven and B. M. Baysal, *Polymers for Advanced Technologies*, 2004, **15**, 528-532.
107. H. Y. Jiang, S. Kelch and A. Lendlein, *Advanced Materials*, 2006, **18**, 1471-1475.
108. A. Serres, M. Baudys and S. W. Kim, *Pharmaceutical Research*, 1996, **13**, 196-201.
109. Y. H. Kim, Y. H. Bae and S. W. Kim, *Journal of Controlled Release*, 1994, **28**, 143-152.
110. H. Suzuki, *Journal of Intelligent Material Systems and Structures*, 2006, **17**, 1091-1097.
111. Y.-R. Kim, S. Jung, H. Ryu, Y.-E. Yoo, S. Kim and T.-J. Jeon, *Sensors (Basel, Switzerland)*, 2012, **12**, 9530-9550.
112. J. Ä. Mano, *Advanced Engineering Materials*, 2008, **10**, 515-527.

113. I. Idziak, D. Avoce, D. Lessard, D. Gravel and X. X. Zhu, *Macromolecules*, 1999, **32**, 1260-1263.
114. M. R. Guilherme, R. Silva, E. M. Giroto, A. F. Rubira and E. C. Muniz, *Polymer*, 2003, **44**, 4213-4219.
115. M. R. Guilherme, E. A. Toledo, A. F. Rubira and E. C. Muniz, *Journal of Membrane Science*, 2002, **210**, 187-194.
116. X.-Z. Zhang and C.-C. Chu, *Journal of Applied Polymer Science*, 2003, **89**.
117. T. Ueki, A. Yamaguchi, N. Ito, K. Kodama, J. Sakamoto, K. Ueno, H. Kokubo and M. Watanabe, *Langmuir*, 2009, **25**, 8845-8853.
118. Z. Ahmed, E. Gooding, K. Pimenov, L. Wang and S. Asher, *The Journal of Physical Chemistry B*, 2009, **113**, 4248-4304.
119. M. Kano and E. Kokufuta, *Langmuir*, 2009, **25**, 8649-8704.
120. C. de Las Heras Alarcon, S. Pennadam and C. Alexander, *Chemical Society Reviews*, 2005, **34**, 276-285.
121. P. Hiemenz and T. P. Lodge, *Polymer Chemistry*, 2007.
122. L. Shan-Yang, C. Ko-Shao and R. C. Liang, *Polymer*, 1998, **40**, 2619-2624.
123. H. Ringsdorf, J. Venzmer and F. Winnik, *Macromolecules*, 1991, **24**, 1678-1686.
124. P. Mi, L. Y. Chu, X. J. Ju and C. H. Niu, *Macromolecular Rapid Communications*, 2007, **29**, 27-32.
125. U. Rauwald, J. del Barrio, X. Loh and O. Scherman, *Chemical Communications* 2011, **47**, 6000-6002.
126. K. S. Soppimath, L. H. Liu, W. Y. Seow, L. H. Liu, R. Powell, P. Chang and Y. Y. Yang, *Advanced Functional Materials*, 2007, **17**, 355-362.
127. W. Xue and I. Hamley, *Polymer*, 2002, **43**, 3069-3077.
128. D. Y. Teng, J. L. Hou, X. G. Zhang, X. Wang, Z. Wang and C. X. Li, *Journal of Colloid and Interface Science*, 2008, **322**.
129. S. Choi, J. Yoon and T. Park, *Journal of Colloid and Interface Science*, 2002, **251**, 57-63.
130. J. P. Gong, Y. Katsuyama, T. Kurokawa and Y. Osada, *Advanced Materials*, 2003, **15**, 1155-1558.
131. M. E. Harmon, D. Kuckling and C. W. Frank, *Langmuir*, 2003, **19**, 10660-10665.

132. T. Friedrich, B. Tieke, F. J. Stadler and C. Bailly, *Soft Matter*, 2011, **7**, 6590-6597.
133. Muniz EC and G. G., *Macromolecules*, 2001, **14**, 4480-4484.
134. X.-Z. Zhang, D.-Q. Wu and C.-C. Chu, *Biomaterials*, 2004, **25**, 3793-3805.
135. T.-A. Asoh, T. Kaneko, M. Matsusaki and M. Akashi, *Macromolecular bioscience*, 2006, **6**, 959-965.
136. Y. Hao, J. Peng, J. Li, M. Zhai and G. Wei, *Carbohydrate Polymers*, 2009, **77**, 779-784.
137. T. Ueki, Y. Nakamura, A. Yamaguchi, K. Niitsuma, T. P. Lodge and M. Watanabe, *Macromolecules*, 2011, **44**, 6908-6914.
138. J. Hoffmann, M. Plotner, D. Kuckling and W.-J. Fischer, *Sensors and Actuators*, 1999, **77**, 139-144.

# **Chapter 2: Ionic Liquid modulation of swelling and LCST behaviour of *N*-isopropylacrylamide polymer gels**

Simon Gallagher<sup>1</sup>, Andrew Kavanagh<sup>1</sup>, Bartosz Ziolkowski<sup>1</sup>, Larisa Florea<sup>1</sup>, Douglas R. MacFarlane<sup>2</sup>, Kevin J. Fraser<sup>1</sup> and Dermot Diamond<sup>1</sup>.

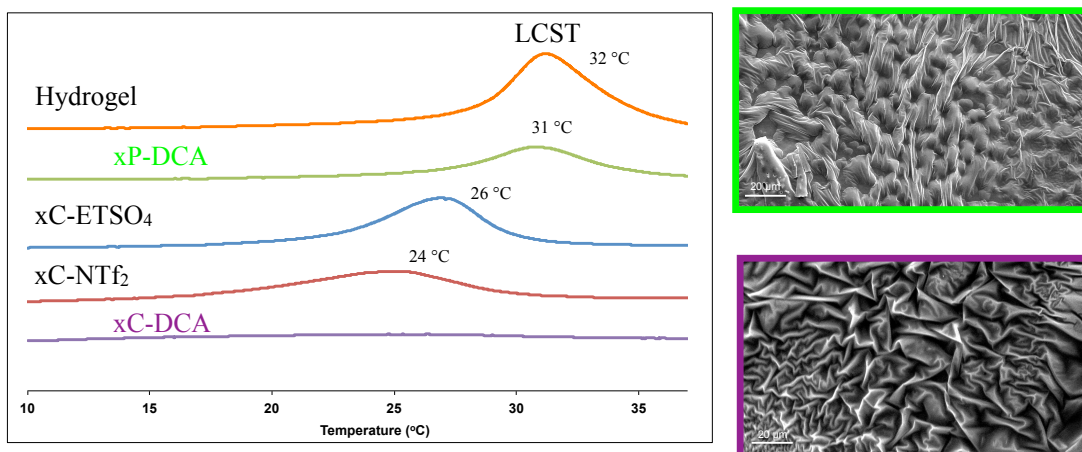
Physical Chemistry Chemical Physics, 3610-3616, **16**, 2014 DOI:

10.1039/C3CP53397B

<sup>1</sup>CLARITY: Centre for Sensor Web Technologies, National Centre for Sensor Research, Dublin City University, Dublin 9, Ireland

<sup>2</sup> School of Chemistry, Monash University, Wellington Road, Clayton, 3800, Vic, Australia

For Supplementary Information see pg. 69



## Abstract

The physicochemical properties of free-standing cross-linked poly(*N*-isopropylacrylamide) (pNIPAAm) gels, generated in the presence of the Ionic Liquids (ILs), 1-ethyl-3-methylimidazolium [C<sub>2</sub>mIm]<sup>+</sup> salts of ethylsulphate [EtSO<sub>4</sub>]<sup>-</sup>, dicyanamide [DCA]<sup>-</sup>, *bis*(trifluoromethylsulfonyl)imide [NTf<sub>2</sub>]<sup>-</sup>, and Trihexyltetradecylphosphonium dicyanamide ([P<sub>6,6,6,14</sub>][DCA]) are described. The Lower Critical Solution Temperature (LCST) of the resulting ionogel was found to vary between 24 – 31 °C. The behaviour of swelling is found to be as high as 31.55% (± 0.47, triplicate) from the initial dehydrated state, while 28.04% (± 0.42, triplicate) shrinking from the hydrated swollen state is observed. For ionogels based on the [DCA]<sup>-</sup> anion an unexpected complete loss of the shrinking behaviour occurs, attributed to water interactions with the nitrile group of the [DCA]<sup>-</sup> anion. Scanning Electron Microscopy also reveals distinct morphological changes, for example [C<sub>2</sub>mIm][EtSO<sub>4</sub>] displays a highly porous, nodule type morphology, efficiently pre-disposed for water uptake.

## 2.1 Introduction

Hydrogels are porous, hydrophilic polymers capable of absorbing large amounts of water. The absorption process leads to bulk swelling, which is dependent on the polymeric chemical structure and the density of cross-linking agents <sup>1</sup>. Stimuli responsive hydrogels can actuate in the swollen state in response to external forces such as applied heat <sup>2</sup>, a change in pH <sup>3</sup> or ionic strength <sup>4</sup>, and incident electromagnetic fields <sup>5</sup>.

One example of a well-studied thermally responsive hydrogel platform is poly(*N*-isopropylacrylamide) (pNIPAAm) <sup>6</sup>. In the presence of an aqueous solution, pNIPAAm displays inverse solubility properties upon heating above and below what is known as its Lower Critical Solution Temperature (LCST) <sup>6, 7</sup>. Experimentally, below the LCST, pNIPAAm is swelled with water through hydration of the polymerized aliphatic chain and hydrogen bonding interactions with its amide moiety, generating a gel network <sup>8</sup>. Above the LCST, the gel collapses along the polymer backbone before water molecules are expelled <sup>9,10</sup>. This process is driven by a changeover from polymer-solvent interactions dominating at low temperatures to polymer-polymer and solvent-solvent interactions and structures dominating at the higher temperatures <sup>6</sup>.

Ionic liquids (ILs) have received much attention over recent years, across diverse disciplines <sup>11-13</sup>. ILs commonly consist of a low symmetry organic cation and an inorganic / organic anion held together via weak electrostatic interactions, which reduce the lattice energy of the salt. This chemical environment (in most cases) contributes to factors such as negligible vapour pressures and generally high thermal stability <sup>14, 15</sup>.

Three dimensional gel networks that are generated with the addition of ILs are known as ionogels. Ionogels are solid-state materials that retain unique IL properties, by allowing the IL to act as the liquid component of the gel. Recent reviews on the area <sup>16-18</sup>, applications such as solid-state electrolytes <sup>19,20</sup> and optical displays <sup>21</sup>, are now available. Popular research avenues to date involving pNIPAAm are to improve the viscoelastic properties of the gels in its various states (initial, swollen and contracted) <sup>22</sup>, modification of the LCST threshold to suit a given application <sup>23</sup> and liquid phase replacement which leads to mechanical issues, when volatile solvents are used <sup>16</sup>. LCST modifications have, however, been found to weaken and even eliminate the thermal sensitivity of the pNIPAAm-based hydrogels due to the introducing of the non-thermosensitive moiety <sup>24</sup>.

The addition of ILs to the pNIPAAm network provides an opportunity to avoid these limitations, leading to stable responsive materials that have improved viscoelastic properties with modified LCST <sup>9</sup>. Compared to a traditional hydrogel, an ionogel was found to have greater thermal actuation, increased viscoelasticity, and induce a downshift in LCST to a more ambient 26 °C <sup>25</sup>. It is clear therefore, that the addition of the IL to the pNIPAAm network provides several advantageous routes toward the development of materials that improve some of the limitations of the traditional hydrogel model.

In this study, we further investigate this triumvirate of interactions, namely, between the polymer network, and both independent liquid phases within the network (ILs and the absorbed water). This is achieved through variation of the IL phase within the material, ranging from water miscible to strongly alkylated materials. As ILs exhibit negligible vapour pressure, these materials have the potential to be employed under open atmospheres with variable LCST. The mechanical and actuation properties of

these thermally responsive ionogel materials are investigated, allowing for their continued functional use in important applications such as drug delivery <sup>26</sup>, polyelectrolytes <sup>27</sup> and actuators <sup>28</sup>.

## 2.2 Experimental

### 2.2.1 Chemical and Materials

*N*-isopropylacrylamide 98% (NIPAAM), *N,N'*-methylenebisacrylamide 99% (MBIS), Aluminum Oxide (activated, basic, Brockmann I), Potassium Bromide and 2,2-Dimethoxy-2-phenylacetophenone 98% (DMPA) were purchased from Sigma Aldrich®, Ireland and used as received. Trihexyltetradecylphosphonium dicyanamide [P<sub>6,6,6,14</sub>][DCA] (CYPHOS IL 105), was kindly donated by Cytec® Industries, Ontario, Canada. 1-ethyl-3-methylimidazolium ethylsulphate [C<sub>2</sub>mIm][EtSO<sub>4</sub>] and 1-ethyl-3-methylimidazolium dicyanamide [C<sub>2</sub>mIm][DCA] were supplied by Merck® industries. 1-ethyl-3-methylimidazolium *bis*(trifluoromethanesulfonyl)imide [C<sub>2</sub>mIm][NTf<sub>2</sub>] was synthesized via an ion-exchange metathesis reaction as previously described <sup>29</sup>. Materials used in this study are shown in Figure 2.1.

All ILs were column cleansed using aluminium (activated, basic, Brockmann I) with dichloromethane used as the mobile phase. This was then removed under vacuum at 40 °C for 48 hrs at 0.1 Torr <sup>30</sup>.

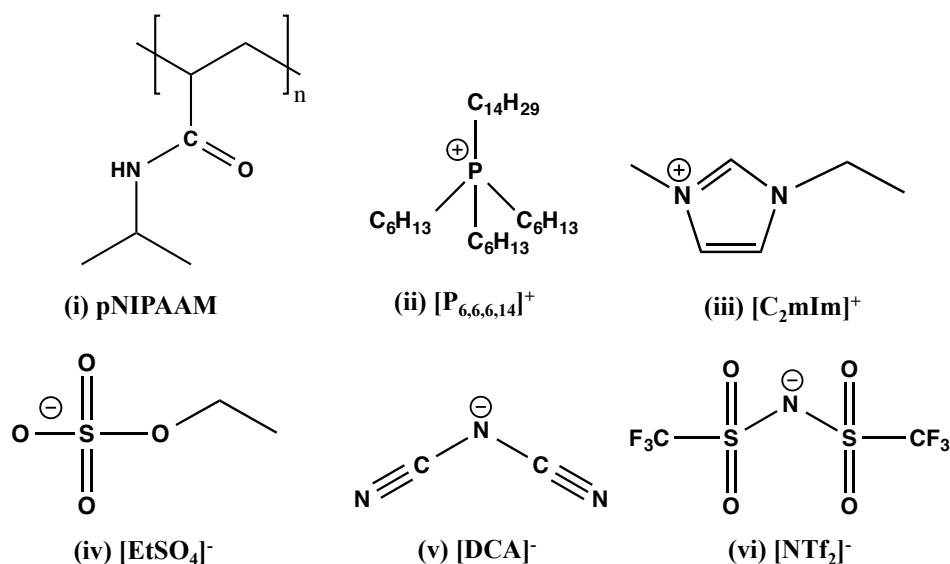


**Figure 2.1.** Molecular structures of the components used for the fabrication of an ionogel; (i) poly(*N*-isopropylacrylamide), (ii) trihexyltetradecylphosphonium  $[P_{6,6,6,14}]^+$ , (iii) 1-ethyl-3-methylimidazolium  $[C_2mIm]^+$ , (iv) ethylsulphate  $[EtSO_4]^-$ , (v) dicyanamide  $[DCA]^-$  and (vi) *bis*(trifluoromethanesulfonyl)imide  $[NTf_2]^-$ .

## 2.2.2 Preparation of Crosslinked Ionogels

pNIPAAAM ionogels were prepared by mixing 400 mg of NIPAAAM monomer (3.53 mmol), 27 mg of MBIS crosslinker (0.18 mmol), 18 mg photoinitiator (DMPA (0.07 mmol) (Final molar ratio 100:5:2), with 1.2 ml of the relevant IL. The mixture was heated to 50 °C and sonicated for 5 min. until a transparent solution was observed. Table 2.1 shows details of the compositions of mixtures studied and their abbreviations. 200  $\mu$ L of the monomeric solution were then dispensed into a Teflon mould, 12 mm in radius, and photo-polymerized using a Connecticut 20 W UV Bond Wand set at 365 nm for 10 min<sup>25</sup>. The synthesized gels were immersed in distilled water at room temperature for 48 hrs and the water was refreshed several times in order to allow the unreacted chemicals to leach out.

## 2.2.3 Preparation of Linear Homopolymers

Preparation of linear pNIPAAm homopolymers were synthesized in the absence of crosslinker MBIS, keeping all other experimental conditions the same as mentioned in the synthesis of crosslinked ionogels (Table 2.1). All resulting polymerized mixtures were dissolved in acetone. Then C-EtSO<sub>4</sub>, C-DCA and the standard hydrogel were precipitated from water at 50 °C, while C-DCA and P-DCA were precipitated from diethyl ether. This process was repeated twice and the purified polymer was then dried in a vacuum oven at 50 °C, for 24 hours.

Sample Abbreviation	IL (1.2ml)	NIPAAm (mmol)	MBIS (mmol)	DMPA (mmol)
xC-EtSO <sub>4</sub>	[C <sub>2</sub> mIm][EtSO <sub>4</sub> ]	3.53	0.18	0.07
C-EtSO <sub>4</sub>	[C <sub>2</sub> mIm][EtSO <sub>4</sub> ]	3.53	-	0.07
xC-NTf <sub>2</sub>	[C <sub>2</sub> mIm][NTf <sub>2</sub> ]	3.53	0.18	0.07
C-NTf <sub>2</sub>	[C <sub>2</sub> mIm][NTf <sub>2</sub> ]	3.53	-	0.07
xC-DCA	[C <sub>2</sub> mIm][DCA]	3.53	0.18	0.07
C-DCA	[C <sub>2</sub> mIm][DCA]	3.53	-	0.07
xP-DCA	[P <sub>6,6,6,14</sub> ][DCA]	3.53	0.18	0.07
P-DCA	[P <sub>6,6,6,14</sub> ][DCA]	3.53	-	0.07

**Table 2.1.** Abbreviations and compositions of samples used in this study.

Details of the characterisation techniques used throughout this work can be found in the accompanying supplementary information.

## 2.3 Results and Discussion

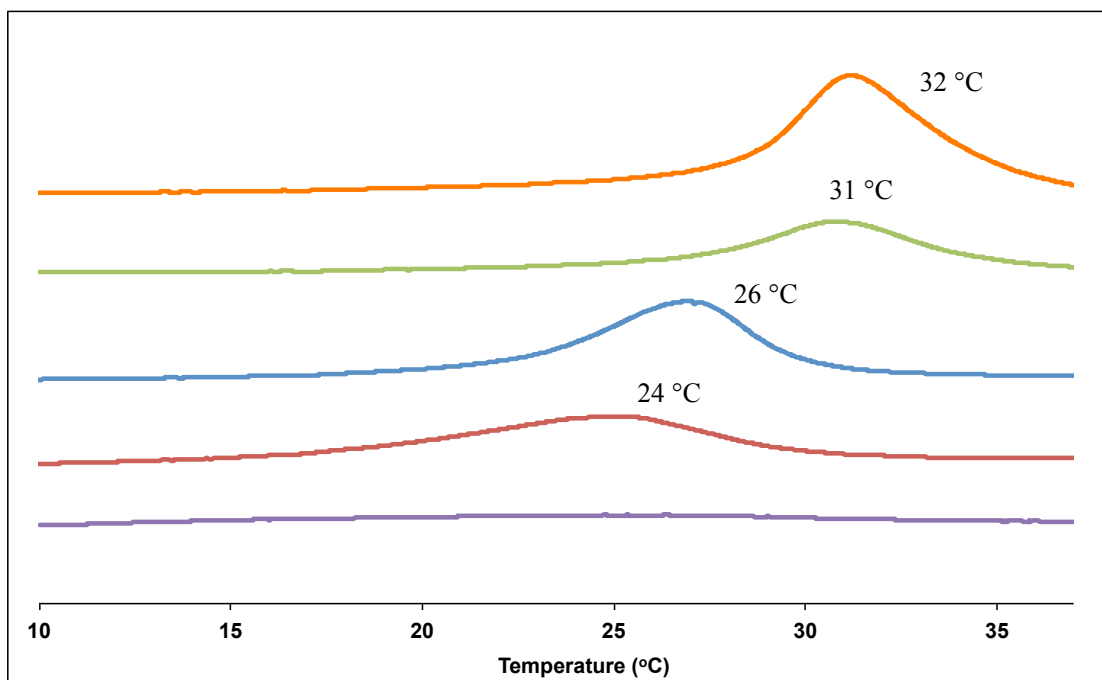
### 2.3.1 Swelling and Shrinking Properties

Table 2.2 is a summary of the individual LCST thresholds, % swelling increase from the dehydrated state and % contractions from the fully hydrated state recorded for all ionogels. As a control experiment, the same parameters for a conventional hydrogel were also recorded.

All samples were prepared using the same monomer, cross-linker and photoinitiator ratios (100:5:2). As with previous studies, the liquid phase is the only experimental variant in all cases<sup>25, 31</sup> thus all physical parameters recorded are a function of the unique chemical environment of the solvent employed.

It was noted that the extent of swelling for most ionogels was greater than the hydrogel control, with xC-NTf<sub>2</sub> being the notable exception. The degree of shrinking was less in all cases however, with xC-EtSO<sub>4</sub> being the exception, and interestingly, no LCST behaviour for ionogels based on the [DCA]<sup>-</sup> anion was apparent.

Figure 2.2 is an overlay of the thermal LCST behaviour for all ionogels and the hydrogel sample, as measured using differential scanning calorimetry. In Figure 2.2, all ionogel LCST parameters obtained were found to deviate from the pNIPAAm literature value (32 °C)<sup>6</sup>, with a range from 24 to 31 °C observed.



**Figure 2.2.** Thermal scans showing endothermic LCST transitions of hydrated pNIPAAm-gels, (orange) hydrogel, (green) xP-DCA, (blue) xC-EtSO<sub>4</sub>, (red) xC-NTf<sub>2</sub>, (purple) xC-DCA.

It has been reported that phase transition temperatures, swelling and shrinking properties of the crosslinked pNIPAAm gels have varied as a function of the isotacticity of their corresponding pNIPAAm homopolymers<sup>32, 33</sup>. The degree of isotacticity of the polymer chain segment is estimated by calculating the proportion of meso (m) and racemo (r) dyads from the region of the backbone methylene protons at ~1.2 – 1.8 ppm. With an increase in isotacticity, interactions among side-chain functional groups of the polymer become stronger, leading to less interaction with water and a decrease in the hydrophilicity of the polymer. This decrease of interactions between the side groups and water has been found to increase swelling, decrease shrinking and lower the pNIPAAm phase transition temperature<sup>32, 33</sup>.

To investigate the effect of the IL on the tacticity of the pNIPAAm chain segment, <sup>1</sup>H NMR spectroscopy was carried out on the corresponding linear homopolymers.

Isotacticity values were determined from Figure SI2-1. The isotacticity ( $m$ ) is calculated by the fraction of the meso dyads equal to the twice of its peak area divided by the peak areas of all three methylene peaks in the region (Table 2.2). In the absence of an IL, the conventional hydrogel with an isotacticity  $m = 47\%$ , is formed in ethanol:water (1:1, v/v). C-EtSO<sub>4</sub> and C-NTf<sub>2</sub> are found to have a higher isotacticity  $m = 52$  and  $50\%$ , respectively. These isotacticity values are found to correlate with the hydrogel phase transition temperature at  $32\text{ }^{\circ}\text{C}$ . This is consistent with previous reports, which have also found higher isotacticity to associate with lower pNIPAAm LCST<sup>33</sup>. Both ionogels studied have a lower LCST than the standard hydrogel, with xC-EtSO<sub>4</sub> and xC-NTf<sub>2</sub> occurring at  $26\text{ }^{\circ}\text{C}$  and  $24\text{ }^{\circ}\text{C}$ , respectively. However, a clear trend in the swelling and shrinking properties of the ionogels cannot be directly correlated with the isotacticity values obtained for the linear polymers. This is due to the effect of the hydrophilic character of the IL itself which clearly can exert a substantial influence on the swelling and shrinking properties of the resulting pNIPAAm ionogels; i.e. water uptake and release behaviour is dominated by the hydrophilicity of the polymerization medium rather than the tacticity of the polymer chain segment formed.

Ionogel	LCST	Tacticity	Swollen	% Swelling	Contracted	% Contraction
	(°C)	(m/r)	Diameter/mm (1)	Increase (a)	Diameter/mm (2)	Decrease (b)
xC-EtSO <sub>4</sub>	26	52/48	15.71 (± 0.18)	30.9 (± 0.69)	11.3 (± 0.26)	28.04 (± 0.42)
xC-NTf <sub>2</sub>	24	50/50	13.9 (± 0.17)	15.83 (± 0.85)	12.02 (± 0.06)	13.51 (± 0.63)
xC-DCA	-	47/53	15.78 (± 0.24)	31.55 (± 0.47)	-	-
xP-DCA	31	45/55	15.3 (± 0.11)	27.5 (± 0.66)	-	-
Hydrogel	32	47/53	14.23 (± 0.21)	18.6 (± 0.92)	11.47 (± 0.2)	19.38 (± 0.72)

**Table 2.2.** 1: Increase in disc diameter (a) from dehydrated state to fully hydrated state at T = 20 °C (triplicate). 2: Decrease in disc diameter (b) from fully hydrated state (a) when T = 40 °C (triplicate). Initial diameter in the dehydrated state is 12 mm for all gels. Tacticity determined by <sup>1</sup>H NMR at 120 °C (meso (m) and racemo (r) dyads).

Infrared Spectroscopy has been used successfully to determine the correlation between the LCST behaviour and amide interactions via the intramolecular hydrogen bonded N-H band (1551 cm<sup>-1</sup>)<sup>32,33</sup>. These interactions were studied on the ionogels when hydrated, with respect to the standard hydrogel (initial and hydrated states). Table 2.3 provides a summary of the IR analysis of all hydrated ionogels and the spectra can be found in Figure SI2-2.

The amide II band representing the N-H group of the standard hydrogel is located at 1550 cm<sup>-1</sup> (Figure SI2-1), while the hydrated hydrogel shows a shift of 5 cm<sup>-1</sup> to 1555 cm<sup>-1</sup> with respect to the dry hydrogel. However, in contrast, the ionogels show a much larger shift when hydrated, with xC-EtSO<sub>4</sub> and xC-NTf<sub>2</sub> undergoing a shift of 10 and 12 cm<sup>-1</sup>, respectively. With a LCST of 24 °C, xC-NTf<sub>2</sub>, shows a greater shift than xC-EtSO<sub>4</sub>, which has a LCST of 26 °C. It has been found that addition of the IL leads to weakening of hydrogen bonding between polymer and water molecules<sup>9</sup>. The results in Figure SI2-2, suggest that, when hydrated, the ILs increased interaction with the

amide group of the polymer results in a decrease in polymer/ water interactions leading to less energy input needed to allow a hydrophobic collapse, and therefore a lower temperature to reach the phase transition.

<b>Sample</b>	<b><math>\nu</math> (cm<sup>-1</sup>)</b>	<b><math>\Delta \nu</math> (cm<sup>-1</sup>)</b>	<b>LCST (°C)</b>
Hydrogel	1550	-	-
Hydrated Hydrogel	1555	<b>5</b>	<b>32</b>
Hydrated xC-EtSO <sub>4</sub>	1560	<b>10</b>	<b>26</b>
Hydrated xC-NTf <sub>2</sub>	1562	<b>12</b>	<b>24</b>
Hydrated xC-DCA	1560	<b>10</b>	-
Hydrated xP-DCA	1550	-	<b>31</b>

**Table 2.3.** Summary of the wavenumber positioning from infrared spectroscopy for the amide II band of various hydrated gels.

It is notable that there is a shift in the amide II band for xC-DCA, however, it does not show an LCST transition, nor any shrinking behaviour. While xP-DCA does not display any shift in the amide II band, but yet also exhibits no shrinking behaviour. This implies that there is more to the LCST than the amide interactions suggest. To investigate this and the high variation in swelling and shrinking behaviour further, a deeper understanding of the thermally dependent physicochemical processes is required, beginning with ionogels of the [DCA]<sup>-</sup> anion.

## 2.4 Ionogels based on the [DCA]<sup>-</sup> anion

In order to gain an insight into the liquid phase activity of the ionogel, we performed an independent physicochemical study centred on IL/H<sub>2</sub>O interactions over the temperature range corresponding to the LCST behaviour. Karl-Fischer, thermal viscosity and density analysis showed [C<sub>2</sub>mIm][DCA] exhibited high water miscibility, manifesting in a high viscosity change (94.53 %, Figure 2.3) but little deviation in density at 20 °C (Tables SI2-1, SI2-2).

As the ionogel is essentially anhydrous at the onset, there is large chemical potential for swelling in the presence of water, with the gel swelling by 31.55 % from the initial dehydrated state (See Table 2.2). The ionogel exhibited no LCST transition and did not contract as the temperature was raised which is in accordance with the DSC data that shows that no transition over the temperature range 10 - 50 °C.

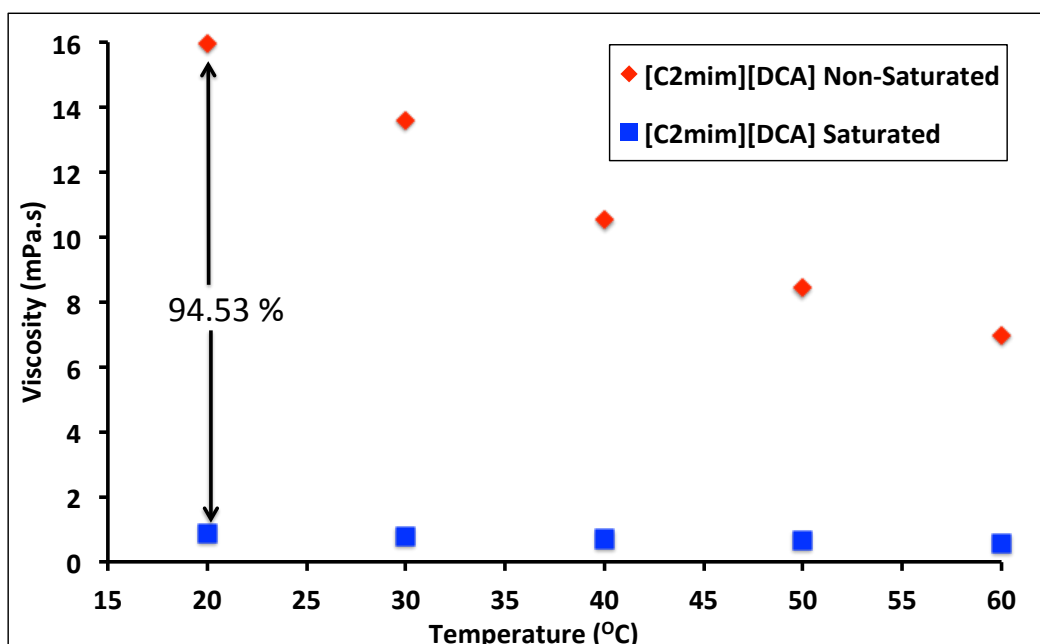


**Figure 2.3.** Viscosity values obtained for [C<sub>2</sub>mIm][DCA], dry (red) and water saturated (blue) as a function of temperature.

To investigate this phenomenon further, a more hydrophobic ionogel based on  $[DCA]^-$  was prepared. In the  $[P_{6,6,6,14}]^+$  cation the phosphonium charge centre is well shielded by long-chain alkyl groups, which leads to less interaction with water molecules<sup>34</sup>. Not surprisingly therefore,  $[P_{6,6,6,14}][DCA]$  is less miscible with water (mole fraction 0.43  $x_w$ , Table SI2-1), leading to little change in viscosity and density at 20 °C (Table SI2-2). The xP-DCA ionogel was found to swell by 27.5 % from the initial dehydrated state, but like xC-DCA, no contraction occurred above the LCST (31 °C) (Table 2.2).

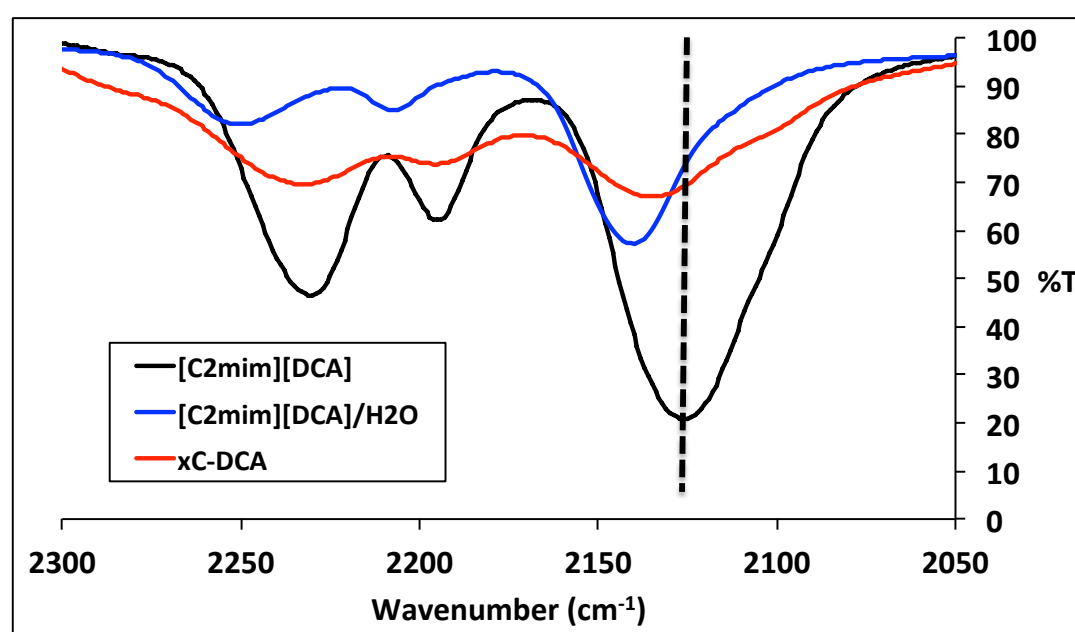


**Figure 2.4.** Infra-red spectroscopy recorded between 2050-2300  $cm^{-1}$  of  $[C_2mIm][DCA]$  (black),  $[C_2mIm][DCA]: H_2O, 1:1 (v/v)$  (blue), and xC-DCA (red).

It appears that this unusual behaviour is an anionic effect, and given the nature of the materials under question, vibrational spectroscopy was again used to examine interactions at the molecular level. The nitrile stretch of the  $[DCA]^-$  anion is well known to absorb in the infrared region, with the absorbance wavelength sensitive to strong molecular interactions, such as metal ion co-ordination<sup>35</sup>. Figures 2.4 and 2.5

provide a summary of the individual IR spectra for both  $[DCA]^-$  based ionogels in the nitrile region.

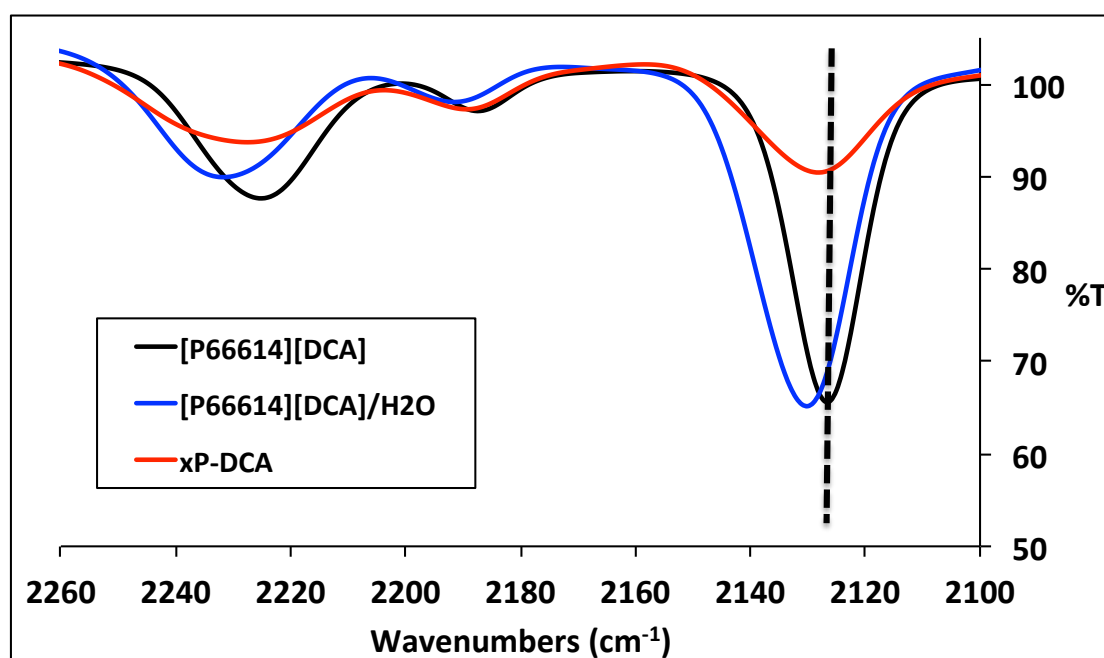


**Figure 2.5.** Infra-red spectroscopy recorded between 2100-2260  $cm^{-1}$  of  $[P_{66614}][DCA]$  (black),  $[P_{66614}][DCA]:H_2O$ , 1:1 (v/v) (blue), and xP-DCA (red).

Analysis of the IL, the IL/water mixture and the ionogel (IL/polymer) was performed in each case, to investigate the IL/anion interactions with both water and the polymer. In Figure 2.4, the asymmetric nitrile stretch for  $[C_2mIm][DCA]$  is located at 2127  $cm^{-1}$ , whilst with the dry ionogel (IL/polymer) and IL/ $H_2O$  (1:1 v/v) stretches are shifted significantly by 10 and 18  $cm^{-1}$ , respectively.

The nitrile stretch of  $[P_{6,6,6,14}][DCA]$  is shown at 2128  $cm^{-1}$ , with the respective IL/polymer and IL/ $H_2O$  interactions inducing spectral shifts to a lesser degree (most likely due to the increased IL hydrophobicity in this case).

From these findings, it can be postulated that dominating molecular interactions between the  $[DCA]^-$  anion and its co-constituents, mainly water, serve to act as a

competing stabilising influence, thereby inhibiting the LCST contraction mechanism. Consequently, no shrinking of the ionogel is observed, as the absorbed water is retained and the swollen state maintained at elevated temperatures (up to 45 °C). A summary of the wavenumber positioning of the asymmetric nitrile stretch of various [DCA]<sup>-</sup> IR spectral shifts are presented in Table 2.4.

An interesting aspect of pNIPAAm is its contrasting surface topographies as the preparation solvent is varied<sup>36</sup>. Distinct features on the micron scale have been reported with respect to the formulation solvent used<sup>37</sup>, and with the use of pore-forming agents, such as poly(ethyleneglycol)<sup>38</sup>. In Figure SI2-3 illustrates the changes in surface morphology associated with water uptake and swelling in a standard hydrogel<sup>25</sup>.

Sample	$\nu$ (cm <sup>-1</sup> )	$\Delta \nu$ (cm <sup>-1</sup> )
[C <sub>2</sub> mIm][DCA]	2127	-
[C <sub>2</sub> mIm][DCA]: H <sub>2</sub> O (1:1, (v/v))	2145	<b>18</b>
xC-DCA	2137	<b>10</b>
[P <sub>6,6,6,14</sub> ][DCA]	2128	-
[P <sub>6,6,6,14</sub> ][DCA]: H <sub>2</sub> O mixture	2131	<b>3</b>
xP-DCA	2130	<b>2</b>

**Table 2.4.** Summary of the wavenumber positioning from infrared spectroscopy for the asymmetric nitrile stretch of various [DCA]<sup>-</sup> IL samples.

Figure 2.6 demonstrates similar solvent dependent behaviour for the [DCA]<sup>-</sup> ionogels studied, in their swollen states. The effect of the IL is clear as the xC-DCA sample (water miscible, 31.55% swelling) exhibits a saturated pore-free exterior, in contrast

to the xP-DCA sample ( $0.428 x_w$ , 27.5% swelling), which appears less stressed, more fibrous, with visible signs of pores even after hydration.

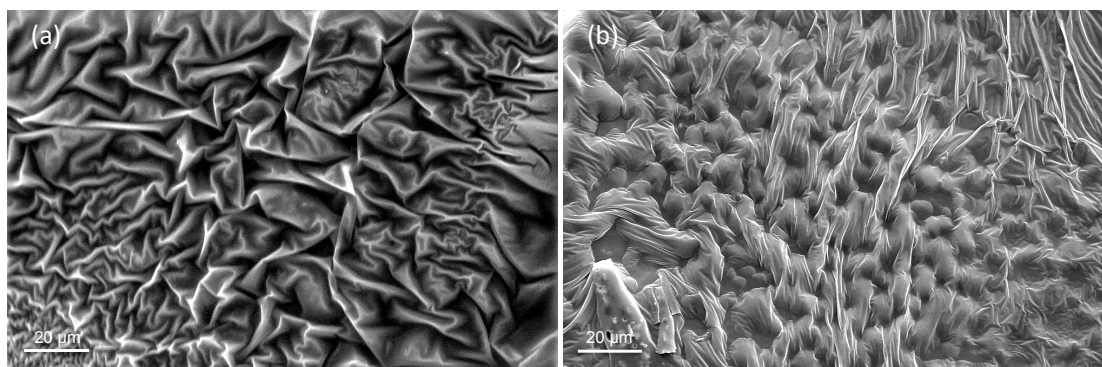


**Figure 2.6.** SEM images of swollen ionogels based on [DCA]<sup>-</sup>. (a) xC-DCA and (b) xP-DCA.

## 2.5 Enhanced Viscoelastic Ionogels

As previously described, a primary research avenue of pNIPAAm explored thus far is the improvement of the bulk viscoelastic properties, which have been shown to be unfavourable in some circumstances, due to the volatility of the gelled liquid phase<sup>39</sup>. Co-polymerised ionic surfactants have been shown to stabilise the viscoelasticity of pNIPAAm at a fixed cross-linking density through micellular aggregation,<sup>4, 40</sup>

For viscoelastic materials, the general mechanical properties are often characterised via the storage and loss moduli<sup>31</sup>. The storage modulus is related to the elastic energy of the hydrated gel as it contracts, whilst the loss modulus is the energy dissipated as heat flow from the gel<sup>41</sup>. The viscoelastic properties of xC-EtSO<sub>4</sub>, xC-NTf<sub>2</sub>, and a hydrogel equivalent are presented as a function of time and temperature in Figures 2.7 and SI2-4.

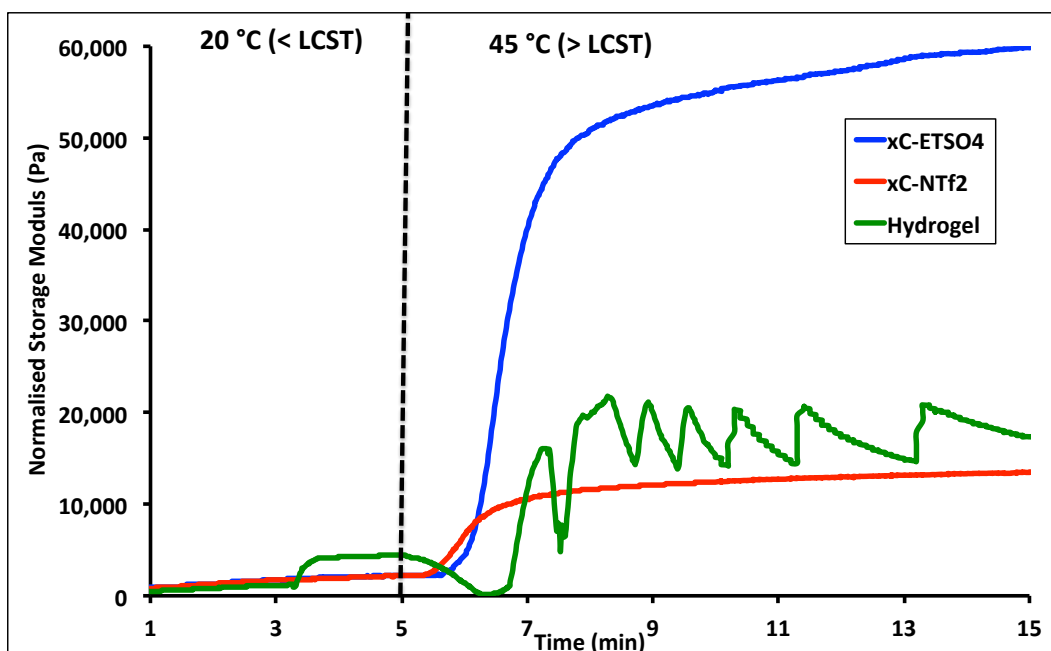


**Figure 2.7.** Storage modulus of (blue) xC-EtSO<sub>4</sub>, (red) xC-NTf<sub>2</sub>, and hydrogel (green), plotted against time during a temperature ramp from 20 °C to 45 °C at 20 °C / min.

Initially (0 to 5 min), all samples are in their hydrated states below the LCST (20 °C), and the shear frequency is kept constant. It can be seen from Figure 2.7 that both ionogels exhibit a stable mechanical response over this time period. Under the same experimental conditions the brittle hydrogel's mechanical stability is sporadic and fluctuates across a ~3,000 Pa range. At  $t = 5 \text{ min}$ , the sample plate is heated from 20 to 45 °C, ensuring that any thermally sensitive processes related to the LCST are completed. As the temperature is increased, the storage modulus increases as the polymer contracts and its mechanical energy is stored internally in response to the applied stress. The sharp peaks produced by the hydrogel are due to the instrument readjusting the normal force on the sample. As the sample shrinks and changes modulus the reaction force of the sample drops and the instrument corrects for this (as described in the experimental section – see ESI) <sup>40, 44</sup>. The increase in the storage modulus of the hydrogel is erratic at higher temperatures, which reflects the material's inability to maintain the stored energy as it contracts, indicative of a material with

fragile mechanical stability<sup>43</sup>. In contrast, the ionogel responses for the same experimental parameters plateau smoothly. Thus, the ionogel template yields a more energetically stable contracted gel compared to the hydrogel under these conditions. The corresponding loss moduli of both gel platforms were found to correlate with the temperature dependent storage moduli features (Figure SI2-4). Thus, from the rheological effects described, both ionogels xC-EtSO<sub>4</sub> and xC-NTf<sub>2</sub> display improved viscoelastic properties compared to the hydrogel. Significantly, this means that a relatively high density of cross-linking sites can exist within a yet flexible ionogel material. For the experiment depicted in Figure 2.7, the rheological features are consistently higher for xC-EtSO<sub>4</sub> over xC-NTf<sub>2</sub>, indicating superior viscoelastic traits, which correlates well with the observed swelling and contracting behaviour (Table 2.2).

To differentiate the deviation in ionogel behaviour further, Raman spectroscopy was used to investigate the symmetrical  $\text{SO}_3^-$  stretch commonly found in [C<sub>2</sub>mIm][EtSO<sub>4</sub>] (Figure SI2-5). The sulfoxide stretch of the IL is located at 1022 cm<sup>-1</sup><sup>45</sup>. The Raman spectrum of an aqueous phase aliquot released via LCST actuation contains the same sulfoxide stretch, although it is slightly shifted to 1025 cm<sup>-1</sup> (Figure SI2-5). Also, in 1:1 (v/v) mixtures of H<sub>2</sub>O and IL, Karl-Fischer analysis shows [C<sub>2</sub>mIm][EtSO<sub>4</sub>] to be miscible with water, while [C<sub>2</sub>mIm][NTf<sub>2</sub>] is found to contain a mole fraction of 0.22  $x_w$  of water (Table SI2-1). This provides evidence that [C<sub>2</sub>mIm][EtSO<sub>4</sub>], is expelled with the liquid phase through hydrogen bonding as the xC-EtSO<sub>4</sub> undergoes LCST phase transition. The release of IL, as well as absorbed water, causes a further decrease in polymer-solvent interactions, and an increase in polymer-polymer interactions, leading to a more compact format of the gel. In

contrast, no evidence of  $[\text{C}_2\text{mIm}][\text{NTf}_2]$  was found in the released aqueous phase from the  $\text{xC-NTf}_2$  ionogel (Figure SI2-6).

Figure 2.8 shows the morphology of the ionogels  $\text{xC-NTf}_2$  and  $\text{xC-EtSO}_4$  in their initial dehydrated and swollen states. Similar to the results presented in Figure 2.6, the presence of different ILs in the polymer matrix appears to have a significant effect on the surface topography.

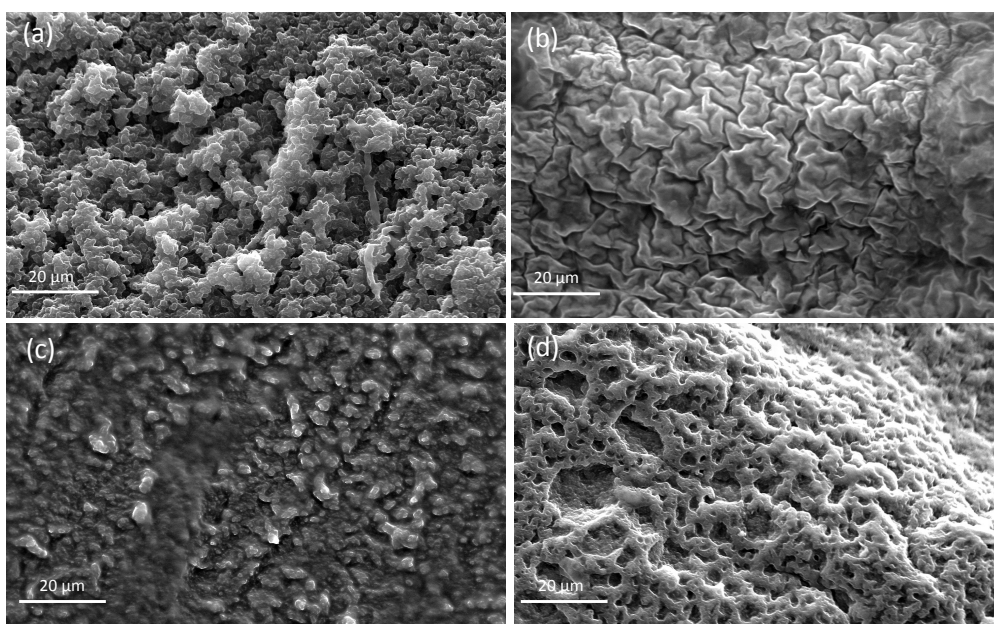


**Figure 2.8.** SEM images of  $\text{xC-EtSO}_4$ , after (a) polymerisation and (b) after swelling, and  $\text{xC-NTf}_2$ , after (c) polymerisation and (d) after swelling. Both ionogels were swelled in deionised water.

Figure 2.8 (a) and (c) show clear changes in the non-hydrated ionogel surface as the solvent used to prepare the ionogel is varied. The ionogel based on  $[\text{C}_2\text{mIm}][\text{EtSO}_4]$  displays a highly porous, nodule type morphology, efficiently pre-disposed for water uptake, which changes further as it swells (Figure 2.8, (b)). The ionogel based on  $[\text{C}_2\text{mIm}][\text{NTf}_2]$  exhibits hydration dependent surface features (Figure 2.8, (d)), although the topography is less nodular when non-hydrated and is less compact in the swollen state.

The morphology in the dehydrated state of both ionogels indicates that the polymer is obtained in its more collapsed state (globular structure) rather than its common expanded coil. This is found to favour shrinking behaviour, which is supported by results found in Table 2.2 (% contraction).

## 2.6 Conclusion

Compared to a traditional free-standing pNIPAAm hydrogel the LCST of a range of imidazolium and phosphonium based ionogels varied between 24 – 31 °C. Each IL dictates a unique LCST value, xP-DCA being the highest (31 °C) and xC-NTf<sub>2</sub> being the lowest (24 °C). Actuation behaviour of the ionogel based on [C<sub>2</sub>mIm][EtSO<sub>4</sub>] was found to be as large as 30.09% (± 0.69, triplicate) from the hydrated swollen state, while contraction from the swollen hydrated state was found to be 28.04% (± 0.42, triplicate).

For ionogels based on the [DCA]<sup>-</sup> anion an unexpected loss of the contraction behaviour occurs. Competing interactions involving the [DCA]<sup>-</sup> anion with water (specifically the nitrile stretch) were found to prevent a LCST triggered contraction, despite the initial high levels of swelling ([C<sub>2</sub>mIm][DCA]: 31.55% ± 0.47, triplicate).

Polymer rheology confirmed that whilst the actuation behaviour varies, the viscoelasticity of these ionogels is far greater and more stable than the hydrogel equivalent at the same cross-linker density. At this concentration of crosslinking (5 mol %), a flexible material is still obtained providing a suitable environment for combining high mechanical stability and actuation.

Scanning Electron Microscopy also reveals distinct morphological changes between ionogels and a standard hydrogel, for example [C<sub>2</sub>mIm][EtSO<sub>4</sub>] displays a highly porous, nodule type morphology, efficiently pre-disposed for water uptake.

As a result of this study it is clear that there are well defined interactions between the polymer network, ILs and water that determine the “tailorability” of the ionogels such as the LCST and actuation behaviour.

## Acknowledgements

S.G. acknowledges support under the Marie Curie IRSES- MASK project (PIRSES-GA-2010-269302), Science Foundation Ireland grant (07/CE/I1147), Marie Curie Actions re-integration grant PIRG07-GA-2010-268365 and the Irish Research Council. D.R.M. is grateful to the Australian Research Council for his Federation and Australian Laureate Fellowships.

## 2.7 References

1. G. Gulten and G. Aysegul, *Industrial & Engineering Chemistry Research*, 2011, **50**.
2. M. R. Guilherme, R. d. Silva, A. F. Rubira, G. Geuskens and E. C. Muniz, *Reactive and Functional Polymers*, 2004, **61**.
3. J. Hee Kyung, K. So Yeon and L. Young Moo, *Polymer*, 2001, **42**.
4. T. Friedrich, B. Tieke, F. J. Stadler and C. Bailly, *Soft Matter*, 2011, **7**, 6590-6597.
5. M. Molina, C. Rivarola, M. Miras, D. Lescano and C. Barbero, *Nanotechnology*, 2011, **22**, 245504.
6. H. G. Schild, *Progressive Polymer Science*, 1992, **17**, 163-249.
7. T. Ueki and M. Watanabe, *Chemistry Letters*, 2006, **35**.
8. T. Ueki, A. Yamaguchi, N. Ito, K. Kodama, J. Sakamoto, K. Ueno, H. Kokubo and M. Watanabe, *Langmuir : the ACS journal of surfaces and colloids*, 2009, **25**, 8845-8853.

9. P. Reddy and P. Venkatesu, *The Journal of Physical Chemistry*, 2011, **115**, 4752-4759.
10. Z. Ahmed, E. Gooding, K. Pimenov, L. Wang and S. Asher, *The journal of physical chemistry. B*, 2009, **113**, 4248-4304.
11. K. Fukumoto, M. Yoshizawa and H. Ohno, *Journal of the American Chemical Society*, 2005, **127**, 2398-2399.
12. K. R. Seddon, A. Stark and M.-J. Torres, *Pure Applied Chemistry*, 2000, **72**, 2275-2287.
13. M.-C. Tseng and Y.-H. Chu, *Chemical communications (Cambridge, England)*, 2010, **46**, 2983-2985.
14. L. Vidal, M.-L. Riekkola and A. Canals, *Analytica chimica acta*, 2012, **715**, 19-60.
15. P. Wasserscheid and T. Welton, *Wiley Online Library*, 2003, **1**.
16. T. Ueki and M. Watanabe, *Macromolecules*, 2008, **41**, 11.
17. A. Kavanagh, R. Byrne, D. Diamond and K. J. Fraser, *Membranes*, 2012, **2**, 16-55.
18. J. Le Bideau, L. Viau and A. Vioux, *Chemical Society reviews*, 2011, **40**, 907-932.
19. A. Kavanagh, R. Copperwhite, M. Oubaha, J. Owens, C. McDonagh, D. Diamond and R. Byrne, *Journal of Materials Chemistry*, 2011, **21**, 8687.
20. D. Khodagholya, V. F. Curto, K. J. Fraser, M. Gurfinkel, R. Byrne, D. Diamond, G. G. Malliaras, F. Benito-Lopez and R. M. Owens, *Journal of Materials Chemistry*, 2012, **22**, 4440-4443.
21. K. Lunstroot, K. Driesen, P. Nockemann, K. Van Hecke, L. Van Meervelt, C. Görrler-Walrand, K. Binnemans, S. Bellayer, J. Le Bideau and A. Vioux, *Chemistry Materials*, 2006, **18**, 5711-5715.
22. K. Anseth, C. Bowman and L. Brannon-Peppas, *Biomaterials*, 1996, **17**, 1647-1704.
23. H.-N. Lee and T. Lodge, *The Journal of Physical Chemistry. B*, 2011, **115**, 1971-1977.
24. W. Xue and I. Hamley, *Polymer*, 2002, **43**.
25. S. Gallagher, A. Kavanagh, L. Florea, D. R. MacFarlane, K. Fraser, J. and D. Diamond, *Chemical Communications*, 2013, **49**, 4613-4615.
26. F. Yhaya, J. Lim, Y. Kim, M. Liang, A. M. Gregory and M. H. Stenzel, *Macromolecules*, 2011, **44**, 8433-8445.
27. S. Amajjahe, S. Choi, M. Munteanu and H. Ritter, *Angewandte Chemie (International ed. in English)*, 2008, **47**, 3435-3442.

28. H. Suzuki, *Journal of Intelligent Material Systems and Structures*, 2006, **17**.
29. L. Li, J. Wang, T. Wu and R. Wang, *Chemistry (Weinheim an der Bergstrasse, Germany)*, 2012.
30. M. Earle, J. Esperanca, M. Gilea, J. Lopes, L. Rebelo, J. Magee, K. Seddon and J. Widegren, *Nature*, 2006, **439**, 831-834.
31. B. Ziolkowski, Z. Ates, S. Gallagher, R. Byrne, A. Heise, K. Fraser, J. and D. Dermot, *Macromolecular Chemistry and Physics*, 2013.
32. C. Biswas, N. Vishwakarma, V. Patel, A. Mishra, S. Saha and B. Ray, *Langmuir : the ACS journal of surfaces and colloids*, 2012, **28**, 7014-7022.
33. C. Biswas, V. Patel, N. Vishwakarma, A. Mishra, S. Saha and B. Ray, *Langmuir : the ACS journal of surfaces and colloids*, 2010, **26**, 6775-6782.
34. Z. Xian-Zheng, Y. Yi-Yan, C. Tai-Shung and M. Kui-Xiang, *Langmuir*, 2001, **17**.
35. L. Shan-Yang, C. Ko-Shao and R. C. Liang, *Polymer*, 1998, **40**, 2619-2624.
36. M. S. S. N. Catarina, J. C. Pedro, G. F. Mara and A. P. C. Joso, *The Journal of Chemical Thermodynamics*, 2011, **43**.
37. L. Ficke and J. Brennecke, *The journal of physical chemistry. B*, 2010, **114**, 10496-10501.
38. Z. Xian-Zheng, X. Xiao-Ding, C. Si-Xue and Z. Ren-Xi, *Soft Matter*, 2008, **4**.
39. A. Suk-kyun, M. K. Rajeswari, K. Seong-Cheol, S. Nitin and Z. Yuxiang, *Soft Matter*, 2008, **4**.
40. S. Hashmi, A. GhavamiNejad, F. O. Obiweluzor, M. Vatankhah-Varnoosfaderani and F. J. Stadler, *Macromolecules*, 2012, **45**, 9804-9815.
41. J. P. Gong, Y. Katsuyama, T. Kurokawa and Y. Osada, *Advanced Materials*, 2003, **15**.
42. T. Friedrich, B. Tieke, F. J. Stadler, C. Bailly, T. Eckert and W. Richtering, *Macromolecules*, 2010, **43**, 9964-9971.
43. P. C. Hiemenz and T. P. Lodge, *Polymer Chemistry, Second Edition*, CRC Press; 2 edition, Florida, 2007.
44. B. Ziółkowski, Z. Ates, S. Gallagher, R. Byrne, A. Heise, K. J Fraser and D. Diamond, *Macromolecular Chemistry and Physics (accepted)*, 2013, **214**, 787-796.
45. J. Kiefer, J. Fries and A. Leipertz, *Applied spectroscopy*, 2007, **61**, 1306-1311.

## **Chapter 2: Supporting Information**

# **Ionic Liquid modulation of swelling and LCST behaviour of *N*-isopropylacrylamide polymer gels**

Simon Gallagher<sup>1</sup>, Andrew Kavanagh<sup>1</sup>, Bartosz Ziolkowski<sup>1</sup>, Larisa Florea<sup>1</sup>, Douglas  
R. MacFarlane<sup>2</sup>, Kevin J. Fraser<sup>1</sup> and Dermot Diamond<sup>1</sup>.

Physical Chemistry Chemical Physics, 3610-3616, **16**, 2014 DOI:

10.1039/C3CP53397B

<sup>1</sup>CLARITY: Centre for Sensor Web Technologies, National Centre for Sensor  
Research, Dublin City University, Dublin 9, Ireland

<sup>2</sup> School of Chemistry, Monash University, Wellington Road, Clayton, 3800, Vic,  
Australia

# Analytical Techniques

## Karl Fischer Titration Analysis

The IL and the water phases 1:1 wt. %, were vigorously agitated in glass vials and allowed to reach the saturation equilibrium by the separation of both phases for at least 72 hours. This period, as well as in previous studies <sup>1, 2</sup> proved to be the minimum time required guaranteeing a complete separation of the two phases and that no further variations in water mole fractions occurred for longer periods.

The miscibility of water in the IL-rich phase was determined, where the samples were taken from the vials using glass syringes maintained dry and at the same temperature of measurements. All measurements of the miscibility of water with the ILs in question were performed at ambient temperature and pressure conditions, using a Mettler-Toledo® V20 Volumetric Karl Fischer Titrator.

## Density

Densities were measured using a DMA-500 from Anton-Paar® (Australia). The density meter uses the “oscillating U-tube principle” <sup>3</sup> to determine the density of the liquid. Measurements were performed at atmospheric pressure from 20 to 60 °C for both neat and water-saturated ILs.

## Viscosity

Viscosity measurements were performed at atmospheric pressure in the temperature range 20 to 60 °C on both neat and water-saturated ILs using an Anton-Paar® AMVn Viscometer, which employs a falling ball technique <sup>4</sup>.

## Differential Scanning Calorimeter

Differential Scanning Calorimetry (DSC) was performed using the Perkin Elmer® Pyris 1 Calorimeter. Individual scans were performed in the temperature range from 10 to 50 °C at a scan rate of 5 °C per minute. Thermal scans below room temperature were calibrated with the cyclohexane solid-solid transition and melting point at – 87.0 °C and 6.5 °C, respectively. Thermal scans above room temperature were calibrated using indium, tin and zinc with melting points at 156.60, 231.93 and 419.53 °C, respectively. Transition temperatures were taken from the peak maximum of the thermal transition.

## Ionogel Diameter Measurements

Each polymerized ionogel was placed in de-ionized water at 20 °C for 24 hours and the swelling behaviour recorded. Next, the gels were then placed in de-ionized water at 45 °C for 1 min. This temperature ensures the swollen hydrated ionogels undergo the LCST phase transition (as individually measured using DSC) <sup>5</sup>.

All measurements were performed using a Mitutoyo® digital micrometer calibrated to a resolution of 1 µm.

## NMR of Linear Homopolymers

<sup>1</sup>H NMR spectra of purified linear polymers were recorded at 120 °C

C on a 400 MHz Bruker NMR in DMSO-*d*<sup>6</sup> solvent and are reported in parts per million (δ) from the residual solvent peak. The meso diad % of the polymer samples were calculated from the backbone methylene proton peaks of the homopolymers.

## Rheometry

All measurements were performed on an Anton-Paar® MCR301 rheometer equipped with a steel bottom plate. Initially, all polymerized ionogels (12 mm diameter) were immersed in deionized water for 24 hours. The swollen gels were then analysed for changes in the loss and storage moduli through the LCST by using a temperature step program. All the swollen ionogels were analysed in oscillation mode with a parallel plate PP15 tool 15 mm diameter at 0.05 % strain and frequency of 10 Hz. The data points were collected every second and the following temperature ramp was applied: isotherm at 20 °C below the measured LCST for 5 min, increase to 45 °C (20 °C /min)<sup>5</sup>.

## Infra-red Spectroscopy

Fourier transformed Infrared (FT-IR) measurements were taken with a Perkin Elmer Spectrum GX FT-IR System® instrument equipped with an attenuated total reflectance accessory in transmittance mode from 1000 to 3000  $\text{cm}^{-1}$  at 20 scans with 2  $\text{cm}^{-1}$  resolution. For solution samples, a droplet was transferred onto an ATR crystal, while ionogel samples were pressed into a KBr pellet.

## Raman Spectroscopy

Raman spectroscopy was performed using a Perkin Elmer® Raman Station 400F. Measurements were taken from 800 to 3200  $\text{cm}^{-1}$  at 20 scans with 2  $\text{cm}^{-1}$ .

## Scanning Electron Microscopy

Ionogel and hydrogel were imaged using scanning electron microscopy (SEM) performed on a Carl Zeiss EVOLS 15 system at an accelerating voltage of 26.11 kV. Gold Sputtering of all gels was performed on a Polaron® SC7640 Auto/Manual High Resolution Sputter Coater. All gels were coated with a 10 nm gold layer, under the following conditions: Voltage 1.5 kV, 15 mA for 2 minutes at a coating rate of 5 nm/min.

## NMR of Ionic Liquids

1-Ethyl-3-Methylimidazolium Ethylsulphate [C<sub>2</sub>mIm][EtSO<sub>4</sub>]

<sup>1</sup>H NMR,  $\delta_{\text{H}}$  (400 MHz; CD<sub>3</sub>CN): 1.14 (t, 3H, CH<sub>3</sub>), 1.34 (t, 3H, CH<sub>3</sub>), 3.73 (s, 3H, CH<sub>3</sub>), 3.95 (m, 2H, CH<sub>2</sub>), 4.05 (m, 2H, CH<sub>2</sub>), 4.69 (s, H, CH), 7.24 (d, H, CH), 7.32-7.33 (d, H, CH) ppm.

1-Ethyl-3-Methylimidazolium *bis*(trifluoromethanesulfonyl)imide [C<sub>2</sub>mIm][NTf<sub>2</sub>]

<sup>1</sup>H NMR,  $\delta_{\text{H}}$  (400 MHz; CD<sub>3</sub>CN): 1.54 (t, 3H, CH<sub>2</sub>CH<sub>3</sub>), 3.93 (s, 3H, N-CH<sub>3</sub>), 4.26 (q, 2H, N-CH<sub>2</sub>), 7.61 (m, 2H, H, CH and H, CH), 8.88 (s, 1H, CH) ppm.

1-Ethyl-3-Methylimidazolium Dicyanamide [C<sub>2</sub>mIm][DCA]

<sup>1</sup>H NMR  $\delta_{\text{H}}$  (400 MHz; CD<sub>3</sub>CN): d 1.42 (t, CH<sub>3</sub>), 3.84 (s, n-CH<sub>3</sub>), 4.19 (q, N-CH<sub>2</sub>), 7.67 (s, CH), 7.76 (s, CH), 9.10 (s, N-CH-N) ppm.

Trihexyltetradecylphosphonium Dicyanamide [P<sub>6,6,6,14</sub>][DCA]

<sup>1</sup>H NMR δ<sub>H</sub> (400 MHz; CDCl<sub>3</sub>): 1.15 (m, 8H, CH<sub>2</sub>), 1.45 (m, 16H, CH<sub>2</sub>), 1.25 (m, 32H, CH<sub>2</sub>), 0.83 (m, 12H, CH<sub>3</sub>) ppm.

## NMR of Linear Homopolymers

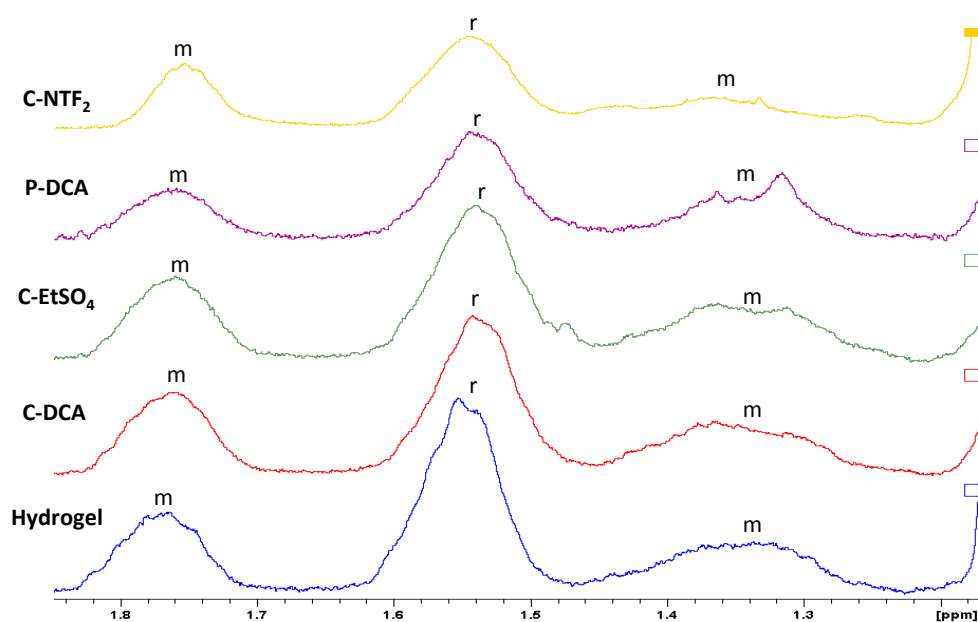


**Figure 1.** <sup>1</sup>H NMR (400 MHz, DMSO-*d*<sup>6</sup>, 120 °C) spectra of linear pNIPAAm homopolymers prepared in various solvents. Shown are the meso (m) and racemo (r) dyads from the region of the backbone methylene protons at 1.2 - 1.8 ppm.

## Vibrational Spectroscopy of Swollen Gels

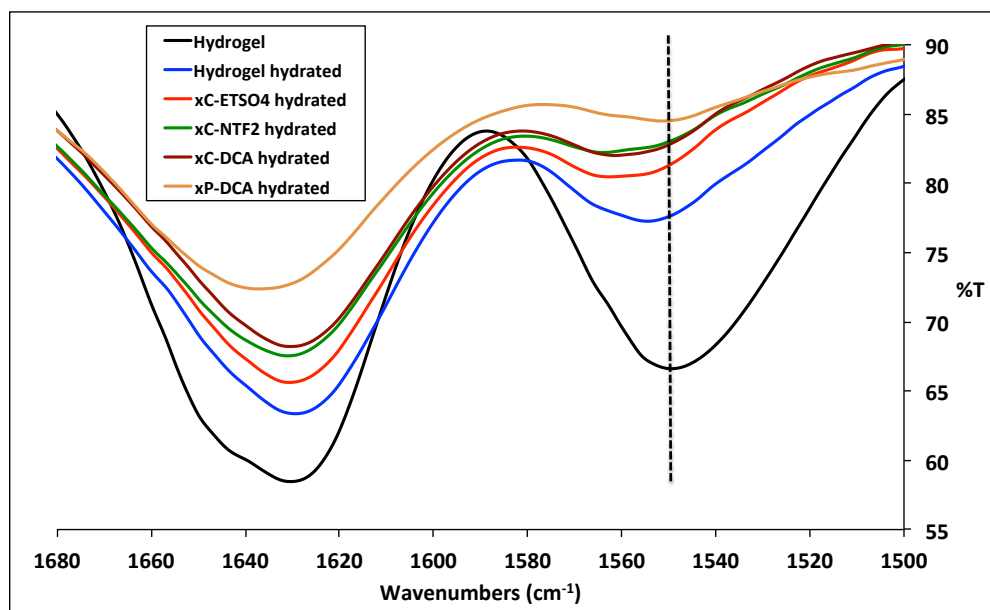


**Figure 2.** Infra-red spectroscopy recorded between 1500-1680  $\text{cm}^{-1}$  of hydrogel (black), a hydrated hydrogel (red), and xC-NTf<sub>2</sub> hydrated (blue).

## Karl-Fischer Analysis of IL/Water Mixtures

Ionic Liquid	$M_{IL}/\text{g mol}^{-1}$	Mole Fraction ( $x_w$ )
[C <sub>2</sub> mIm][EtSO <sub>4</sub> ]	236.29	Miscible
[C <sub>2</sub> mIm][NTf <sub>2</sub> ]	391.31	0.2156
[C <sub>2</sub> mIm][DCA]	177.21	Miscible
[P <sub>6,6,6,14</sub> ][DCA]	549.9	0.4284

**Table 1.** Experimental mole fraction solubilities of water ( $x_w$ ) in Imidazolium- and Dicyanamide-based ILs at 20 °C.

## Density and Viscosity of IL/Water Mixtures

Ionic Liquid	Temperature (°C)	Non-hydrated	Hydrated	Non-hydrated	Hydrated
		Density (g/cm <sup>3</sup> )	Density (g/cm <sup>3</sup> )	Viscosity (mPa.s)	Viscosity (mPa.s)
[C <sub>2</sub> mIm][EtSO <sub>4</sub> ]	20	1.2413	1.1754	93.6088	3.433
	30	1.2345	1.1114	74.6075	3.0444
	40	1.2277	1.1050	49.7062	2.4212
	50	1.221	1.0984	34.6231	1.9927
	60	1.212	1.0916	19.2359	1.7316
[C <sub>2</sub> mIm][NTf <sub>2</sub> ]	20	1.5154	1.4641	32.4902	23.9337
	30	1.5062	1.4534	27.3582	16.8197
	40	1.4965	1.4429	20.0407	12.7826
	50	1.4868	1.4327	15.1803	10.0548
	60	1.457	1.4226	12.2837	8.1369
[C <sub>2</sub> mIm][DCA]	20	1.0953	1.0478	15.940	0.8713
	30	1.0887	1.0415	13.597	0.8030
	40	1.0822	1.0351	10.5365	0.7028
	50	1.0757	1.0284	8.4365	0.6346
	60	1.0693	1.0214	6.9552	0.5840
[P <sub>6,6,6,14</sub> ][DCA]	20	0.8978	0.9012	330.6532	208.6054
	30	0.892	0.8952	252.8495	119.6639
	40	0.8863	0.8892	154.6302	74.5571
	50	0.8806	0.8832	99.7411	49.1904
	60	0.8759	0.8772	67.6314	34.1912

**Table 2.** Summary of density and viscosity values obtained for imidazolium- and dicyanamide-based ILs as a function of addition of water and increasing temperature.

# Scanning Electron Microscopy

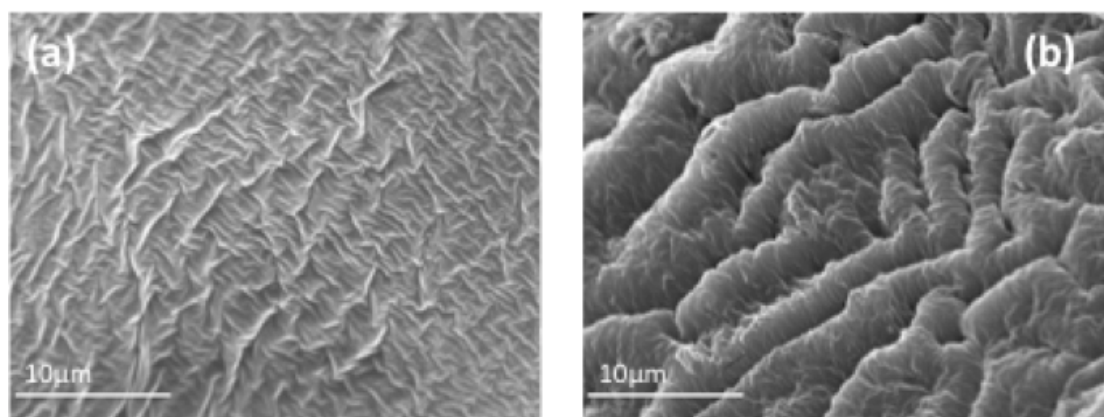


**Figure 3.** SEM images of pNIPAAm hydrogel, (a) after polymerization and (b) after swelling in deionized water <sup>5</sup>.

## Rheometry of Actuating Gels

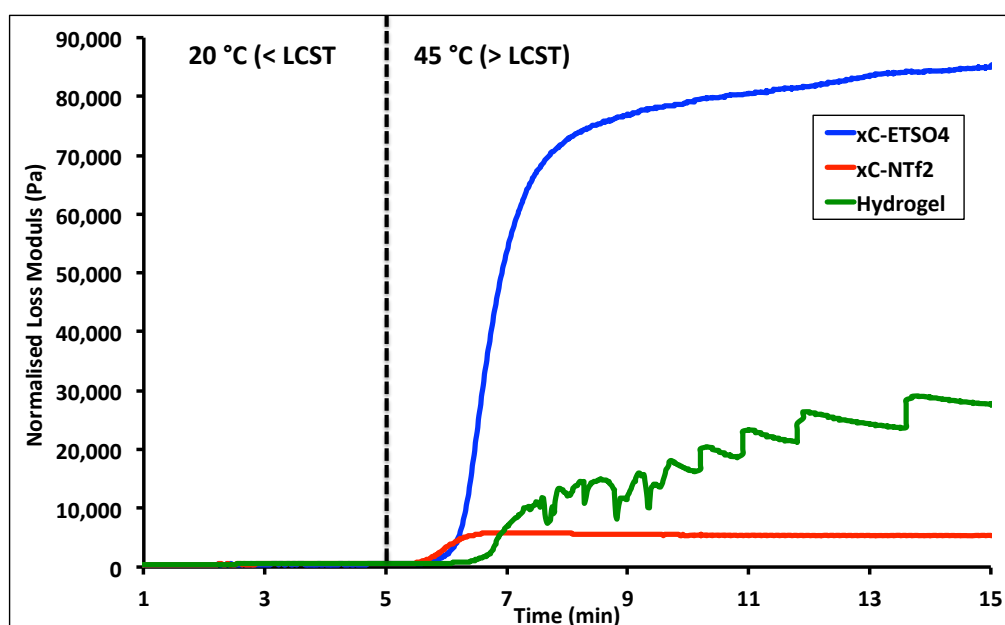


**Figure 4.** Loss modulus of (red) xC-EtSO<sub>4</sub> and (blue) xC-NTf<sub>2</sub> plotted against time during a temperature ramp from 20 °C to 45 °C at 20 °C / min.

# Raman Spectroscopy of Ionogel Leaching

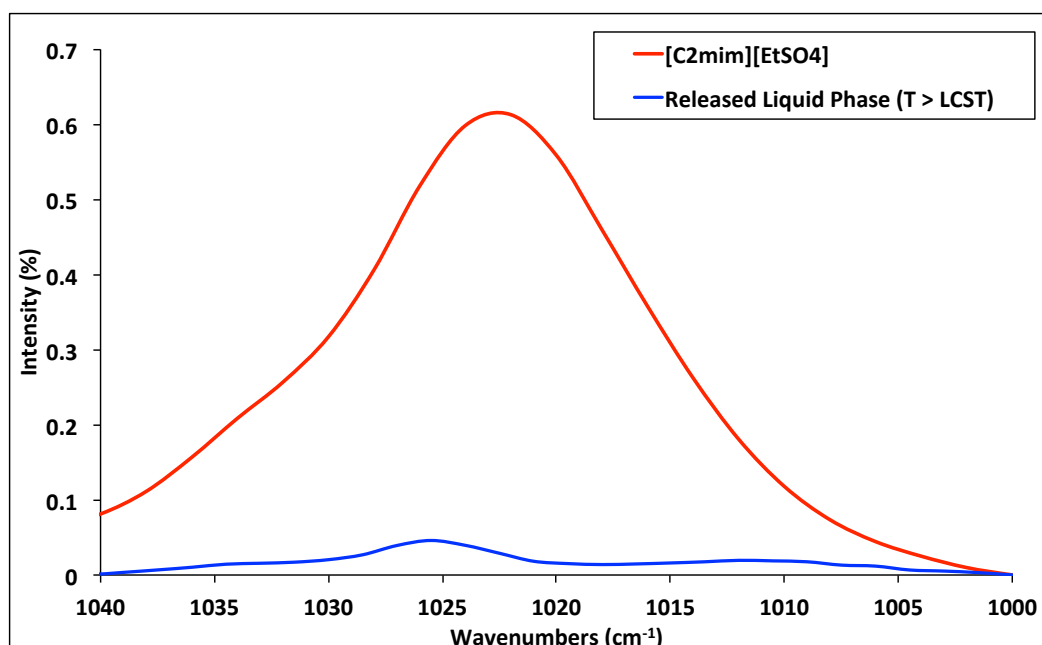


**Figure 5.** Raman spectra of symmetrical  $\text{-SO}_3^-$  stretch found in (red)  $[\text{C}_2\text{mIm}][\text{EtSO}_4]$  and (blue) aliquot of released liquid phase from  $x\text{C-EtSO}_4$  above the LCST.

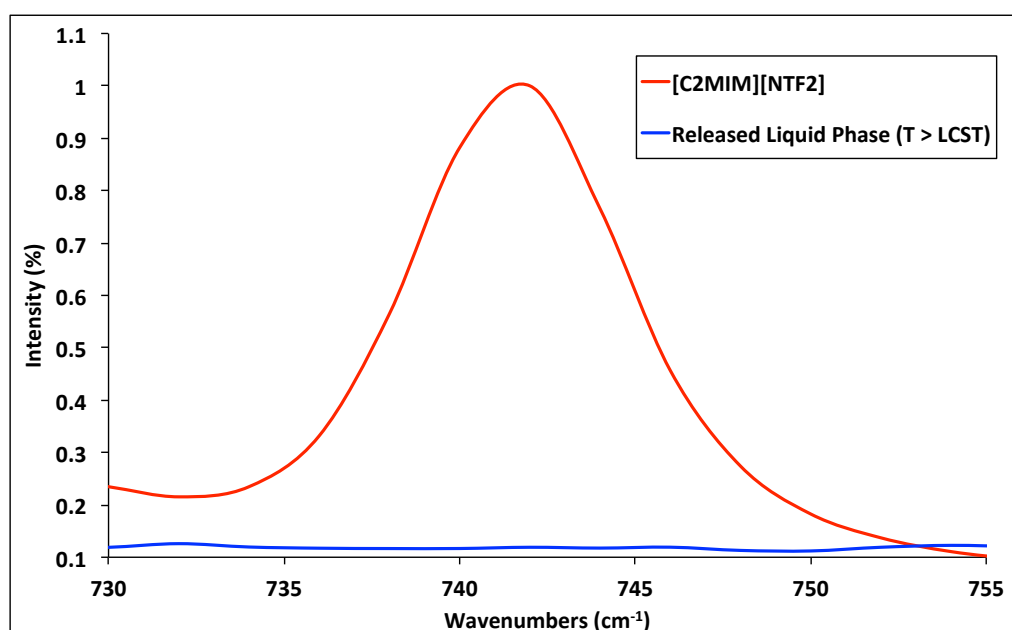


**Figure 6.** Raman spectra of symmetrical  $\text{CF}_3$  bend found in (red)  $[\text{C}_2\text{mIm}][\text{NTf}_2]$  and (blue) aliquot of released liquid phase from  $x\text{C-NTf}_2$  above the LCST.

## References

1. L. E. Ficke, R. R. Novak and J. F. Brennecke, *Journal of Chemical & Engineering Data*, 2010.
2. J. Jacquemin, P. Husson, *Green Chemistry*, 2005, **8**, 172-180.
3. D. Fitzgerald and C. Du, *H&D Fitzgerald Ltd Publ*, 2000.
4. M. Brizard, M. Megharfi, E. Mahe and C. Verdier, *Review of Scientific Instruments*, 2005, **76**, 25109.
5. S. Gallagher, A. Kavanagh, L. Florea, D. R. MacFarlane, K. Fraser, J. and D. Diamond, *Chemical Communications*, 2013, **49**, 4613-4615.

**Chapter 3: Temperature & pH triggered  
release characteristics of water/fluorescein  
from 1-ethyl-3-methylimidazolium  
ethylsulphate based ionogels.**

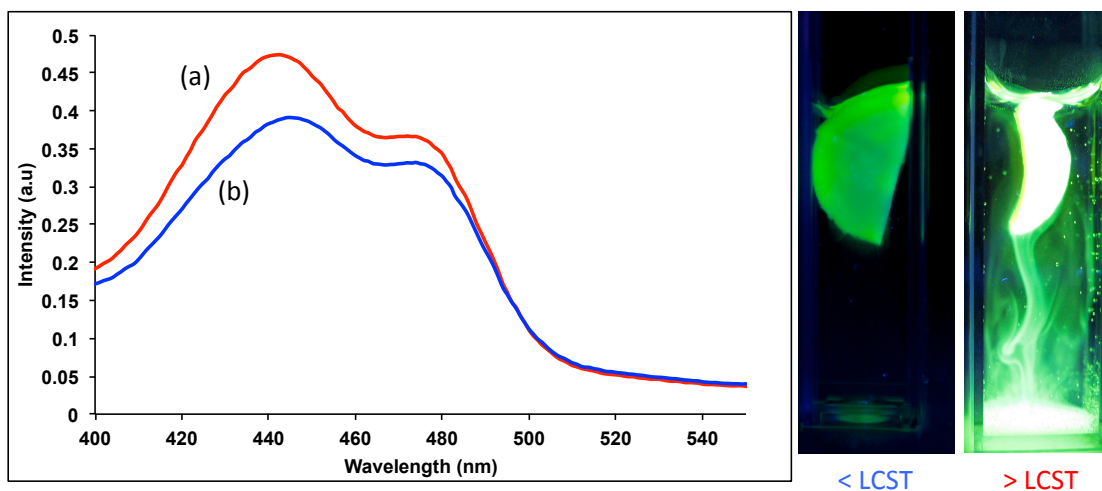
Simon Gallagher<sup>1</sup>, Andrew Kavanagh<sup>1</sup>, Larisa Florea<sup>1</sup>, Douglas R. MacFarlane<sup>2</sup>,  
Kevin J. Fraser<sup>1</sup> and Dermot Diamond<sup>1</sup>.

Chemical Communications, 4613, **49**, 2013, DOI: 10.1039/C3CC41272E

<sup>1</sup>CLARITY: Centre for Sensor Web Technologies, National Centre for Sensor  
Research, Dublin City University, Dublin 9, Ireland

<sup>2</sup> School of Chemistry, Monash University, Wellington Road, Clayton, 3800, Vic,  
Australia

For Supplementary Information see pg. 94



## Abstract

A crosslinked Poly(*N*-isopropylacrylamide) ionogel encapsulating an ionic liquid exhibits improved transmittance properties, enhanced water uptake/release, greater thermal actuation behaviour and distinct solvatomorphology over its hydrogel equivalent. It was also found that the rate of release of fluorescein pre-loaded into membranes was considerably enhanced for ionogels compared to equivalent hydrogels, and could be triggered through changes in pH and temperature.

## 3.1 Introduction

Poly(*N*-isopropylacrylamide) (pNIPAAm) hydrogels have been the subject of particular attention due to their well-known actuation behaviour<sup>43</sup>. This expansion/contraction behaviour is associated with a temperature threshold, known as the Lower Critical Solution Temperature (LCST)<sup>44</sup>. pNIPAAm-based hydrogels have been shown to swell and solvate important pharmacological substances, and subsequently release these substances as the polymer contracts above its LCST<sup>45</sup>. It has been demonstrated previously that the pNIPAAm LCST threshold can be fine tuned depending on the polymer composition<sup>46</sup>. This requires chemical modification of the polymer backbone and, as a general rule, hydrophilic modifications have been shown to lower the LCST<sup>47</sup>. However, the brittleness and inflexibility of pNIPAAm at high crosslink densities in the dehydrated state can pose handling problems<sup>48</sup>. Even more importantly, water volatility means the lifetime of pNIPAAm-based hydrogels is dramatically reduced when used in open atmospheres<sup>49</sup>.

A novel alternative proposed by some has been to replace the aqueous phase of these materials with Ionic Liquids (ILs)<sup>50</sup>. The employment of ILs as a replacement for water in gel-based polymers has led to the emergence of ionogels as a relatively new sub-class of materials. To date, ionogels have been the subject of reviews detailing their preparation, and their applications in sensor science<sup>51</sup>. The ionogel template is an ideal matrix as the properties of the IL are hybridized with those of the polymer component combining the favourable characteristics of both independent phases in one material.

As pNIPAAm is well known as a platform for drug delivery, dyes have been used such as Methylene blue<sup>52</sup> and Orange II<sup>53</sup> to monitor their uptake and release

properties of the hydrogels. The study of release of pre-loaded organic molecules is of great interest for example as a model platform for precise delivery (space, time, amount) of active drugs (in vitro). In order to study the effect of temperature and pH on the release characteristics of organic molecules (Figure SI3-1) loaded into ionogels, we used fluorescein as a model compound due to its ease of optical visualization<sup>54</sup>. It is well known that Fluorescein can exist in several isomeric forms dependent on the pH (Figure SI3-2). It is also an excellent probe due to its high quantum yield, absorption ( $\lambda_{\max}$  494 nm) and emission ( $\lambda_{\max}$  521 nm) in the visible region of the spectrum<sup>54</sup>.

In this work, rheometry was used to quantify the change in mechanical moduli of two polymer gel templates (hydrogel vs. a 1-ethyl-3-methylimidazolium ethylsulphate ([C<sub>2</sub>mIm][EtSO<sub>4</sub>]) based ionogel) as a function of temperature, and scanning electron microscopy was employed to investigate differences in the solvatomorphological microstructures. Gel samples were loaded with fluorescein (3 mM) and exposed to water buffered at pH 4.0, 7.0 and 9.2, with the dynamics of fluorescein release observed using video imaging and by measuring the concentration of fluorescein in the bathing solution after 1 min. The experiments were repeated using the same buffers for water above and below the LCSTs of the gels (40 °C and 20 °C, respectively).

## 3.2 Results & Discussion

It was found that the two gels display differences in physical characteristics after polymerisation. For example, it is evident that the ionogel is more flexible and transparent than the equivalent hydrogel (Figure SI3-3 (a, b)). Unlike ILs, which have negligible vapour pressure under ambient conditions, water is gradually lost from the hydrogels and the material becomes increasingly brittle over time. Additionally, the rate constant obtained for the rate of water uptake for the ionogel was found to be  $\sim 30$  times larger (Figures SI3-4 and SI3-5).

The neat hydrophilic IL undergoes a 96.3% change in viscosity under ambient conditions, when mixed with water in a 1:1 v/v ratio (Table SI3-1 and Figure SI3-6). As the ionogel is essentially anhydrous at the outset, the chemical potential drive for water absorption into the hydrophilic IL is large. As a result, ionogel structures swell considerably on exposure to water. For example, the diameter of ionogel disks increased by 30% above their initial value, in some of the structures we have worked with (Table 3.1 and Table SI3-2). Similar to chemical modifications of the polymeric backbone, the ionogel LCST can be considerably affected by the presence of the IL (Table 3.1 and Figure SI3-7).

Above the LCST, the ionogel contracts by 31.4% of its initial swollen diameter indicating expulsion of the absorbed water and some of the IL originally present, whereas the equivalent hydrogel was found to swell by 18.6% and contract by 21.6%.

Sample	LCST (°C)	Dehydrated gel diameter (mm)	(a) Swelling % increase	(b) Contraction % decrease
Ionogel	26	3.46	28.7	31.4
Hydrogel	31	3.25	18.6	21.6

**Table 3.1.** Increase in disc diameter from dehydrated state to (a) fully hydrated state at T = 20 °C (triplicate). (b): Decrease in disc diameter from fully hydrated state (a) when T = 40 °C (triplicate).

The difference in actuation % between the hydrogel and ionogel can be attributed to the presence of the IL within the polymer network. It is well known that lower crosslinking density results in increased water uptake, however this can result in a weaker mechanical stable gel. Therefore a compromise between physical/mechanical integrity (high degree of cross linking) and extent of actuation (low degree of cross-linking) has been established for these materials.

For viscoelastic materials, rheology experiments (Figure 3.1 and Figure SI3-8) provide information about the storage modulus (energy stored in the material) and the loss modulus (energy dissipated as heat) of these gels. These parameters are commonly used to characterise general mechanical properties. The rheology experiments were designed to enable the behaviour of the sample to be monitored in both its swollen and contracted states over a period of 15 min.

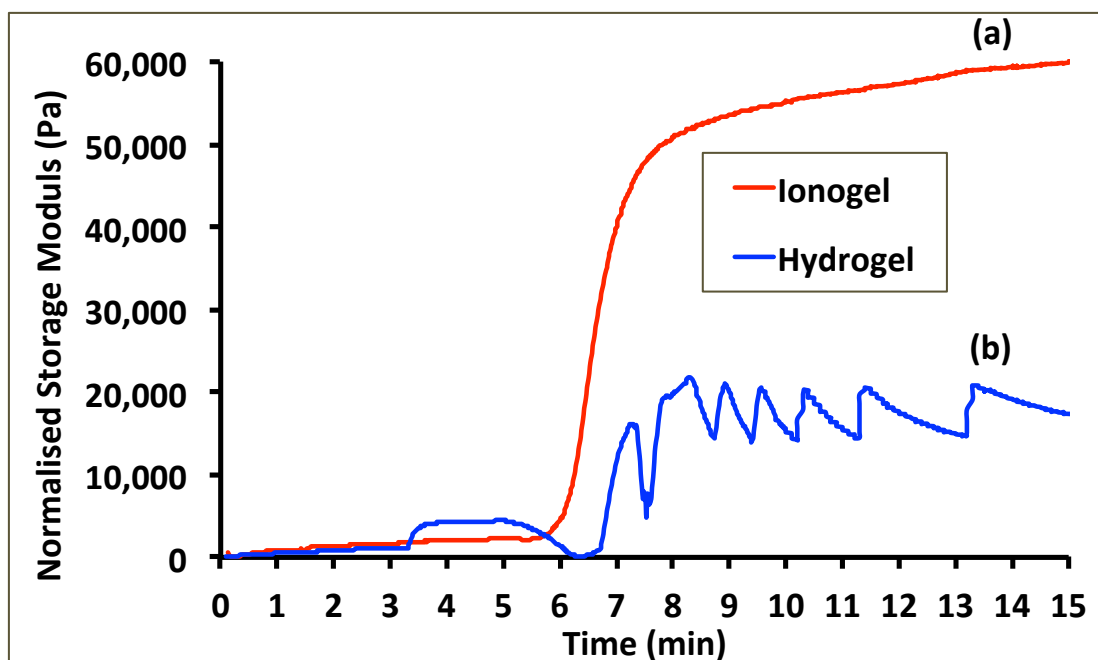


**Figure 3.1** Storage moduli as a function of LCST phase transition for (a) Ionogel and (b) hydrogel (Heating Rate: 20 °C to 45°C at 20 °C per min starting after 5 minutes).

Initially (0 to 5 min), both gels are in their hydrated states below the LCST (20 °C), and the shear rate frequency is kept constant. It can clearly be seen from Figure 3.1 that the ionogel exhibits a stable mechanical response over this time period. Under the same experimental conditions the brittle hydrogel's mechanical stability is sporadic and fluctuates across a ~3,000 Pa range.

At  $t = 5 \text{ min}$ , the sample plate is heated from 20 to 45 °C, ensuring that any thermally sensitive processes related to the LCST are completed in both samples. As the temperature is increased, the storage modulus increases in tandem as the polymer contracts and its mechanical energy is stored internally in response to the applied stress. The increase in the storage modulus of the hydrogel is erratic at higher temperatures. This reflects the materials inability to maintain the stored energy as it contracts, indicative of a material with fragile mechanical stability<sup>55</sup>. The more consistent ionogel thermo-responsive behaviour is evident as the temperature is

increased, with the substantially increased storage modulus plateauing at approximately 10 minutes. Thus it yields a much more energetically stable contracted gel compared to the hydrogel under these conditions.

The corresponding loss moduli of both gel platforms were found to correlate with the temperature dependent storage moduli features (Figure SI3-8). From the point of view of the liquid phase therefore, the ionogel displays an increased dissipation of the converted energy over the hydrogel control. Thus, from the rheological effects described, the ionogel displays improved viscoelastic properties compared to the hydrogel. Significantly, this means that a relatively high density of cross-linking sites can exist within a yet flexible ionogel material.

An interesting feature of pNIPAAm is its contrasting porosities as the preparation solvent is varied. Solvatomorphological effects have been found to correlate with the mole fraction of the formulation solvent<sup>37</sup>, and with the use of porosigens, such as biologically prevalent sugars<sup>38</sup>. In Figure SI3-9 shows the effect of hydration on the hydrogel surface morphology, changing from a relatively dense ribbed type surface (a) to a much more swollen form (b). Under equivalent conditions, the ionogel has a distinctly different surface morphology in the non-hydrated and hydrated states (Figure 3.2 (a) and (b), respectively). In its initial non-hydrated state, the ionogel displays a highly porous, nodule type morphology, efficiently pre-disposed for water uptake. As the hydration process proceeds, the morphology changes, clearly evolving to a more swollen state.

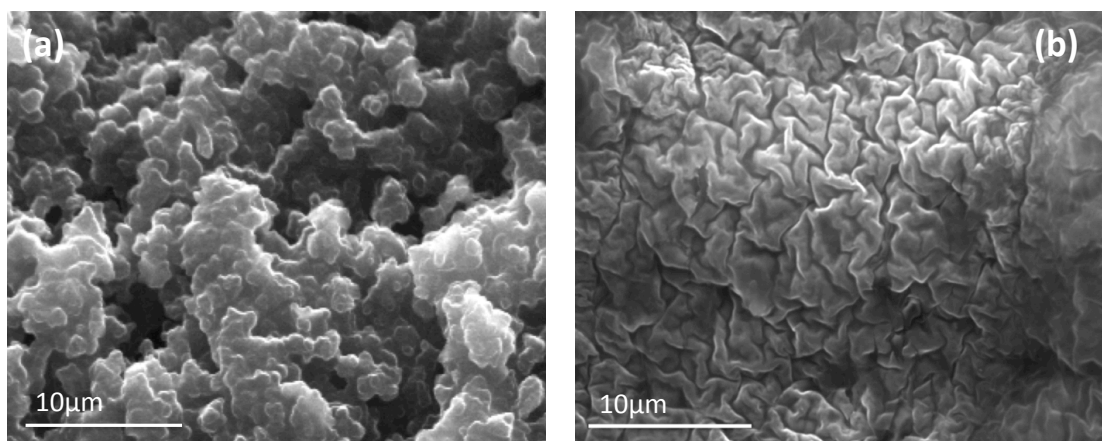


**Figure 3.2** Scanning Electron Microscopy images of (a) Ionogel after polymerisation (non-hydrated) and (b) after hydration in de-ionised water for 24 hours.

Due to the ionogel's very effective hydration characteristics, and its relatively low LCST, we investigated its possible use for the thermally controlled release of solvated organic molecules, using fluorescein as a model system. In Table 3.2 and Table SI3-3 express the quantity of fluorescein expelled after one minute above/below the LCST under acidic, neutral and basic conditions, for the hydrogel and the ionogel. The results show that at over the pH range 4.0 - 9.2, when the temperature is below the LCST ( $T = 20\text{ }^{\circ}\text{C}$ ), the release of fluorescein is minimal for both gels (Table 3.2 and Figure SI3-10). However, at pH 4, and  $40\text{ }^{\circ}\text{C}$  (i.e;  $T > \text{LCST}$  for both gels), there is a striking difference in the rate at which fluorescein is released from the ionogel. Samples taken from the ionogel bathing solution after 1 minute show a fluorescein concentration of 0.3 mM, compared to negligible concentrations in the hydrogel bathing solution. When the temperature is held above the LCSTs ( $T = 40\text{ }^{\circ}\text{C}$ ), the rate of release of fluorescein increases for both gels with increasing pH, but the rate of release is always greater for the ionogel.

There are several interesting outcomes arising from these experiments. For both gels, fluorescein release is clearly dependent on whether the temperature is above or below

the LCST. As the capacity for polymer-fluorescein interactions decrease, the fluorescein-solvent interactions increase, manifesting in an increase in the rate of fluorescein release ( $T > \text{LCST}$ ). This effect is further enhanced in the ionogel due to stronger interactions between the solvent (H-bonding, electrostatic interactions) and fluorescein. In general, fluorescein release is favoured when  $T > \text{LCST}$  and release is impaired when  $T < \text{LCST}$ . For both gels, fluorescein release is enhanced as the pH is increased ( $\text{pH } 9.2 > \text{pH } 7.0 > \text{pH } 4.0$ ) and finally the fluorescein release is enhanced by the presence of the  $[\text{C}_2\text{mIm}][\text{EtSO}_4]$  in the gel (ionogel  $>$  hydrogel). These trends can be explained as follows; when the gels are above the LCST, solvent (IL, water) and solute (fluorescein) interactions with the polymer backbone (e.g. hydrogen bonding with pNIPAAm amide groups) are reduced in favour of increasingly strong polymer-polymer hydrogen bonding as the gel contracts, adopting a more compact format, which also reduces the free volume available for the solvent/solute to occupy. This effect is more apparent in the ionogel than the hydrogel, leading to a 31.4 % dimension change in the diameter of ionogel discs compared to 21.5 % for equivalent hydrogel disks.

	Hydrogel (mM)		Ionogel (mM)	
	< LCST	> LCST	< LCST	> LCST
pH 4	-	-	-	0.3023 (2.96 x 10 <sup>-4</sup> )
pH 7	-	0.0082 (4.97 x 10 <sup>-3</sup> )	-	0.3510 (1.57 x 10 <sup>-2</sup> )
pH 9.2	-	0.1970 (1.20 x 10 <sup>-1</sup> )	-	0.5382 (4.49 x 10 <sup>-2</sup> )

**Table 3.2.** Concentration of fluorescein (mM) found in the bathing solution for both gels below the LCST (20 °C,) and above the LCST (40 °C) after 1 min. Standard deviation is presented in brackets (triplicate).

Therefore, the rate of release of the loaded fluorescein is enhanced above the LCST for both gels, and the effect is greater for the ionogel than the hydrogel.

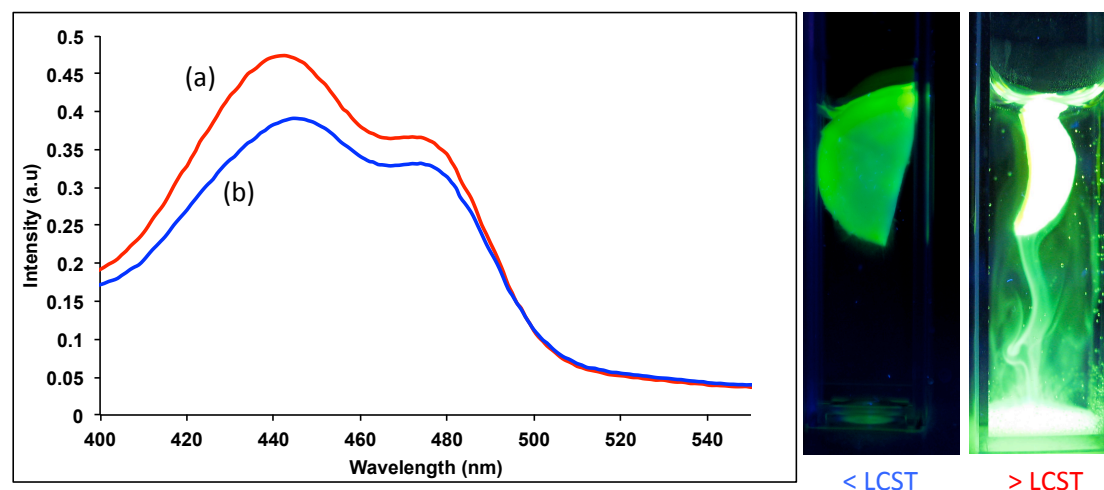


**Figure 3.3 Left: Absorbance spectra** obtained for the Fluorescein dye in (a pH 4 buffered solution and (b 1:1 (v/v) pH 4 buffered/[C<sub>2</sub>mIm][EtSO<sub>4</sub>] solution after 1 min. **Right:** Snapshot images of the ionogel after 30 seconds in pH 4 buffered solution above and below its LCST.

The general increase in rate of release of fluorescein with increasing pH is related to the deprotonation of fluorescein from the neutral quinoid form (hydrogen bonding interactions favoured) to the monoanion and dianion forms (Figure SI3-2). The increasing charge on fluorescein renders it more soluble in water and hence more mobile (rate of release generally increases). The presence of the IL enhances the

effectiveness of electrostatic interactions with the anionic forms of fluorescein that predominate at pH 7 and pH 9.2 (Figure SI3-11, SI3-12), and therefore solvation (and release) is enhanced compared to the equivalent hydrogel ( $T > \text{LCST}$ ). Trace amounts of IL in the released solution above the LCST was detected by Raman spectroscopy (Figure SI3-17).

The dramatic enhancement in release of fluorescein at pH 4 observed with the ionogel compared to the hydrogel most likely arises as, at this pH, fluorescein tends to exist predominantly in the neutral (quinoid) form, as shown by the absorbance spectra in Figure 3.3. In the presence of  $[\text{C}_2\text{mIm}][\text{EtSO}_4]$ , the absorbance bands are reduced, suggesting that the neutral quinoid form is, to some extent, converted to the non-absorbing zwitterionic neutral form due to the presence of  $\text{sp}^3$  hybridization which disrupts the conjugation of  $\pi$ -bonds in the xanthene moiety of the fluorescein<sup>56</sup>. The zwitterionic isomer will tend to be stabilized by electrostatic interactions with the IL, rendering it more mobile than the quinoid form, in which hydrogen bonding is the dominant inter-molecular force. Therefore for the hydrogel (pH4,  $T > \text{LCST}$ ), we observe negligible amounts of fluorescein in the bathing solution after 1 minute. Whereas, for the ionogel, a strong flux can be clearly seen in the video under the same conditions, and a significant concentration of fluorescein is found in the bathing solution after 1 minute (0.30 mM, Table 3.2). These results suggest that for these gels, the release of a loaded molecule can be turned on/off by bringing the temperature above/below the LCST, respectively. In addition, the rate of release of pre-loaded molecules can be tuned by controlling the %v/v of IL in the gel formulation, and by changing the pH.

# Acknowledgements

This work is supported by the Marie Curie IRSES-MASK project (PIRSES-GA-2010-269302), and the CLARITY Centre (Science Foundation Ireland grant 07/CE/I1147). K.J.F acknowledges the European Commission for financial support through a Marie Curie Actions re-integration grant (IRG) (PIRG07-GA-2010-268365) and the Irish Research Council. D.R.M. is grateful to the Australian Research Council for a Federation fellowship.

## 3.3 References

1. F. Benito-Lopez, R. Byrne, A. M. Raduta, N. Vrana, G. McGuinness and D. Diamond, *Lab on a Chip*, 2010, **10**, 195-396.
2. H. G. Schild, *Progress in Polymer Science*, 1992, **17**, 163-249.
3. A. Chilkoti, M. R. Dreher, D. E. Meyer and D. Raucher, *Advanced Drug Delivery Reviews*, 2002, **54**, 613-630.
4. H. Ringsdorf, J. Venzmer and F. M. Winnik, *Macromolecules*, 1991, **24**, 1678-1686.
5. U. Rauwald, J. del Barrio, X. J. Loh and O. A. Scherman, *Chemical Communications*, 2011, **47**, 6000-6002.
6. T. Friedrich, B. Tieke, F. J. Stadler and C. Bailly, *Soft Matter*, 2011, **7**, 6590-6597.
7. Hoffmann, M. Plotner, D. Kuckling and W. J. Fischer, *Sensors and Actuators*, 1999, **77**, 139-144.
8. T. Ueki and M. Watanabe, *Macromolecules*, 2008, **41**, 3739-3749.
9. A. Kavanagh, R. Byrne, D. Diamond and K. J. Fraser, *Membranes*, 2012, **2**, 16-39.
10. B. Taşdelen, N. Kayaman-Apohan, O. Güven and B. M. Baysal, *Polymer Advanced Technology*, 2004, **15**, 528-532.
11. M. R. Guilherme, E. A. Toledo, A. F. Rubira and E. C. Muniz, *Journal of Membrane Science*, 2002, **210**, 129-136.

12. M. M. Martin and L. Lindqvist, *Journal of Luminescence*, 1975, **10**, 381-390.
13. P. Hiemenz and T. P. Lodge, *Polymer Chemistry*, Florida, 2007.
14. C. S. Biswas, V. K. Patel, N. K. Vishwakarma, A. K. Mishra, R. Bhimireddi, R. Rai and B. Ray, *Journal of Applied Polymer Science*, 2012, **125**, 2000-2009.
15. X-Z. Zhang, X.-D. Xu, S.-X. Cheng and R.-X. Zhuo, *Soft Matter*, 2008, **4**, 385-391.
16. M. Ali, P. Dutta and S. Pandey, *Journal of Physical Chemistry B*, 2010, **114**, 15042-15051.

## **Chapter 3: Supporting Information**

# **Temperature & pH triggered release characteristics of water/fluorescein from 1- ethyl-3-methylimidazolium ethylsulphate based ionogels.**

Simon Gallagher<sup>1</sup>, Andrew Kavanagh<sup>1</sup>, Larisa Florea<sup>1</sup>, Douglas R. MacFarlane<sup>2</sup>,  
Kevin J. Fraser<sup>1</sup> and Dermot Diamond<sup>1</sup>.

Chemical Communications, 4613, **49**, 2013, DOI: 10.1039/C3CC41272E

<sup>1</sup>CLARITY: Centre for Sensor Web Technologies, National Centre for Sensor  
Research, Dublin City University, Dublin 9, Ireland

<sup>2</sup> School of Chemistry, Monash University, Wellington Road, Clayton, 3800, Vic,  
Australia

# Chemicals and Materials

*N*-isopropylacrylamide 98 % (NIPAAM), *N,N'*-methylenebisacrylamide 99% (MBIS), Aluminum Oxide (activated, basic, Brockmann I), Fluorescein disodium salt, Fluka pH 4, 7 and 9.2 buffer tablets and 2,2-Dimethoxy-2-phenylacetophenone 98 % (DMPA) were purchased from Sigma Aldrich®, Ireland and used as received. 1-ethyl methylimidazolium ethylsulphate  $[C_2mIm][EtSO_4]$  was purchased from Sigma Aldrich® Ireland Ltd and purified as outlined below.

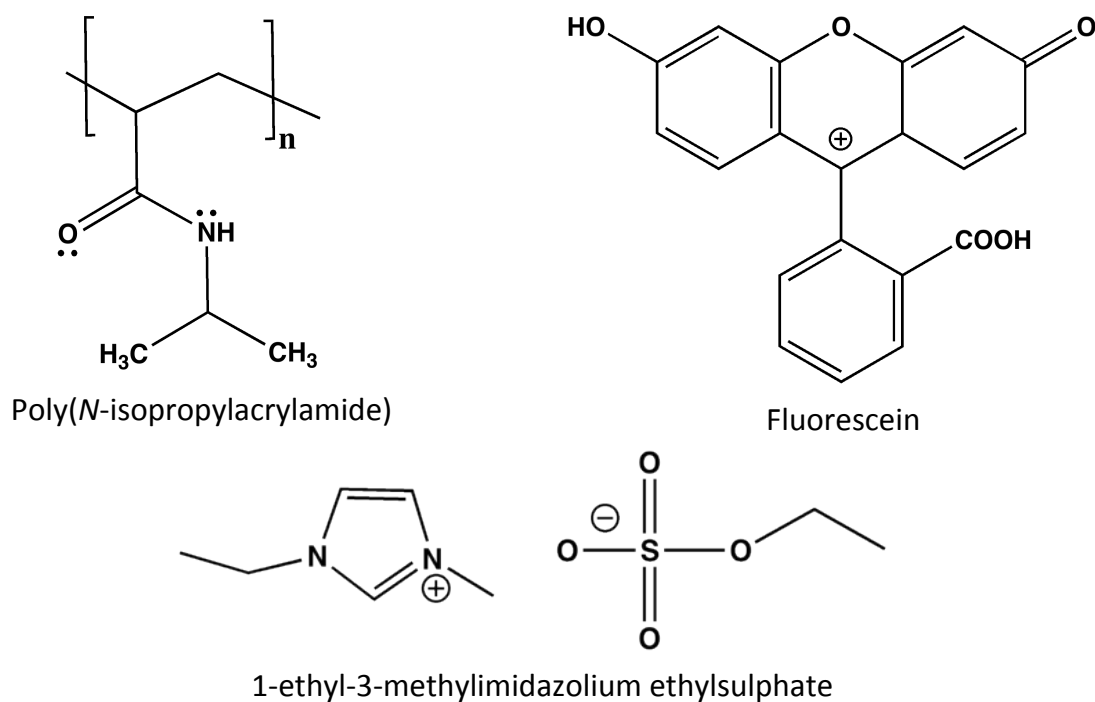


**Figure 1:** (top) pNIPAAM, ionic liquid  $[C_2mIm][EtSO_4]$  and fluorescein in its neutral form.

# Experimental

## IL purification

Before further analyses, [C<sub>2</sub>mIm][EtSO<sub>4</sub>] was column cleansed using alumina (activated, basic, Brockmann I), with dichloromethane used as the mobile phase, which was subsequently removed under vacuum at 40 °C for 48 hrs at 0.1 Torr<sup>1</sup>. The IL was subsequently stored in an inert atmosphere (N<sub>2</sub>) at room temperature.

<sup>1</sup>H NMR,  $\delta_{\text{H}}$  (400 MHz; CD<sub>3</sub>CN): 1.15 (3H, t, CH<sub>3</sub>), 1.34 (3H, t, CH<sub>3</sub>), 3.73 (3H, s, CH<sub>3</sub>), 3.94 (2H, m, CH<sub>2</sub>), 4.07 (2H, m, CH<sub>2</sub>), 4.69 (H, s, CH), 7.24 (H, d, CH), 7.32 (H, d, CH).

## Preparation of polymer gels

pNIPAAm ionogels were prepared by mixing 400 mg of NIPAAm monomer (3.53 mmol), 27 mg of MBIS crosslinker (0.176 mmol), 18.1 mg photoinitiator (DMPA (0.07 mmol) (Final molar ratio 100:5:2), with 1200 mg (5.07 mmol, 960  $\mu$ L) of [C<sub>2</sub>mIm][EtSO<sub>4</sub>] added. The mixture was heated to 30 °C and sonicated for 5 min. until a transparent solution was observed. 200  $\mu$ L of the monomeric solution was then dispensed into a Teflon mold, 12 mm in radius, and photo-polymerized using a Connecticut® 20 W UV BondWand (365 nm) for 10 mins. A 1 mm diameter punch was then used to isolate the sample area for further analyses.

The control hydrogel experiments were performed in the same manner, by substituting 1.2 g of a 1:1 (v/v) mixture of H<sub>2</sub>O: Ethanol for [C<sub>2</sub>mIm][EtSO<sub>4</sub>].

The fluorescent ionogels were prepared by adding 1.083 mg of Fluorescein disodium

salt to the ionogel composition, and polymerised in the same manner as described previously.

## Rate of Fluorescein Expulsion.

100 ml of Standard pH solutions were made using Fluka pH 4, 7 and 9.2 buffer tablets (Sigma-Aldrich, Ireland). Ionogels and hydrogels preloaded with 3 mM of fluorescein dye were allowed to swell overnight in the corresponding pH buffered water solution. The swollen gels were then cut in half and placed in solution of the same pH at 40 °C for 1 min ( $>$  LCST) and 20 °C ( $<$  LCST). The free-standing ionogel membrane was then removed and the resultant solution was stirred for homogeneity. When the sample cooled to room temperature (20 °C), the concentration of fluorescein was measured. Calibration curves can be found in Fig 13 and 14 and emission spectra for the ionogel at pH 4, 7 and 9.2 in Fig 15 and 16 respectively.

## Instrumentation

### Density Measurements

Densities were measured using a DMA-500 vibrating-tube densiometer from Anton-Paar®. The density meter uses the “oscillating U-tube principle”<sup>2</sup> to determine the density of the liquid. Measurements were performed at atmospheric pressure from 20 to 60 °C for both pure and water-saturated ILs.

## Viscosity

Viscosity measurements were performed at atmospheric pressure in the temperature range 20 to 60 °C on both pure and water-saturated ILs using an Anton-Paar® Viscometer, which employs a rolling ball technique<sup>3</sup>.

## Differential Scanning Calorimetry

Differential Scanning Calorimetry (DSC) was performed using the Perkin Elmer® Pyris 1 Calorimeter. Individual scans were performed in the temperature range from 10 to 50 °C, at a scan rate of 5 °C per minute. Thermal scans below room temperature were calibrated with the cyclohexane solid-solid transition and melting point at – 87.0 °C and 6.5 °C, respectively. Thermal scans above room temperature were calibrated using indium, tin and zinc with melting points at 156.60, 231.93 and 419.53 °C, respectively. Transition temperatures were taken from the peak maximum of the thermal transition.

## Polymer Gel Diameter Measurements

Each free-standing polymerized gel was placed in 5.76 mL de-ionized water at 20 °C for 24 hours before the swelling behaviour was recorded. Next, the gels were placed in de-ionized water at 45 °C for 1 minute. This temperature ensures the swollen hydrated ionogels undergo the LCST phase transition (as individually measured using DSC).

De-ionized water was substituted by pH 4, 7 and 9.2 buffer solutions for fluorescence ionogel experiments.

The thickness of the resultant gel samples were calculated using a Mitutoyo® micrometer calibrated to a resolution of 1  $\mu\text{m}$ .

## Rheometry

All measurements were performed on an Anton-Paar® MCR301 rheometer equipped with a steel bottom plate. Initially, all polymerized gels (12 mm diameter) were immersed in deionized water for 24 hours. The swollen gels were then analysed for changes in the loss and storage moduli through the LCST by using a temperature step program. All the swollen gels were analysed in oscillation mode with a parallel plate PP15 tool 15 mm diameter at 0.05 % strain and a frequency of 10 Hz.

The data points were collected every second and the following temperature ramp were applied: Isotherm for 5 min at 20 °C, after which increase to 45 °C (20 °C /min) and isotherm for a total of 9 min thereafter at 45 °C.

## Optical Microscopy

Optical Microscopy studies were performed using an AIGO® GE-5 digital microscope.

## Scanning Electron Microscopy

Ionogel and hydrogel surface areas were imaged using scanning electron microscopy (SEM), performed on a Carl Zeiss EVOLS 15 system at an accelerating voltage of 26.11 kV. Gold Sputtering of all gels was performed on a Polaron® SC7640

Auto/Manual High Resolution Sputter Coater. All gels were coated under the following conditions: Voltage 1.5 kV, 15 mA for 2 minutes at a coating Rate of 5 nm/min. The 10 nm gold coating proved capable of maintaining a saturated ionogel for microscopy imaging.

## UV/Vis Spectroscopy

UV/Vis transmittance / absorbance spectra were obtained using a Perkin Elmer Lambda 900 UV/Vis/NIR® spectrometer. All spectra were obtained in the wavelength region spanning from 300 to 900 nm at 200 nm/minute, using a 1 nm data interval.

## Fluorescence Spectroscopy

Fluorescence measurements were performed using a Perkin Elmer® LS 50B Luminescence Spectrometer, in the spectral range from 300 to 800 nm, at a scan rate of 100 nm/min.

# Different Prototropic Forms of Fluorescein

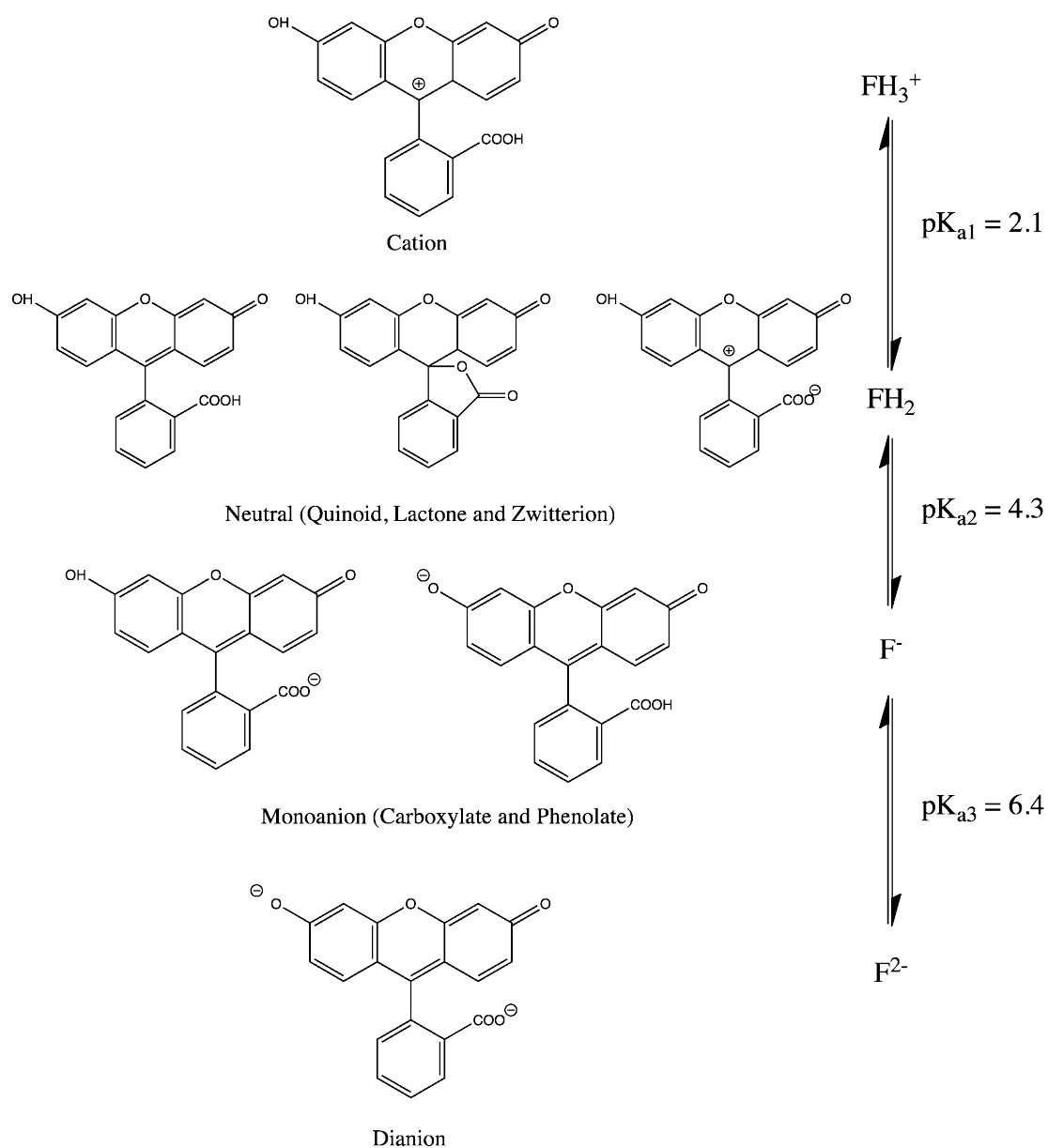


**Figure 2.** pH dependence of prototropic forms of fluorescein in aqueous solution [cation ( $FH_3^+$ ,  $pK_a = 2.1$ ), neutral ( $FH_2$ ,  $pK_a = 4.3$ ), monoanion ( $F^-$ ,  $pK_a = 6.4$ ), and dianion ( $F^{2-}$ )].<sup>4</sup>

## UV-Vis

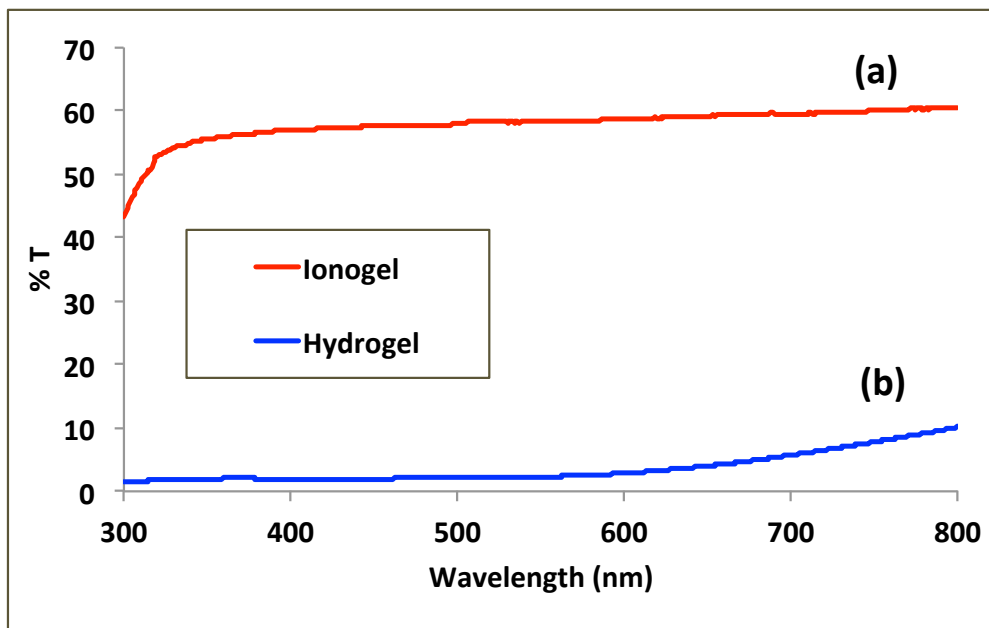


**Figure 3.** Transmittance spectra obtained for (a) Ionogel and (b) Hydrogel after the initial photoinitiation step.

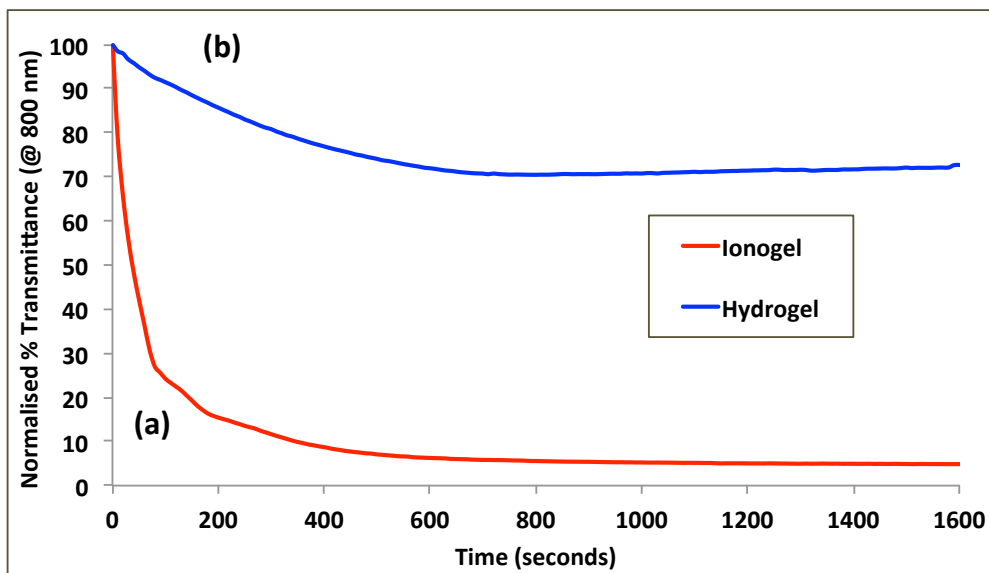
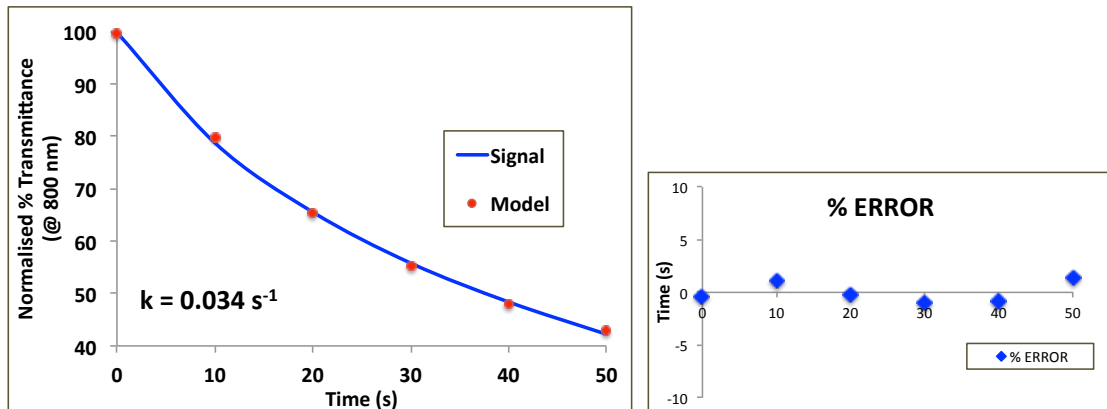


**Figure 4.** Kinetic analysis (@ 20 °C) of the water uptake for (a) Ionogel and (b) Hydrogel after the initial photoinitiation step. As the gel swells it becomes more opaque resulting in decreased transmission at the given wavelength (800 nm).

(a)



(b)

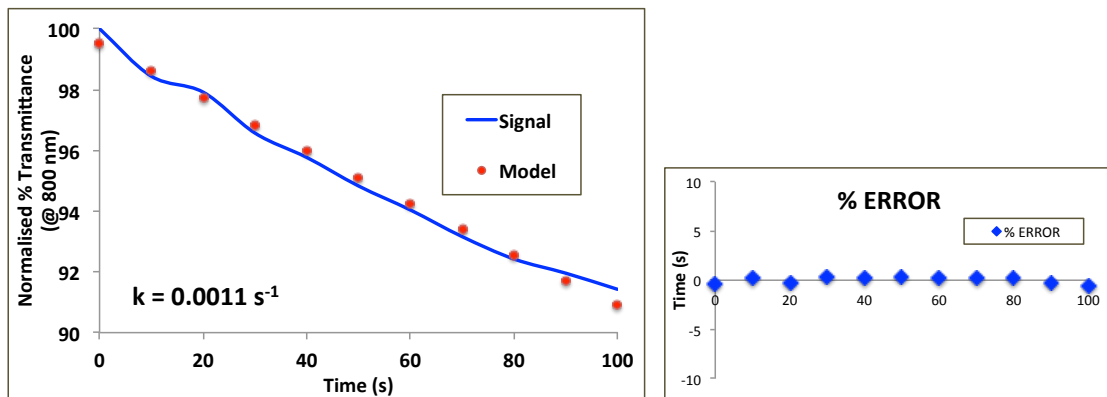


**Figure 5.** Exponential decay analysis used for the determination of rate constants for gel water uptake for (a) the Ionogel and (b) the Hydrogel. As the gel swells it becomes more opaque resulting in decreased transmission at the given wavelength (800 nm). The model was fitted using the SOLVER function in MS Excel® 2011 and the pre-exponential equation,

$$f(t) = [A(1 - e^{-kt})] + z, \text{ where:}$$

$A$  = pre-exponential factor

$k$  = rate constant

$t$  = time

$z$  = baseline offset.

# Viscosity of $[C_2mIm][EtSO_4]$

Ionic Liquid	Temperature (°C)	NON-SATURATED	SATURATED
		Viscosity (mPa.s)	Viscosity (mPa.s)
$[C_2mIm][EtSO_4]$	20	93.61	3.43
	30	74.61	3.044
	40	49.71	2.421
	50	34.62	1.99
	60	19.24	1.73

**Table 1.** Viscosity values of non-hydrated and water-saturated mixtures of  $[C_2mIm][EtSO_4]$  as a function of temperature.

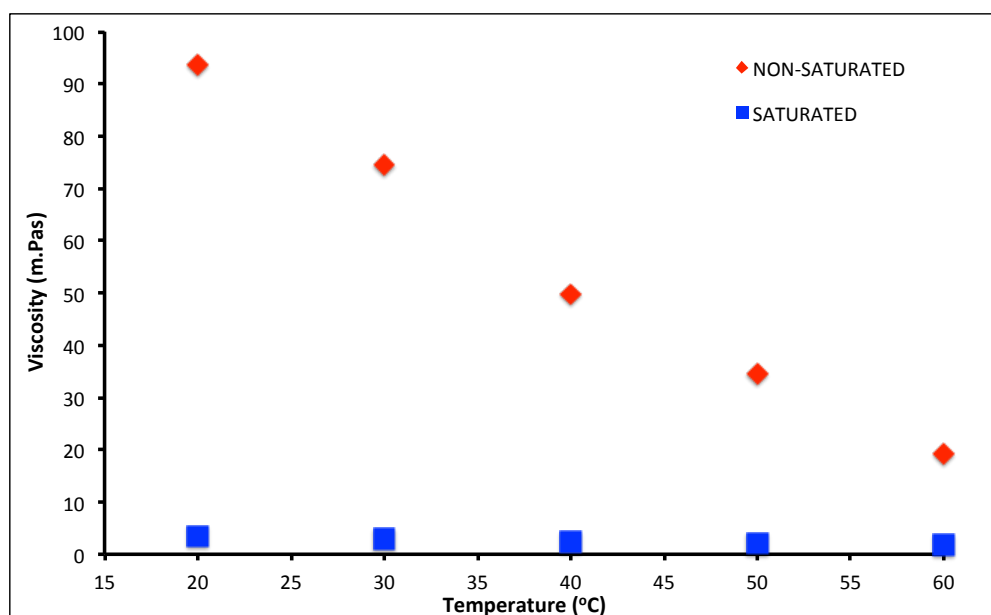


**Figure 6.** Viscosity values of non-hydrated (red) and water-saturated (blue) mixtures of  $[C_2mIm][EtSO_4]$  as a function of temperature.

## Actuation Behaviour.

Sample	LCST (°C)	Swollen	%	Contracted	%
		Diameter/mm (n=3)	Swelling Increase	Diameter/mm (n=3)	Contraction Decrease
Ionogel	26	4.45 (0.09)	28.68	3.05 (0.03)	31.44
Hydrogel	31	3.58 (0.05)	18.59	3.02 (0.09)	21.59

**Table 2.** Summary of the actuation behaviour of both gel templates recorded using the digital micrometer. Here the % changes are expressed after the swelling and LCST phase transition behaviour, respectively.

## Thermal Behaviour

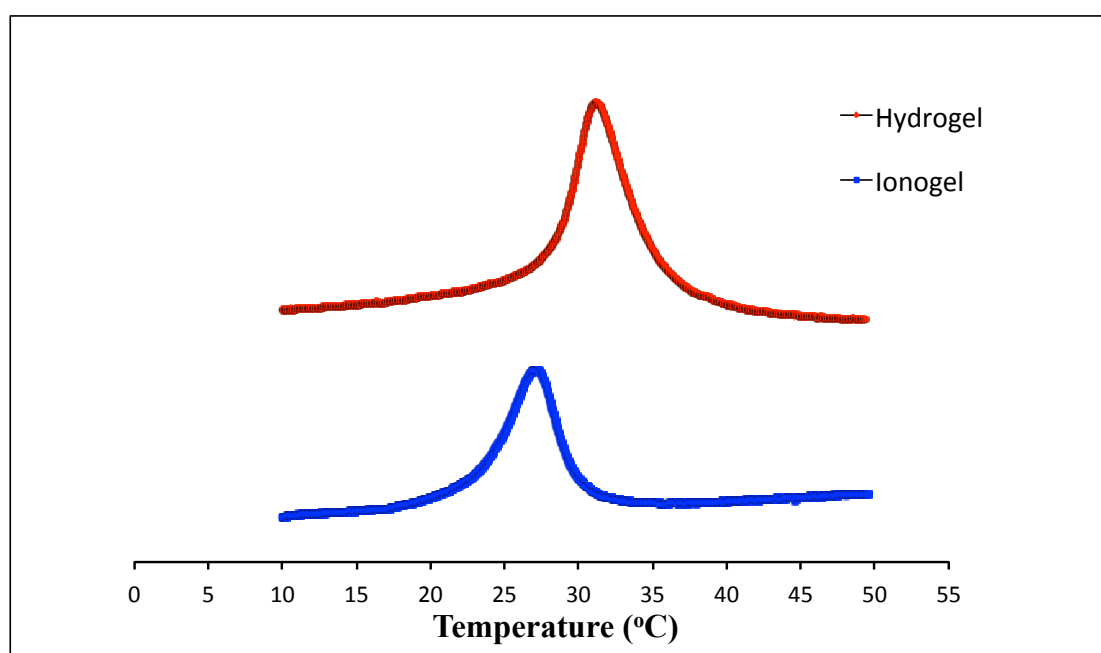


**Figure 7.** DSC temperature profiles obtained for the pNIPAAm LCST transition of Ionogel (26 °C) and Hydrogel (31 °C).

## Mechanical data

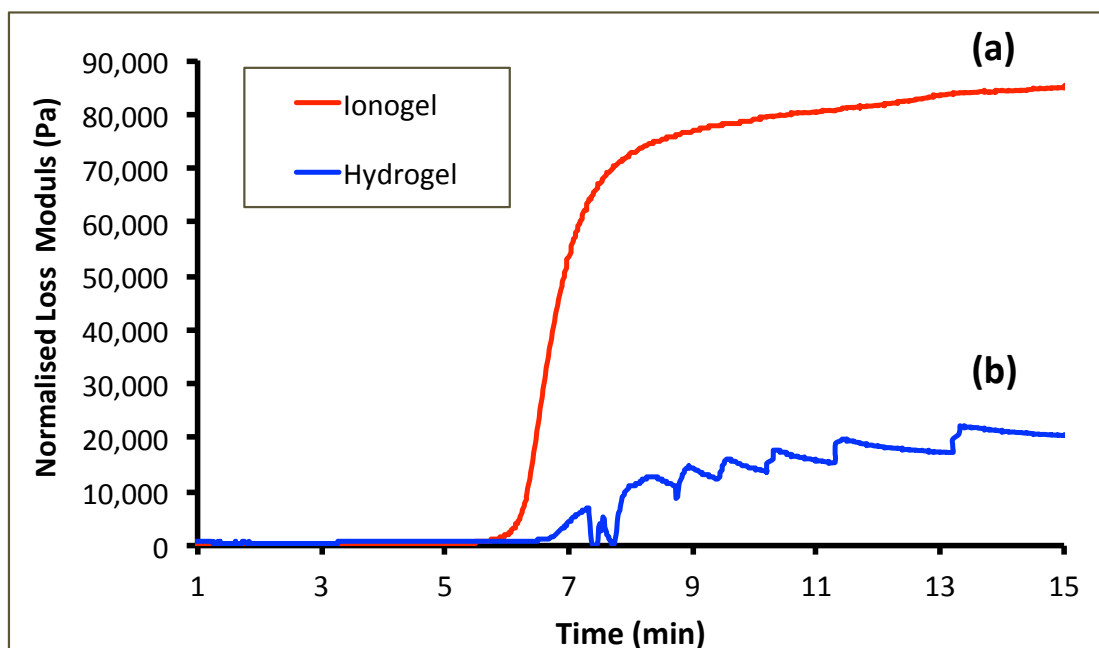


**Figure 8.** Loss moduli as a function of LCST phase transition for (a)  $[C_2mIm][EtSO_4]$  Ionogel and (b) hydrogel (heated from 20 °C to 45 °C @ 20 °C / min, starting after 5 minutes).

## SEM

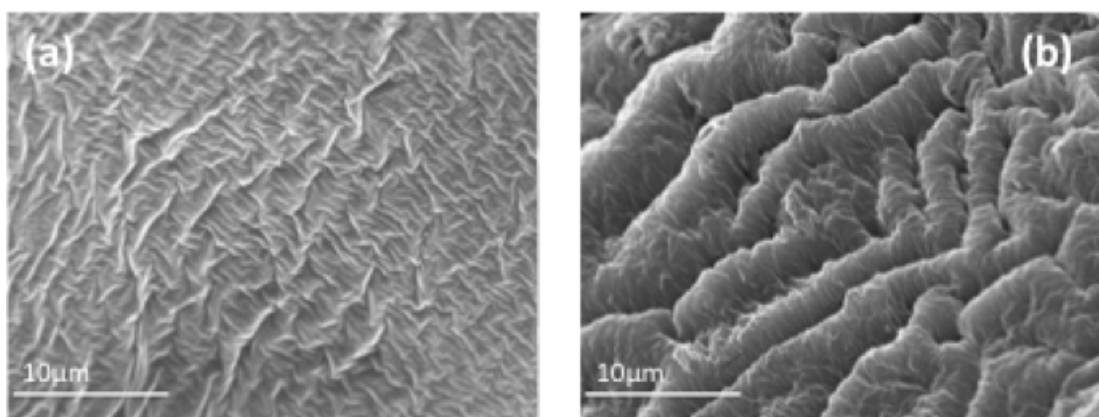


**Figure 9.** SEM Images of pNIPAAm control hydrogel, (a) after polymerisation (non-hydrated) and (b) after hydration in de-ionised water for 24 hours.

## Video Details

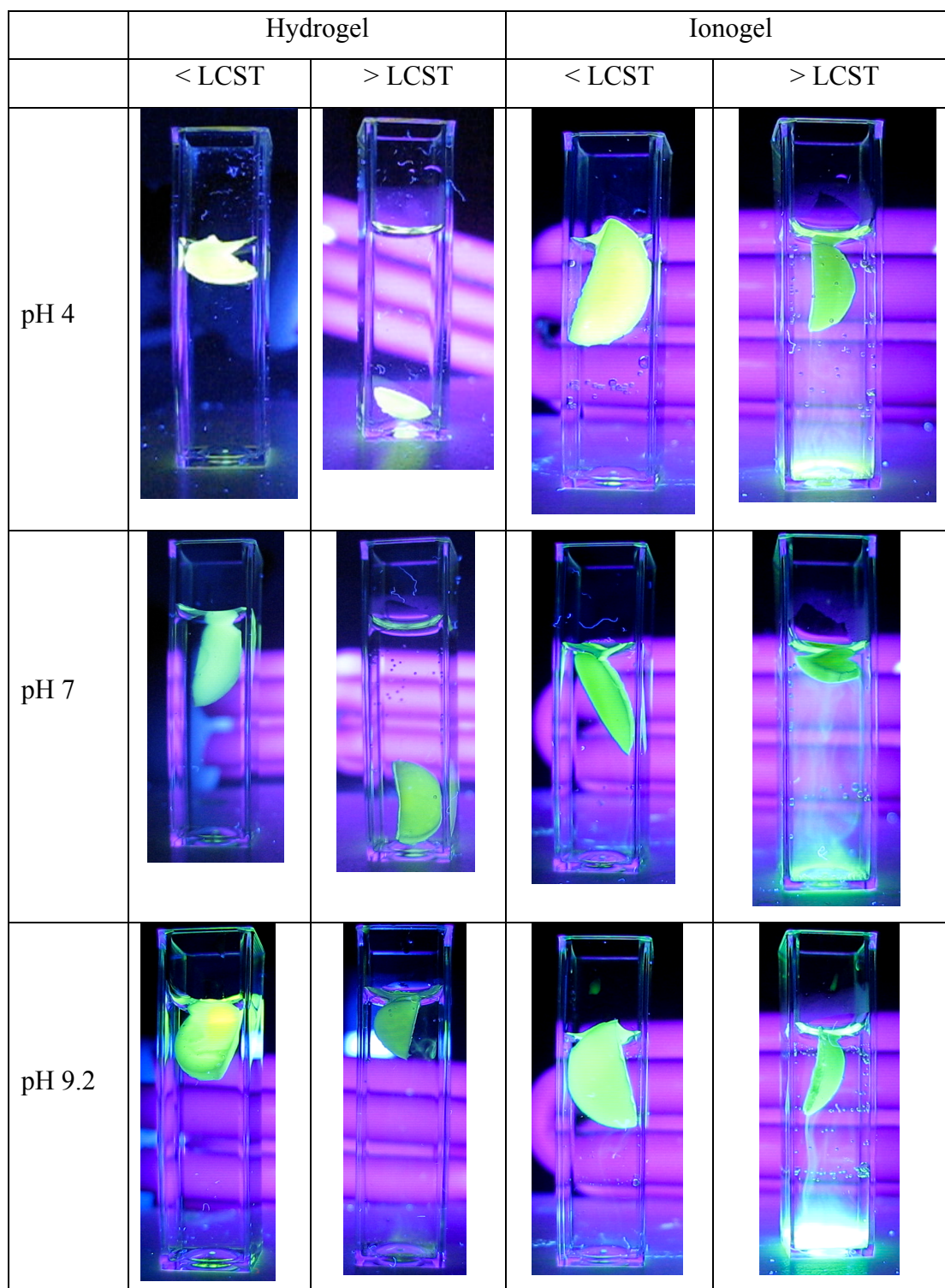


**Figure 10.** Video capture of release of fluorescein from free-standing hydrogel and Ionogel membranes after 1 min, at pH 4.0, 7.0 and 9.2, for  $T < LCST$  (20 °C) and  $T > LCST$  (40 °C). The full videos can be viewed at: <http://tinyurl.com/bhnrfo> (Hydrogel) and <http://tinyurl.com/bha479p> (Ionogel).

## UV-Vis Spectroscopy of Fluorescein

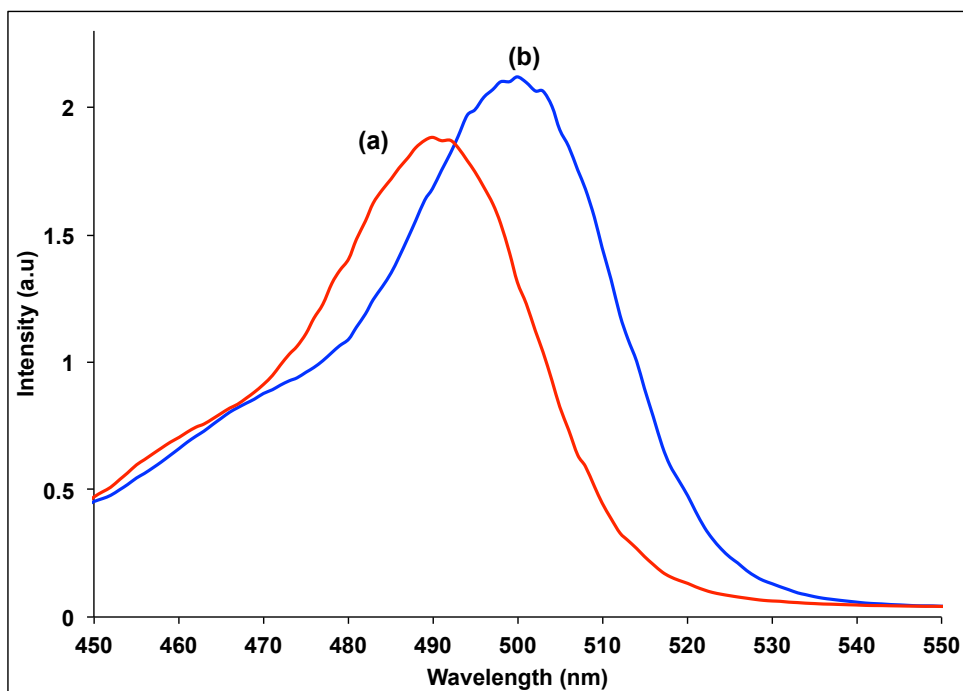


**Figure 11.** Absorbance spectra of fluorescein in (a) pH 7 buffer and (b) (1:1, v/v) IL/pH 7 buffer mixture.

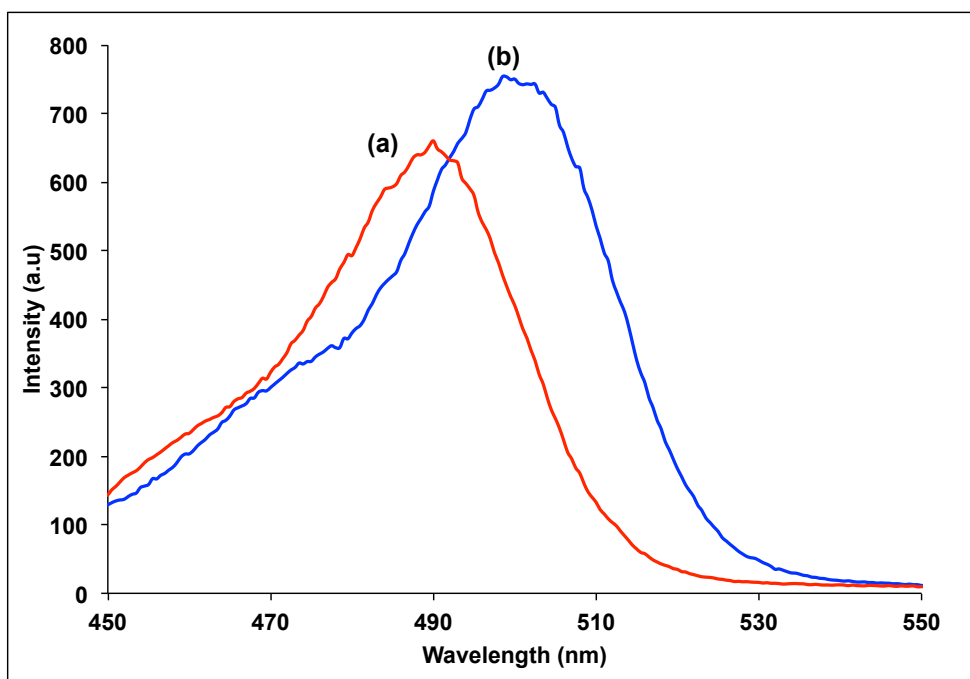


**Figure 12.** Absorbance spectra of fluorescein in (a) pH 9.2 buffer and (b) (1:1, v/v) IL/pH 9.2 buffer mixture.

## Fluorescence Spectroscopy.

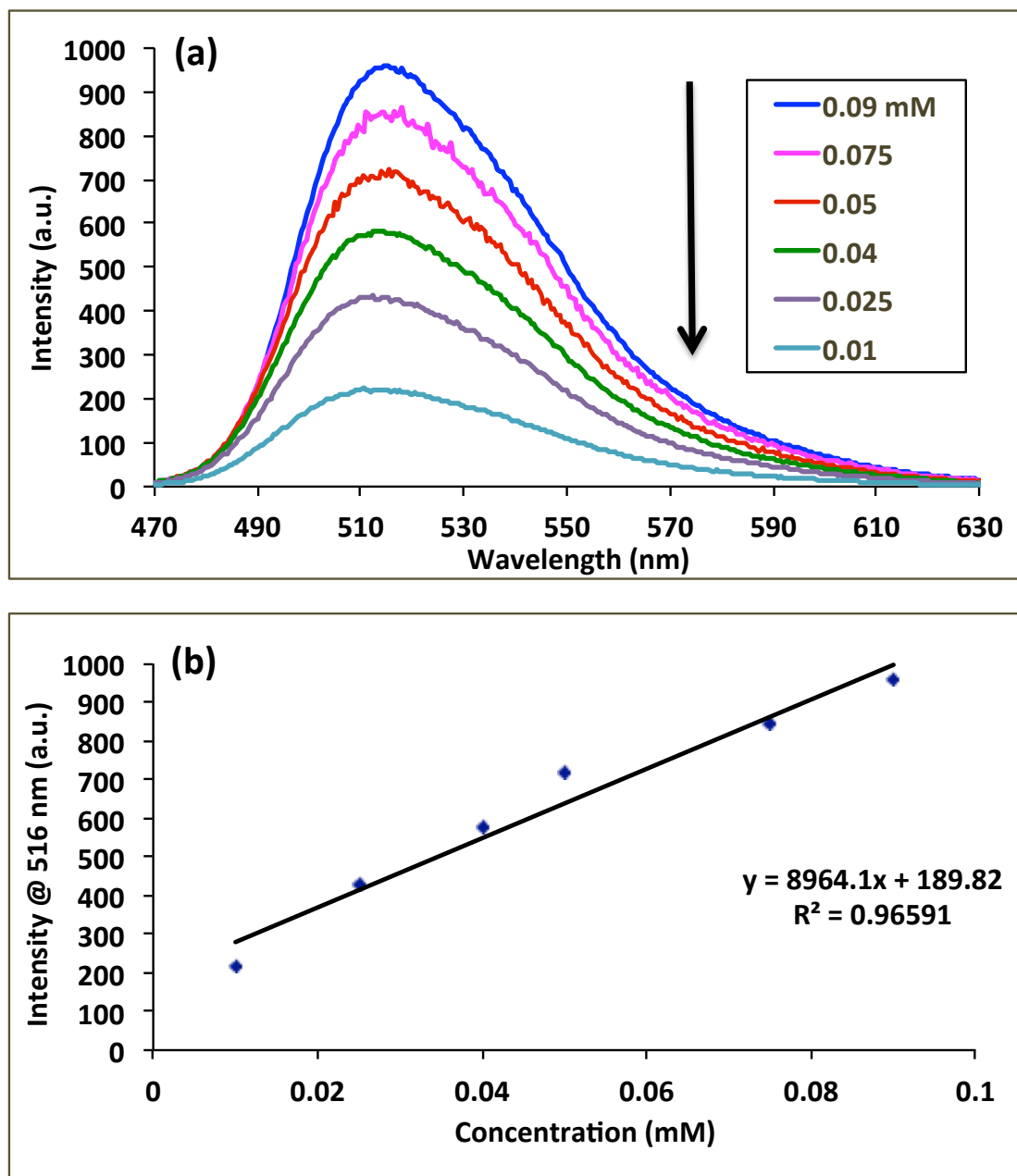


**Figure 13.** (a) Emission spectra of 0.01 – 0.09 mM fluorescein in pH 4 buffer solution (excitation wavelength = 460 nm) and, (b) the calibration plot, taken at emission wavelength = 516 nm.

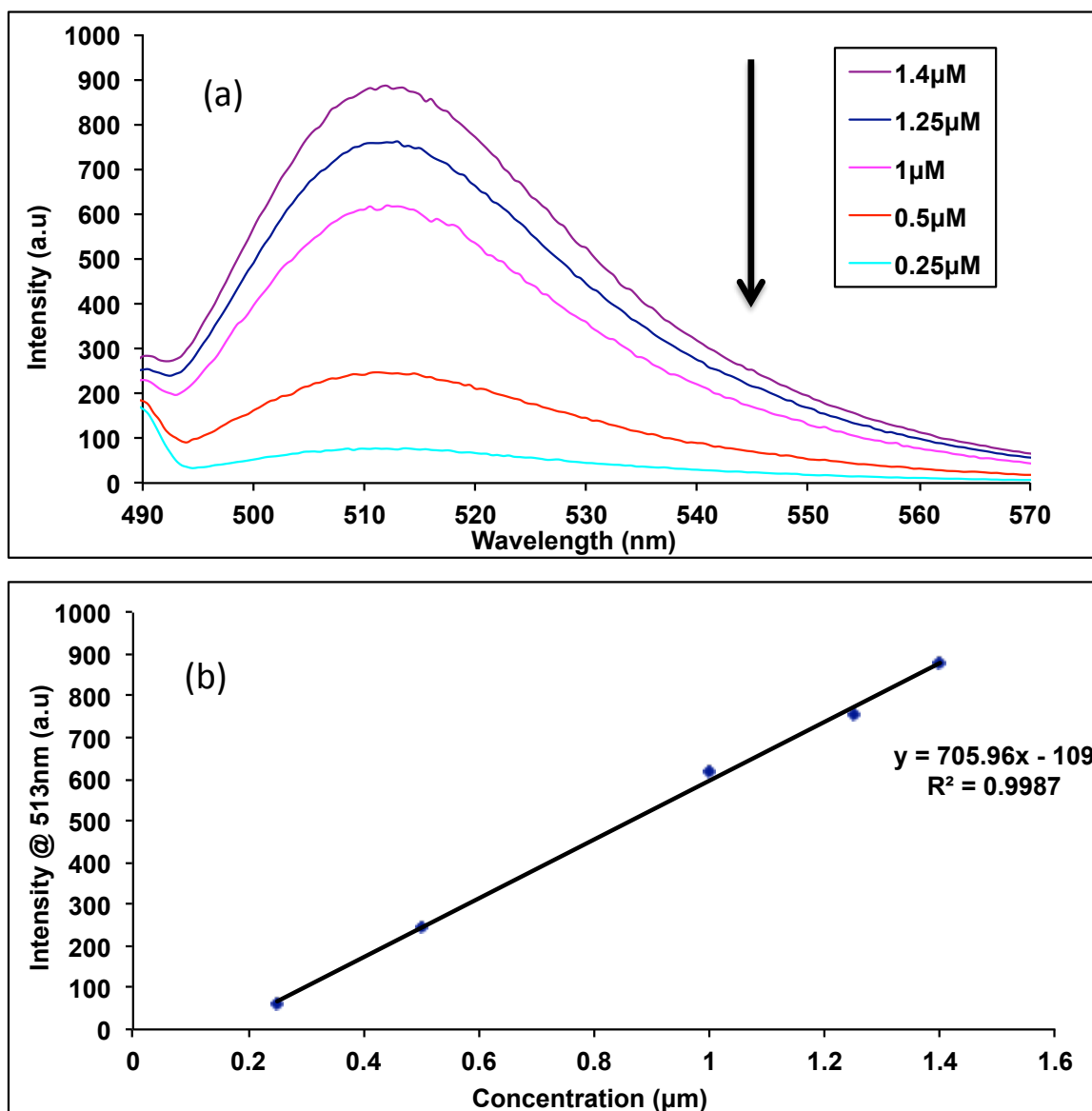


**Figure 14.** (a) Emission spectra of 0.25 – 1.4 μM fluorescein in pH 7 buffer solution (excitation wavelength = 490 nm) and, (b) the calibration plot, taken at emission wavelength = 513 nm.

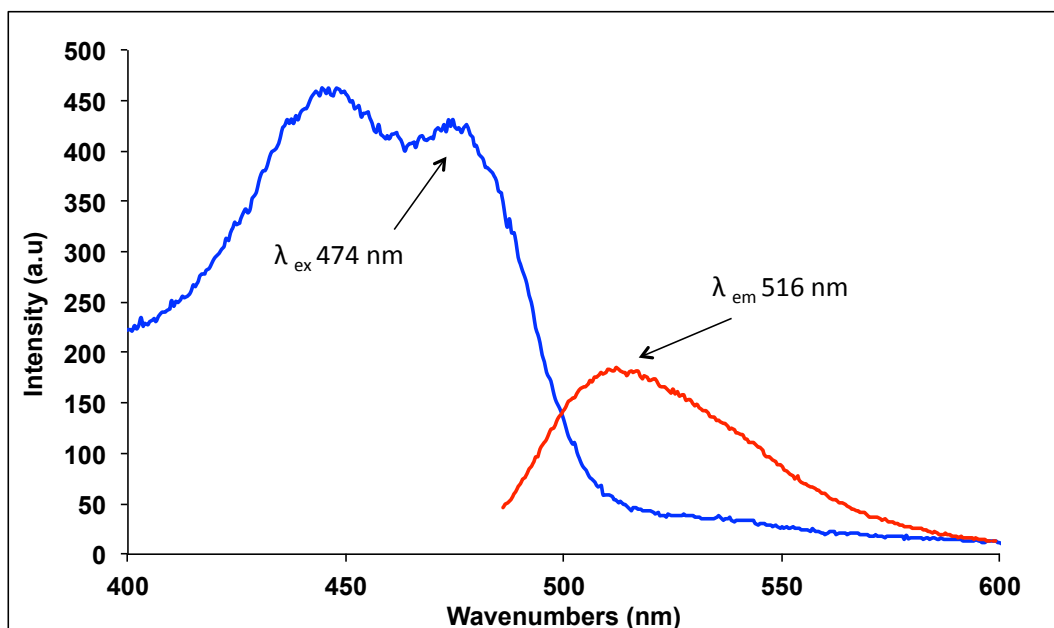


**Figure 15.** Excitation and emission spectra for fluorescein obtained from the bathing solution for the ionogel membrane at pH 4 ( $T > LCST$ ) after 1 min.

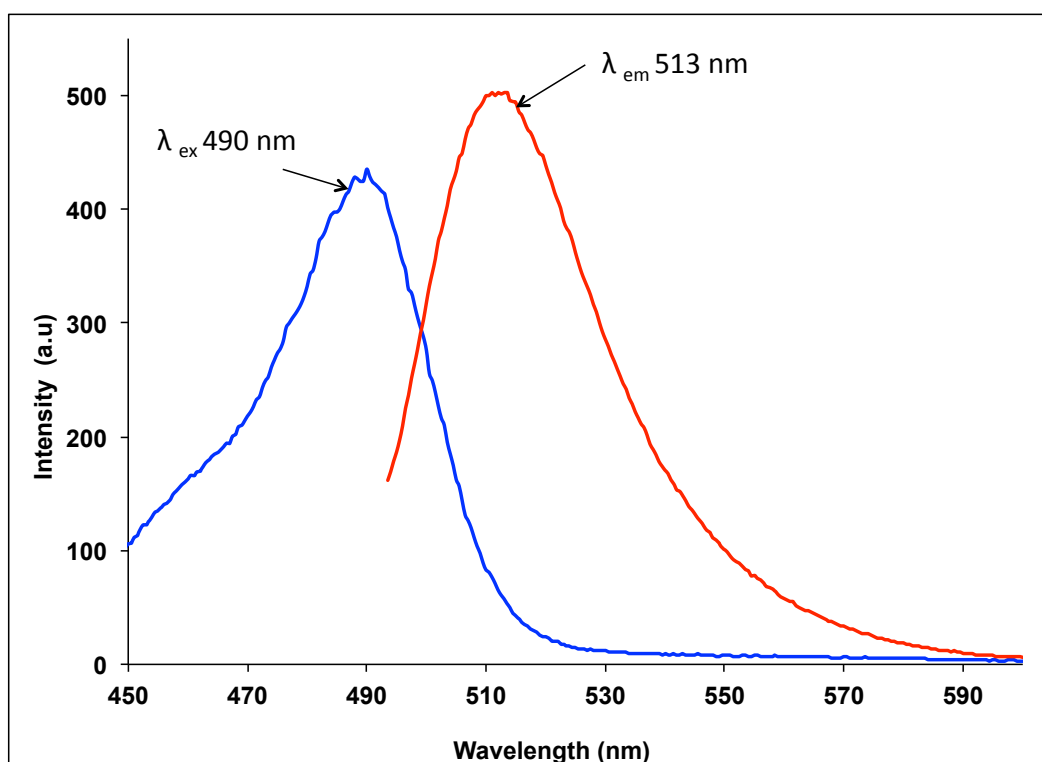


**Figure 16.** Excitation and emission spectra obtained for fluorescein obtained from the bathing solution for the ionogel membrane at pH 7 ( $T > LCST$ ) after 1 min. pH 9.2 yielded the same excitation and emission values. Spectra not shown for clarity.

**Table 3.** Concentration of released fluorescein (mM) for free standing Hydrogel and Ionogel membranes (triplicate) above the LCST (40°C). Standard deviation is presented in brackets.

	pH 4	pH 7	pH 9.2
Hydrogel			
1	-	0.0082	0.1981
2	-	0.0082	0.1971
3	-	0.0081	0.1957
<b>Average</b>	-	<b>0.0082</b>	<b>0.1970</b>
		<b>(4.97 x 10<sup>-5</sup>)</b>	<b>(1.20 x 10<sup>-3</sup>)</b>
Ionogel			
1	0.3025	0.3329	0.4845
2	0.3025	0.3616	0.5589
3	0.3020	0.3584	0.5712
<b>Average</b>	<b>0.3023</b>	<b>0.3510</b>	<b>0.5382</b>
	<b>(2.96 x 10<sup>-4</sup>)</b>	<b>(1.57 x 10<sup>-2</sup>)</b>	<b>(4.49 x 10<sup>-2</sup>)</b>

# Raman Spectroscopy

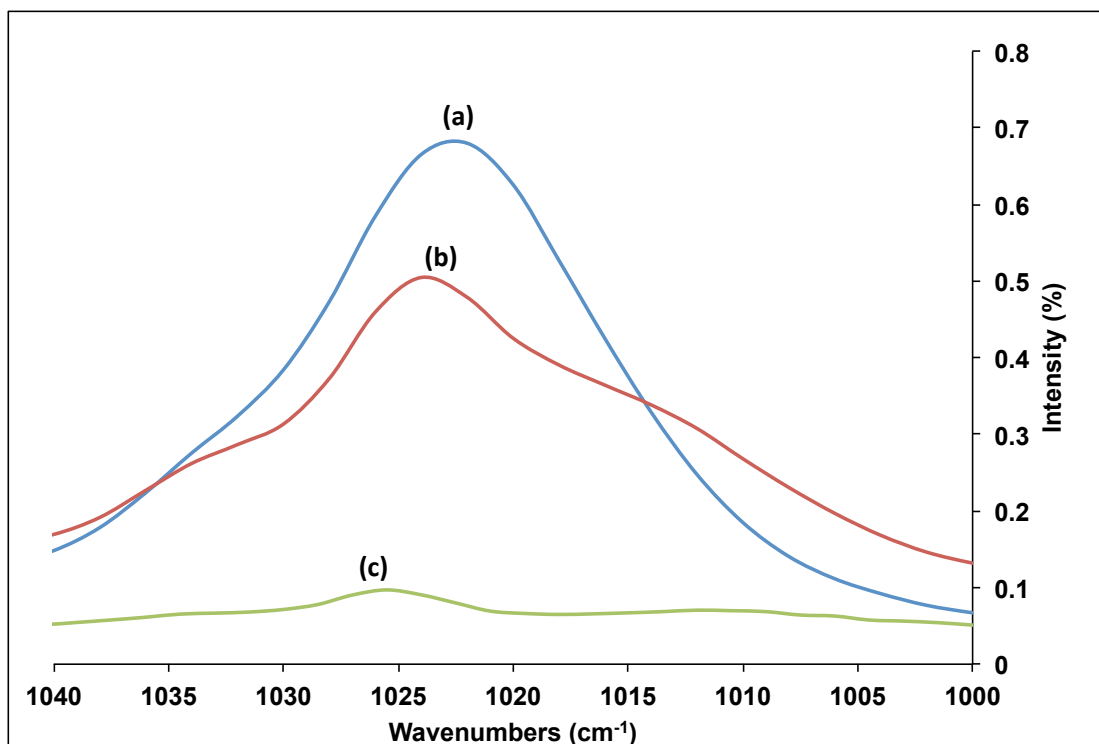


**Figure 17.** Raman spectra of symmetrical  $-\text{SO}_3^-$  stretch found in (a)  $[\text{C}_2\text{mIm}][\text{EtSO}_4]$ , (b) a 1:1 (v/v) IL at pH 4 containing Fluorescein and (c) a sample of the solution expelled from the ionogel above the LCST<sup>5</sup>.

## References

1. J. E. M. J. Earle, M. A. Gilea, J. N. C. Lopes, L. P. N. Rebelo, J. W. Magee, K. R. Seddon and J. A. Widegren, *Nature*, 2006, **439**, 831-834.
2. D. Fitzgerald and C. Du, *H&D Fitzgerald Ltd Publ*, 2000.
3. M. Brizard, M. Megharfi, E. Mahe and C. Verdier, *Review of Scientific Instruments*, 2005, **76**, 25109.
4. M. Ali, P. Dutta and S. Pandey, *J. Phys. Chem. B*, 2010, **114**, 15042-15051.
5. J. Kiefer, J. Fries and A. Leipertz, *Applied spectroscopy*, 2007, **61**, 1306-1311.

**Chapter 4: Swelling and Shrinking**  
**Properties of Thermo-responsive Polymeric**  
**Ionic Liquid Hydrogels with Embedded**  
**Linear pNIPAAm**

Simon Gallagher<sup>1</sup>, Larisa Florea<sup>2</sup>, Kevin J. Fraser<sup>2</sup> and Dermot Diamond<sup>1,2</sup>.

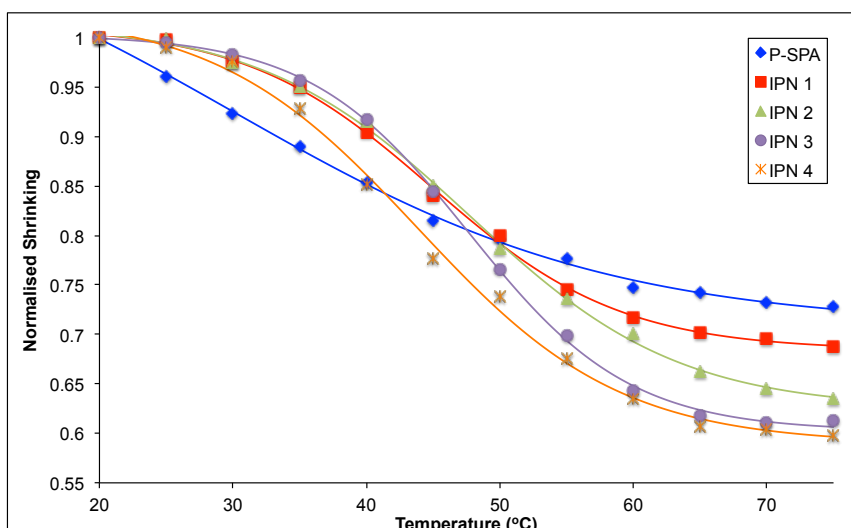
International Journal of Molecular Sciences, 5337-5349, **15**, 2014 DOI;

10.3390/ijms15045337

<sup>1</sup>CLARITY: Centre for Sensor Web Technologies, National Centre for Sensor  
Research, Dublin City University, Dublin 9, Ireland

<sup>2</sup> Insight Centre for Data Analytics, Dublin City University, Dublin, Ireland. Tel:  
+353 1 700 5404

For Supplementary Information see pg. 135



## Abstract

In this study, varying concentrations of linear pNIPAAm have been incorporated for the first time into a thermo-responsive polymeric ionic liquid (PIL) hydrogel, namely tributylhexylphosphonium 3-sulfopropylacrylate (P-SPA), to produce semi-interpenetrating polymer networks. The thermal properties of the resulting hydrogels have been investigated along with their thermo-induced shrinking and reswelling capabilities. The semi-IPN hydrogels were found to have improved shrinking and reswelling properties compared with their PIL counterpart. At elevated temperatures (50 – 80 °C), it was found that the semi-IPN with the highest concentration of hydrophobic pNIPAAm exhibited the highest shrinking percentage of ~ 40 % compared to the conventional P-SPA, (27 %). This trend was also found to occur for the reswelling measurements, with semi-IPN hydrogels producing the highest reswelling percentage of ~ 67 %, with respect to its contracted state. This was attributed to an increase in water affinity due to the presence of hydrophilic pNIPAAm. Moreover, the presence of linear pNIPAAm in the polymer matrix

leads to improved shrinking and reswelling response rates compared to the equivalent PIL.

## 4.1 Introduction

Ionic Liquids are classified as organic salts that possess melting points below 100 °C<sup>1</sup>. They have gained considerable attention in recent years due to their distinctive properties, including very low vapour pressure, good thermal stability and high ion conductivity<sup>2-4</sup>. An innovation that has arisen in recent years is a subclass of ILs called polymeric ionic liquids (PILs), prepared via polymerization of ionic liquid monomers, to form a solid, macromolecular structure.

The main features of PILs are that they combine all the unique properties associated with ILs, while being able to form coatings, gels, films and membranes due to their polymeric nature. Many different kinds of PILs have been designed and have found applications as functional polymers, namely solid polymer electrolytes<sup>5</sup>, lithium batteries<sup>6</sup>, solar cells<sup>7</sup>, biomedical<sup>8</sup> and electrochromic devices<sup>9</sup>.

Recently, a new class of PILs displaying thermo-responsive behaviour has been reported<sup>10-13</sup>. The development of these PILs creates possibilities for new applications such as selective extraction of water-soluble proteins<sup>10, 12, 14</sup>. The first reported thermo-responsive PIL to display phase separation at elevated temperatures; i.e. LCST (Lower Critical Solution Temperature) behaviour, consisted of a tetrabutylphosphonium cation and 4-styrene sulfonate anion<sup>15</sup>. When dissolved in water, this PIL precipitated at a temperature higher than its LCST, and re-dissolved when cooled below the LCST, much like the thermo-responsive polymer *N*-isopropylacrylamide (pNIPAAm)<sup>16</sup>. Following this report, several thermo-responsive

PILs have been developed based on variations of phosphonium cations, such as tetrabutyl or tributyl-hexyl, combined with anion derivatives based on benzenesulfonic acid<sup>10, 12, 13, 17</sup>.

Recently, we reported the polymerization of thermo-responsive monomeric ILs and subsequent formation of thermo-responsive PIL hydrogels<sup>18</sup>. In this work, we established suitable cross-linkers for the production of mechanically robust PIL hydrogels and investigated their endothermic transition behaviour. The cross-linked PILs were found to display a significant broadening of the temperature range over which LCST behaviour occurs compared with conventional thermo-responsive polymers like pNIPAAm.

However, the use of these temperature sensitive PIL hydrogels for applications such as polymer-based microfluidic valves is limited, because of their relatively slow response rate to temperature changes. Previous studies have proposed ways to improve the actuation kinetics of pNIPAAm-based hydrogels<sup>19-25</sup>. One of the most effective strategies has been the use of semi-interpenetrating networks (semi-IPNs)<sup>20, 24-26</sup>. Semi-IPNs are composed of two or more chemically distinct networks wherein one of the polymer components is cross-linked while the other is in its linear form. For example, linear pNIPAAm has been integrated into cross-linked hydrogel networks, to examine whether its rapid response rate could improve the shrinking and reswelling capabilities of the cross-linked polymer<sup>16, 20</sup>.

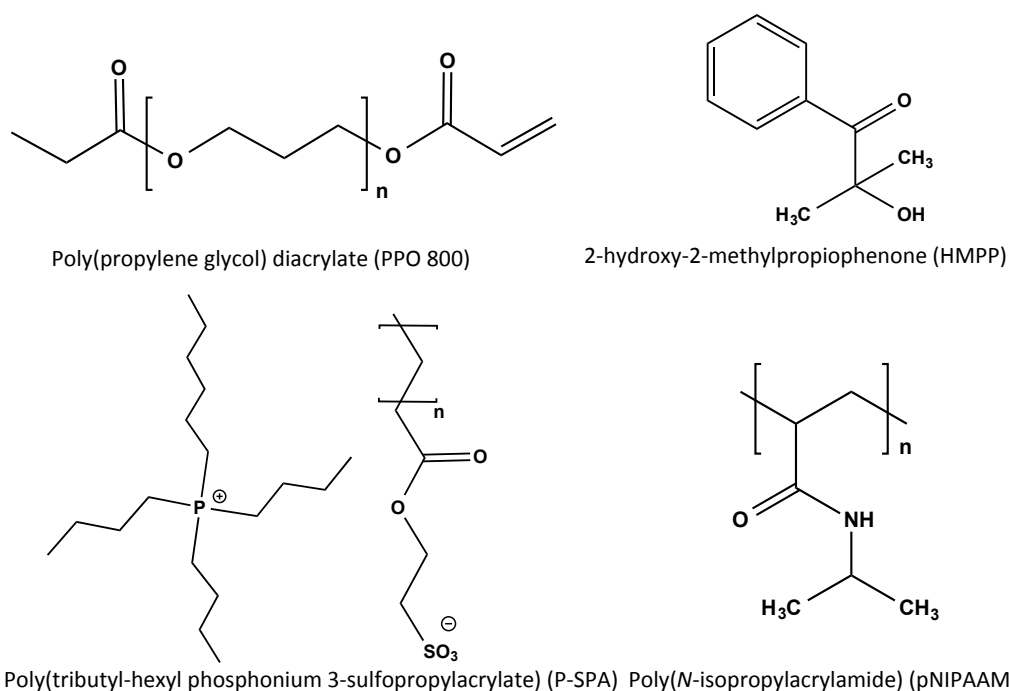


**Figure 4.1** Components used in the formulation of semi-IPN hydrogels used in this study.

In this study, a cross-linked tributylhexylphosphonium 3-sulfopropylacrylate (P-SPA) (Figure 4.1) hydrogel has been prepared with controlled amounts of linear pNIPAAm embedded in the hydrogel network in order to improve its actuation response characteristics. The resulting semi-IPN structures were investigated by measuring the shrinking behaviour of the hydrogels as a function of elevated temperature and the reswelling kinetics at room temperature. DSC was used to further understand the influence of pNIPAAm concentration on the PIL LCST behaviour.

## 4.2 Results and Discussion

### 4.2.1 Morphological Properties of Hydrogels

The feed compositions and sample ID of the semi-IPNs are summarized in Table 4.1. During the crosslinking process, the monomeric IL and linear pNIPAAm chains form

a semi-IPN network. To our knowledge, this is the first time linear pNIPAAm has been embedded in a thermo-responsive PIL hydrogel. In such a network, molecular interactions, such as hydrogen bonding, have been previously shown to occur between distinct polymers<sup>27, 28</sup>. Such interactions can result in different morphological, thermal and actuation properties manifested by the semi-IPN compared to traditional pNIPAAm polymers. Figure 4.2 shows examples of hydrogels with composition ranging from 1:0 to 1:1.2 P-SPA: pNIPAAm mol % ratio after removal from a 3 mm in diameter polydimethylsiloxane (PDMS) mould and exposure to water. In preliminary results, hydrogels exceeding 1:1.2 P-SPA:pNIPAAm mol % ratio were found to fragment when swollen in water. Therefore investigations into LCST swelling/contraction behaviour were restricted to hydrogels of composition 1:0 to 1:1.2 P-SPA:pNIPAAm mol % ratio, as this represented the range over which suitable physical robustness could be formed.

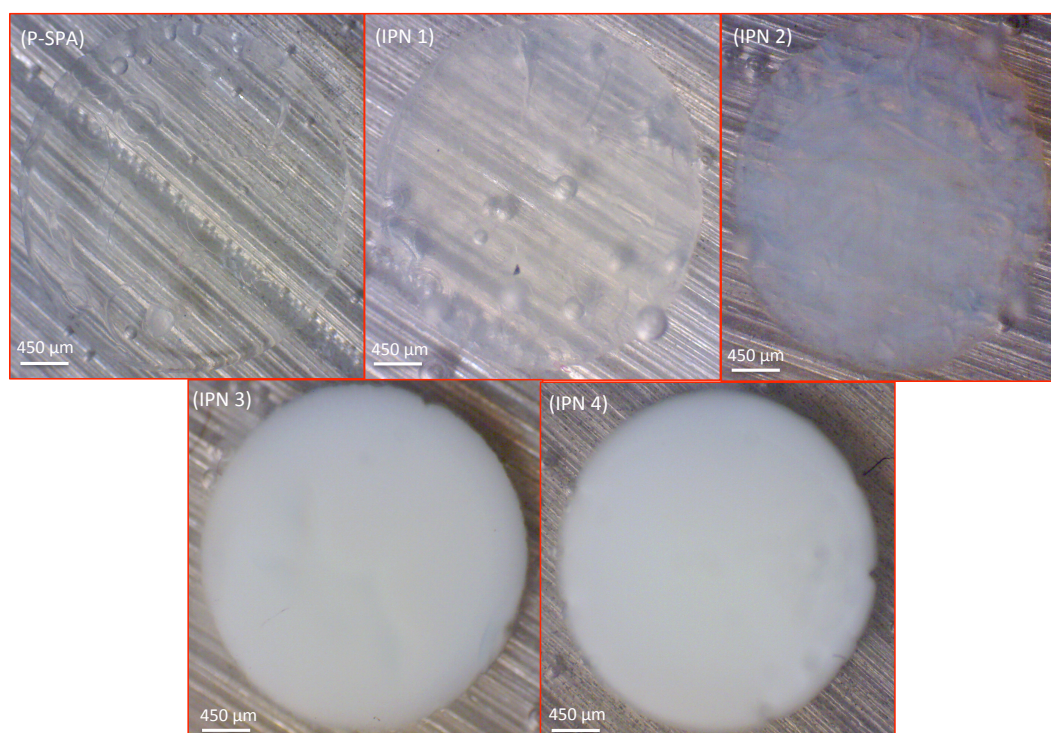
The images were recorded at 40 °C. Under these conditions, the pNIPAAm becomes hydrophobic and forms clathrate structures within the gels, which in turn produces an opaque appearance, as water is no longer bound to pNIPAAm<sup>16</sup>. Clearly, the opaque appearance of the gel increases as the mol % pNIPAAm is increased.

**Table 4.1.** Compositions of the semi-IPN Hydrogels. <sup>a</sup> 5 mol % concentration with respect to PIL. <sup>b</sup> 2 mol % concentration with respect to PIL.

Material	Sample ID				
	P-SPA	IPN 1	IPN 2	IPN 3	IPN 4
P-SPA ( $\mu\text{mol}$ )	800	800	800	800	800
pNIPAAm ( $\mu\text{mol}$ )	0	240	480	800	960
PPO 800 <sup>a</sup> ( $\mu\text{mol}$ )	40	40	40	40	40
HMPP <sup>b</sup> ( $\mu\text{mol}$ )	16	16	16	16	16
<b><i>P-SPA : pNIPAAm (mol ratio)</i></b>	<b><i>1:0</i></b>	<b><i>1:0.3</i></b>	<b><i>1:0.6</i></b>	<b><i>1:1</i></b>	<b><i>1:1.2</i></b>

The hydrogels polymerized in a PDMS mould 1 mm deep and 3 mm in diameter appeared to be mechanically stable in their swollen state after hydration. For example, they did not fragment during the experiments and handling was relatively simple during shrinking and reswelling measurements (Figure 4.2).

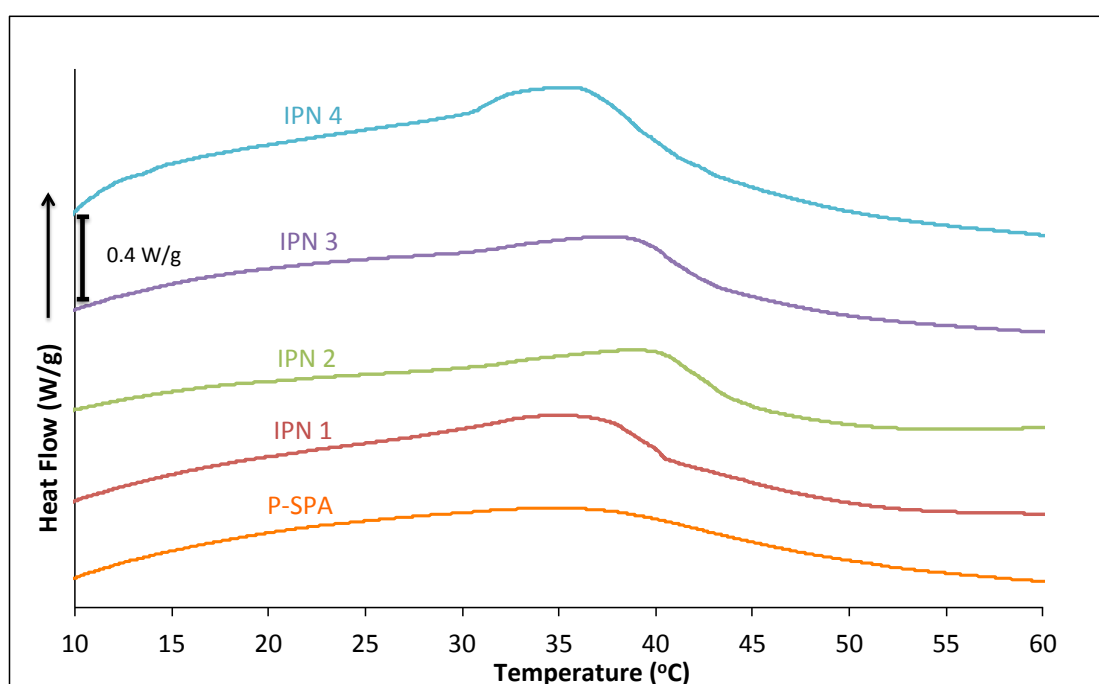
**Figure 4.2.** Hydrogels after polymerization in a circular mould (1 mm deep, 3 mm diameter) and subsequent swelling in deionized water at room temperature for 72 hours, followed by contraction in deionized water at 40 °C for approximately 2 minutes.



## 4.2.2 Thermal Behaviour of Hydrogels

In our previous study, we found that when crosslinked, the thermo-responsive P-SPA exhibited a broad endothermic transition in contrast to the more narrow peak of its linear form<sup>18</sup>. This phenomenon was attributed to the decreased level of freedom due to the bulky and highly charged nature of the PIL when in the cross-linked hydrogel state. Figure 4.3 illustrates that all of the hydrogels analysed in this study exhibit broad LCST transitions, in contrast to linear pNIPAAm, which has a relatively sharp LCST typically appearing around 30-35 °C<sup>16</sup>. The DSC profile for P-SPA is broad and featureless, with a maximum in the range 34-37 °C. In contrast, the hydrogels that containing linear pNIPAAm show a distinct feature in the range 34-40 °C superimposed on the broad P-SPA profile, which is due to the presence of the pNIPAAm (Table SI4-1). This suggests that the PIL and pNIPAAm components are, to some extent, retaining their independent characteristics within the semi-IPN hydrogels.

**Figure 4.3.** DSC endothermic transitions of hydrogels at heating rate 10 °C/min.



### 4.2.3 Shrinking Behaviour of Hydrogels

Prior to the shrinking experiments the hydrogels were allowed to swell in DI water as described in the experimental section. Although the initial diameter after polymerization for all of the hydrogels was 3 mm (equal to the diameter of the mould), they were found to exhibit different degrees of swelling (Table 4.2). The swollen diameter increased with increasing pNIPAAm content with the following trend: P-SPA < IPN 1 < IPN 2 < IPN 3. For hydrogel IPN 4, a reduction in the degree of swelling was observed relative to IPN 3, suggesting that there is an optimum amount of pNIPAAm in the hydrogel matrix around that of IPN 3 that maximises the water uptake. This effect may be due to the increasing concentration of pNIPAAm polymer chains decreasing the elasticity of the hydrogels, which in turn suppress the water uptake<sup>25,30</sup>.

Table 4.2 shows the diameter of the contracted hydrogels at 75 °C and their subsequent shrinking percentage with respect to their fully swollen diameter prior to shrinking. The trend in shrinking percentage follows the trend, P-SPA < IPN 1 < IPN 2 < IPN 3 < IPN 4. The hydrophobic nature of pNIPAAm, above its normal LCST of ~35 °C<sup>16</sup>, seems to have an effect on the semi-IPNs, increasing the degree of contraction. Above the LCST, hydrophobic interactions between isopropyl groups of pNIPAAm increase and polymeric chains start to aggregate and phase separation takes place. Entrapped water molecules are then freed due to broken hydrogen bonds, and the polymer collapses<sup>16</sup>. Previous studies have shown that the addition of linear pNIPAAm to a semi-IPN hydrogel increases shrinking at elevated temperatures<sup>25</sup>. The hydrogel IPN 4 is shown to have the greatest shrinking of 40.3 % at 75 °C. This is a substantial increase compared to the 27.3 % shrinking of P-SPA under the same

conditions. This shows that a greater concentration of hydrophobic pNIPAAm in the hydrogel increases the shrinking percentage at elevated temperatures.

**Table 4.2.** Shrinking properties of hydrogels at 75 °C. <sup>a</sup> Initial swollen diameter of gel after 72 hours in deionized water when temperature is 20 °C (n=3). <sup>b</sup> Contracted diameter of gel from fully hydrated state when temperature is 75 °C (n=3). <sup>c</sup> Percentage of shrinking of gel with respect to initial swollen diameter. <sup>d</sup> The slope of the reduction in diameter (mm) vs. temperature step (5 °C) for the data presented in Figure 4.4 calculated using the Boltzmann sigmoidal function (Equation SI4-1) <sup>31</sup>. Standard deviations are given in parentheses.

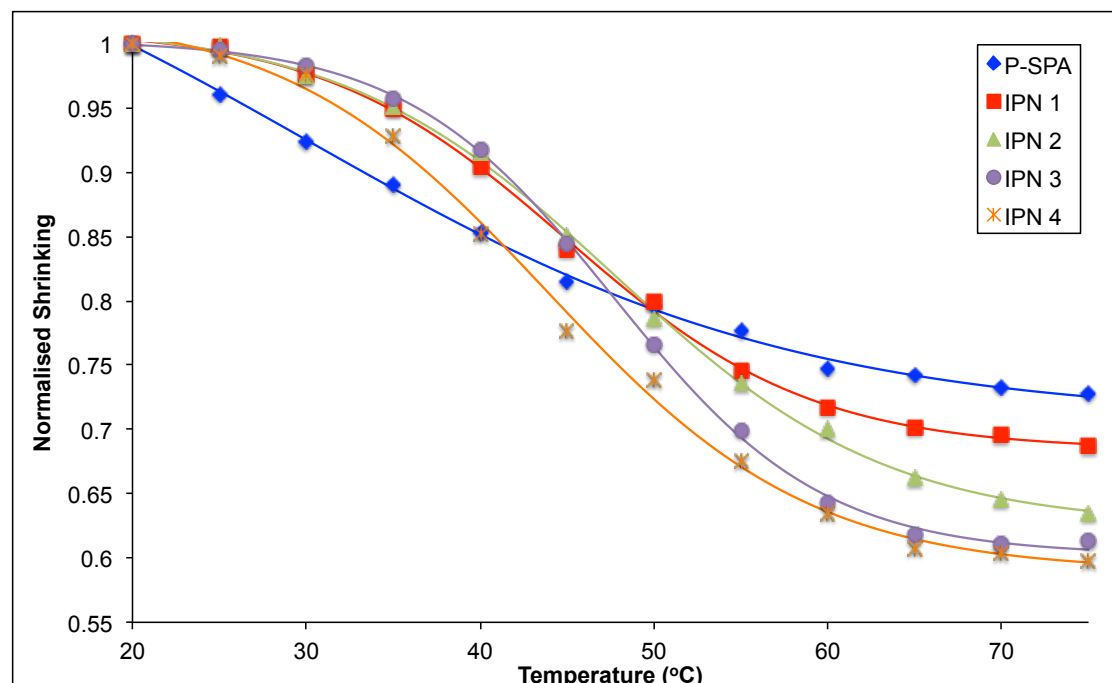
Sample	Initial Swollen Diameter <sup>a</sup> (mm)	Contracted gel diameter <sup>b</sup> (mm)	% Shrinking <sup>c</sup>	Slope <sup>d</sup>
P-SPA	5.33 (0.07)	3.88 (0.07)	27.2	-0.007
IPN 1	5.61 (0.01)	3.85 (0.06)	31.2	-0.011
IPN 2	6.11 (0.17)	3.88 (0.11)	36.4	-0.012
IPN 3	6.22 (0.07)	3.81 (0.14)	38.7	-0.016
IPN 4	5.73 (0.09)	3.43 (0.04)	40.2	-0.014

Figure 4.4 shows the shrinking profiles of the hydrogels from their initial swollen state at 20 °C to their contracted state at 75 °C at 5 °C increments. The normalised shrinking values represent the percentage change of the contracted diameters compared to their initial swollen diameter value. The data shows that all the samples shrink as the temperature is increased from 20 °C to 75 °C, which is in agreement with the endothermic transitions in the DSC study. It can be seen that the shrinking profiles of the semi-IPNs are slightly steeper than that obtained for P-SPA. The slopes of the hydrogel shrinking-profiles (Figure 4.4) give a numerical indication of the extent of the shrinking effect as a function of temperature. The slopes were derived from the best fit of the experimental data sets to the Boltzmann sigmoidal function

using Microsoft Excel Solver<sup>31</sup> and were found to follow the trend, P-SPA < IPN 1 < IPN 2 < IPN 4 < IPN 3 (Table 4.2). The data shows that the PIL-pNIPAAm IPN shrinks to a greater extent from 20 °C to 75 °C compared to the P-SPA. Previous studies have shown that the presence of pNIPAAm increases the number of pores in the morphology of semi-IPN hydrogels<sup>20</sup>. This leads to an increase in the surface area to bulk ratio, which in turn reduces the average diffusion pathlength for water within the material, and leads to more efficient movement of water into/out of the hydrogel. Therefore, the presence of pNIPAAm in the semi-IPNs produces a greater shrinking effect over this temperature range compared with P-SPA. Compared to the IPN samples, the P-SPA shrinking profile is very broad, and the effect very gradual over the entire temperature range studied, reaching ca. 27 % reduction from the initial swollen diameter. In contrast, with all the IPN samples, the effect is much more pronounced in terms of the extent of shrinking, and the temperature range over which it occurs, with a steady state reached at ca. 60 °C. For example, IPN 3 shrinks by ca. 40 % over the temperature range 30-60 °C.

From these data, it is apparent that the degree of temperature dependent contraction of the thermo-responsive PIL hydrogel can be controlled to some extent by varying the composition ratio of PIL/pNIPAAm in the semi-IPN material.

**Figure 4.4.** Temperature induced shrinking profiles of hydrogels from 20 °C to 75 °C at 5 °C increments, showing the best-fit of the experimental data (points) to a Boltzmann sigmoidal function (Equation SI4-1) <sup>31</sup>. Shrinking monitored by the reduction of diameter size relative to the initial swollen diameter (Table 4.1).



#### 4.2.4 Reswelling Behaviour of Hydrogels

Table 4.3 shows the reswelling data of the hydrogels from their contracted state when placed in deionized water at 20 °C as a function of the diameter of the gel disc sample. The reswollen diameters are similar to their initial swollen diameters (Table 4.2) ( $\pm 0.8\%$ ). This shows the gel reswelling behaviour is reasonably consistent with no observable hysteresis effect. The degree of reswelling follows the trend; P-SPA < IPN 1 < IPN 2 < IPN 3 < IPN 4; i.e. the semi-IPNs display greater swelling capabilities than the standard P-SPA hydrogel. The hydrogel IPN 4 exhibited the highest swelling at 67.6 % increase in diameter relative to its contracted state, which is nearly twice that of the P-SPA hydrogel, at 37.6 % diameter increase. The increase in swelling is due to the increasing influence of linear pNIPAAm on the water uptake behaviour of

the semi-IPN. The carbonyl and amide groups of pNIPAAm increase the hydrophilicity of the gel leading to an increase in water uptake and therefore greater tendency to swell in water.

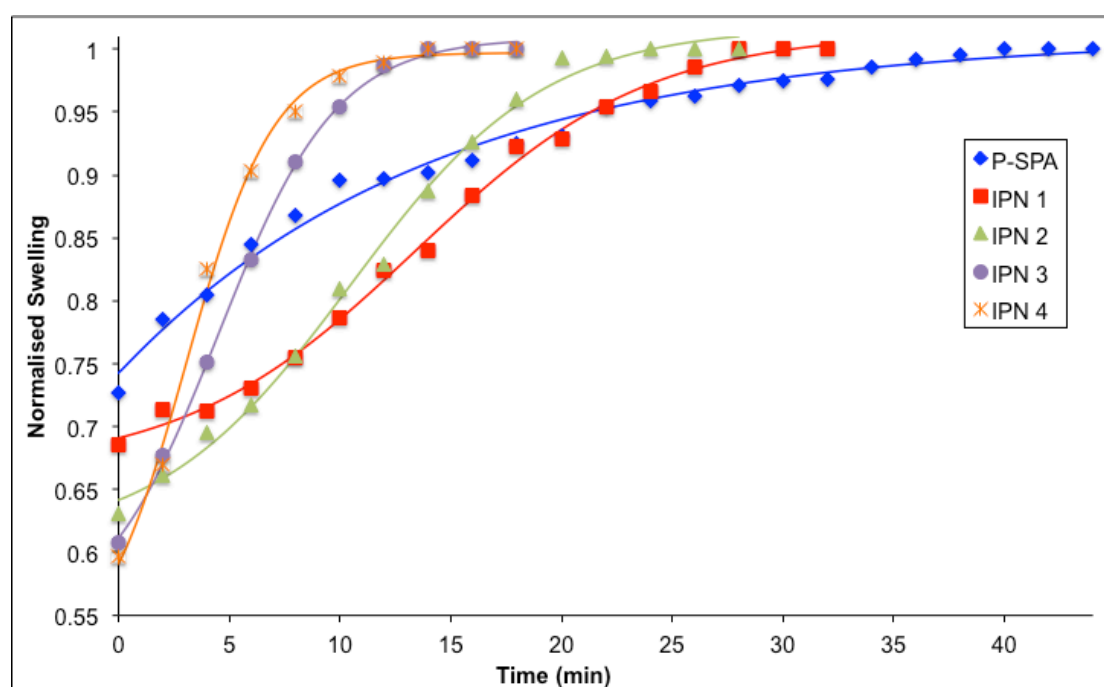
**Table 4.3.** Reswelling properties of hydrogels at room temperature. <sup>a</sup> Contracted diameter of gel at 75 °C (n=3). <sup>b</sup> Reswollen gel diameter from contracted state when temperature is 20 °C (n=3). <sup>c</sup> Percentage of reswelling of gel with respect to contracted gel diameter. <sup>d</sup> The slope of the reswelling kinetics was calculated using the Boltzmann sigmoidal function (Equation SI4-1) <sup>31</sup>. Standard deviations are given in parentheses.

Sample	Contracted gel Diameter	Reswollen gel	% Reswelling <sup>c</sup>	Slope <sup>d</sup>
	<sup>a</sup> (mm)	diameter <sup>b</sup> (mm)		(min <sup>-1</sup> )
P-SPA	3.88 (0.07)	5.34 (0.08)	37.6	0.014
IPN 1	3.85 (0.06)	5.62 (0.01)	45.8	0.016
IPN 2	3.88 (0.11)	6.16 (0.16)	58.8	0.023
IPN 3	3.81 (0.14)	6.27 (0.06)	64.4	0.044
IPN 4	3.43 (0.04)	5.75 (0.09)	67.6	0.062

In Figure 4.5, the reswelling profiles of the contracted hydrogels are shown as a function of time. The obtained diameter values were normalised by dividing them by the final reswollen diameter value. The contracted gels were placed in water at 20 °C and measurements taken over a period of up to 45 minutes. It can be seen that the semi-IPNs cease reswelling much earlier than the standard P-SPA. The slope of the reswelling profiles follows the trend; P-SPA < IPN 1 < IPN 2 < IPN 3 < IPN 4 (Table 4.3). The hydrogel P-SPA reaches its fully hydrated state after ~40 min, and the profile is very broad and gradual. In contrast, with IPN 3 and 4 the processes are essentially complete after ~14 min, and the extent of the swelling is greater at ca. 40% in both cases compared to ca. 25 % for P-SPA after 35 min. This behaviour is

consistent with the shrinking behaviour discussed earlier, which is ascribed to the increasing hydrophilicity and porosity as the %pNIPAAm increases in the semi-IPN.

**Figure 4.5.** Reswelling profiles of hydrogels from contracted state at 20 °C as a function of time. For better visualisation, the experimental data was fitted using a Boltzmann sigmoidal function (Equation SI4-1) <sup>31</sup>.



## 4.3 Experimental Section

### 4.3.1 Chemicals and Materials

*N*-isopropylacrylamide 98 % (NIPAAm), 2-hydroxy-2-methylpropiophenone 97 % (HMPP), Potassium 3-sulfopropylacrylate (SPA), and poly(propylene glycol) diacrylate Mn 800 (PPO 800) were purchased from Sigma Aldrich®, Ireland and used as received. Tetrabutylphosphonium chloride ( $[P_{4,4,4,4}][Cl]$ ) (Cyphos 443W) and tributyl-hexyl phosphonium chloride ( $[P_{4,4,4,6}][Cl]$ ) were supplied by Cytec® (Ontario Canada) which were column cleansed using aluminium (activated, basic, Brockmann

I) with dichloromethane used as the mobile phase. This was then removed under vacuum at 40 °C for 48 hrs at 0.1 Torr<sup>32</sup>.

### 4.3.2 Synthesis of pNIPAAM

The required amount of NIPAAM and HMPP (2 mol %) were dissolved in a vial containing 1:1 volume ratio of distilled water and ethanol. The solution was then stirred until homogenisation. The vial was then placed in a UV curing chamber ( $\lambda = 365$  nm, 3.5 mW/cm<sup>2</sup>) for 20 min. The resulting pNIPAAM was then purified by precipitation in water at 60 °C.

### 4.3.3 Synthesis of Tributyl-hexyl phosphonium 3-sulfopropylacrylate (P-SPA)

The IL monomer, namely tributylhexylphosphonium 3-sulfopropylacrylate (P-SPA) was synthesized according to previous studies<sup>18</sup>. 7 g of phosphonium chloride was mixed with 10 g of water and 1.2 molar equivalents of the anion salt ([Na][4-styrenesulfonate] for [P<sub>4,4,4,4</sub>][Cl] and [K][3-sulfopropylacrylate] for [P<sub>4,4,4,6</sub>][Cl], respectively). The mixture was stirred at room temperature for 48 hours. The IL was extracted from the water phase by dichloromethane (DCM). The DCM phase was reduced by a rotary evaporator and the residual liquid was dried at high vacuum (0.1 mBar) for 24 hours at room temperature. A final product yield of 95 % was obtained.

**P-SPA** <sup>1</sup>H NMR,  $\delta_H$  (400 MHz, CDCl<sub>3</sub>): 0.75-0.79 (t, 3H, CH<sub>3</sub>), 0.84-0.88 (t, 9H, CH<sub>3</sub>), 1.19-1.22 (m, 4H, CH<sub>2</sub>), 1.38-1.44 (m, 16H, CH<sub>2</sub>), 2.07-2.14 (m, 2H, CH<sub>2</sub>), 2.15-2.24 (m, 8H, CH<sub>2</sub>), 2.75-2.79 (m, 2H, CH<sub>2</sub>), 4.13-4.17 (t, 2H, CH<sub>2</sub>), 5.68-5.71 (dd, 1H, CH), 5.93-6.00 (q, 1H, CH), 6.23-6.28 (dd, 1H, CH) ppm.

#### 4.3.4 Preparation of Semi-IPN hydrogel.

The synthesized pNIPAAm was added to a vial containing the required amount of P-SPA, PPO 800 (5 mol %) and HMPP (2 mol %). For each gel, the mole ratios for NIPAAm, crosslinker and initiator were calculated with regard to the IL monomer content. The concentration of crosslinker and initiator are with respect to P-SPA. The contents of the vial were stirred with a magnetic stirrer until the pNIPAAm was dissolved and the result solution was homogenised. The solution was then quickly cast into a PDMS mould. The gels were polymerised for 40 min in a UV curing chamber that produced 365 nm UV light intensity of 3.5 mW/cm<sup>2</sup>.

These semi-IPN structures were then immersed in deionized water at room temperature for at least 72 hours to reach equilibrium and to extract any unreacted monomers. The water was refreshed every several hours during this treatment. The feed compositions and sample ID of the reaction are summarized in Table 4.1.

#### 4.3.5 Thermobehaviour of Semi-IPN Hydrogels

The LCST behaviour of the swollen gels was monitored on a Q200 DSC TA instrument. Thermal scans below room temperature were calibrated with the cyclohexane solid-solid transition and melting point at -87.0 °C and 6.5 °C, respectively. Thermal scans above room temperature were calibrated using indium, tin and zinc with melting points at 156.6, 231.93 and 419.53 °C, respectively. Approximately 10 mgs of the water-swollen samples were placed on a tissue to remove excess water and were weighed on a microscale before the DSC measurement. These samples were then placed on aluminium DSC plates and sealed. The LCST

values for these samples were determined by thermal scans at 10 C/min with the following temperature program: Heat from 0 °C to 90 °C then cool from 90 °C to 0 °C. This process was repeated three times in order to observe if the endothermic process was reproducible. The LCSTs were determined as the endothermic peak during heating.

#### 4.3.6 Measurement of Shrinking of Semi-IPN Hydrogels

After polymerisation in the PDMS mould (1 mm deep and 3 mm diameter), the gels were allowed to fully swell for 72 hours in deionized water at 20 °C, before the shrinking measurements were taken. The imaging was performed using an Aigo GE-5 microscope with a 60x objective lens and the accompanying Aigo ScopeImage 9.0 software. The gels were placed on an aluminium plate resting on an Anton Paar MCR 301 Rheometer peltier holder. The plate was filled with DI water and covered with a glass plate to avoid evaporation of water. The glass plate was also in contact with the filling water to avoid condensation. Temperature of the holder was controlled by the rheometer software and was ramped up from 20 °C to 75 °C by 5 °C steps. During each step the temperature around the sample was checked with a Fluke 62 Mini IR thermometer and the diameter of the gel was taken once the temperature stabilised after approximately 2 min. This experiment was performed for three samples of each type of gel. The microscope software was used to measure the diameter of the gel and this value was compared to a diameter value obtained using a MATLAB R2010a program for validation purposes (Figure SI4-1). For better visualisation, the experimental data was fitted using a Boltzmann sigmoidal function (Equation SI4-1) using Microsoft EXCEL Solver<sup>31</sup>. An example can be found in the supplementary information (Figure SI4-2).

### 4.3.7 Measurement of Reswelling of Semi-IPN Hydrogels

The contracted gels were placed in deionized water on the Anton Paar MCR 301 Rheometer peltier holder. Temperature was controlled by the holder rheometer software and was kept at 20 °C throughout the experiment. Images were taken using an Aigo GE-5 microscope with a 60x objective lens and the accompanying software. Images were taken every two minutes until the gel swelling appeared to stop. This experiment was performed for three samples of each type of gel. The diameter of the gel was measured as described in section *3.6 Measurement of Shrinking of Semi-IPN Hydrogels*. For better visualisation, the experimental data was fitted using a Boltzmann sigmoidal function (Equation SI4-1) using Microsoft EXCEL Solver<sup>31</sup>.

## 4.4 Conclusions

In this study, cross-linked thermo-responsive PIL hydrogels were prepared with different concentrations of linear pNIPAAm chains incorporated in each gel, producing novel semi-IPN networks. The DSC data showed that the presence of pNIPAAm caused a narrowing of the broad LCST transition shown by the PIL hydrogel, which was attributed to the fast response nature of the linear pNIPAAm chains.

At elevated temperatures, the presence of hydrophobic pNIPAAm within the semi-IPN network provided an increased shrinking percentage of 40.3 % compared to the respective 27.3 % of P-SPA. Moreover, the hydrophilic presence of pNIPAAm

provided a platform for higher and quicker reswelling at room temperature. These novel semi-IPN hydrogels are found to exhibit interesting swelling/contraction trends with respect to linear pNIPAAm concentration within the gel. In terms of producing gels with the best actuation characteristics for potential applications such as flow control in microfluidics, a composition around that of IPN 3/IPN 4 would appear to be optimum, as these gels show the largest swollen diameters, the largest degree of shrinking, and the most rapid rate of reswelling (compare data in Table 4.2, Table 4.3).

## Acknowledgments

This publication has emanated from research conducted with the financial support of Science Foundation Ireland (SFI) under grant number's SFI/12/RC/2289 and 07/CE/I1147.

## 4.5 References

1. J. S. Wilkes and M. J. Zaworotko, *Journal of Chemistry Society, Chemical Communications*, 1992, 965.
2. P. Wassersheid and T. Welton, *Wiley-VCH, Weinheim*, 2003, **2nd edition**, 1-380.
3. T. Welton, *Chemistry Review*, 1999, **99**, 2071-2084.
4. K. J. Fraser and D. R. MacFarlane, *Australian Journal of Chemistry*, 2009, **62**, 309-321.
5. H. Ohno, *Macromolecular Symposia*, 2007, **249-250**, 551-556.
6. A.-L. Pont, R. Marcilla, I. De Meazza, H. Grande and D. Mecerreyes, *Power Sources*, 2009, **188**, 558.
7. K. Suzuki, M. Yamaguchi, S. Hotta, N. Tanabe and S. Yanagida, *Journal of Photochemistry and Photobiology A: Chemistry*, 2004, **164**, 81-85.

8. R. Marcilla, M. Sanchez-Paniagua, B. Lopez-Ruiz, E. Lopez-Cabarcos, E. Ochoteco, H. Grande and D. Mecerreyes, *Journal of Polymer Science Part A: Polymer Chemistry*, 2006, **44**.
9. M. Kijima, K. Setoh and H. Shirakawa, *Chemistry Letters*, 2000, **29**, 936.
10. Y. Kohno and H. Ohno, *Physical Chemistry Chemical Physics*, 2012, **14**, 5063-5070.
11. Y. Fukaya, K. Sekikawa, K. Murata, N. Nakamura and H. Ohno, *Chemical Communications (Cambridge, England)*, 2007, 3089-3091.
12. Y. Kohno and H. Ohno, *Chemical Communications (Cambridge, England)*, 2012, **48**, 7119-7130.
13. Y. Kohno, Y. Deguchi and H. Ohno, *Chemical communications (Cambridge, England)*, 2012, **48**, 11883-11885.
14. K. Fujita, D. MacFarlane, M. Forsyth, M. Yoshizawa-Fujita, K. Murata, N. Nakamura and H. Ohno, *Biomacromolecules*, 2007, **8**, 2080-2086.
15. Y. Kohno and H. Ohno, *Australian Journal of Chemistry*, 2011, **65**, 91-94.
16. H. G. Schild, *Progressive Polymer Science*, 1992, **17**, 163-249.
17. Y. Men, H. Schlaad and J. Yuan, *ACS Macro Letters*, 2013, **2**, 456-459.
18. B. Ziolkowski and D. Diamond, *Chemical Communications*, 2013, **49**, 10308-10310.
19. X.-Z. Zhang, X.-D. Xu, S.-X. Cheng and R.-X. Zhuo, *Soft Matter*, 2008, **4**, 385-391.
20. X.-Z. Zhang and C.-C. Chu, *Journal of Applied Polymer Science*, 2003, **89**, 1935-1942.
21. X.-Z. Zhang, Y.-Y. Yang, T.-S. Chung and K.-X. Ma, *Langmuir*, 2001, **17**, 6094-6099.
22. X.-D. Xu, B. Wang, Z.-C. Wang, S.-X. Cheng, X.-Z. Zhang and R.-X. Zhuo, *Journal of Biomedical Materials Research. Part A*, 2008, **86**, 1023-1032.
23. X. S. Wu, A. S. Hoffman and P. Yager, *Journal of Polymer Science Part A: Polymer Chemistry*, 1992, **30**, 2121-2129.
24. M. R. Guilherme, G. M. Campese, E. Radovanovic, A. F. Rubira, E. B. Tambourgi and E. C. Muniz, *Journal of Membrane Science*, 2006, **275**, 187-194.
25. M. R. Guilherme, R. da Silva, A. F. Rubira, G. Geuskens and E. C. Muniz, *Reactive and Functional Polymers*, 2004, **61**, 233-243.

26. F. Vidal, C. Plesse, H. Randriamahazaka, D. Teyssie and C. Chevrot, *Molecular Crystals and Liquid Crystals*, 2006, **448**, 287–291.
27. J. Zhang and N. A. Peppas, *Journal of Applied Polymer Science*, 2001, **82**, 1077-1082.
28. Y. Maeda, T. Higuchi and I. Ikeda, *Langmuir*, 2001, **17**, 7535-7539.
29. L. Hengjie, C. Qianjin and W. Peiyi, *Soft Matter*, 2013, **9**, 3985-3993.
30. E. C. Muniz and G. Geuskens, *Journal of Materials Science: Materials in Medicine*, 2001, **12**, 879-881.
31. S. Walsh and D. Diamond, *Talanta*, 1995, **42**, 561-572.
32. M. Earle, J. Esperanca, M. Gilea, J. Lopes, L. Rebelo, J. Magee, K. Seddon and J. Widegren, *Nature*, 2006, **439**, 831-834.

**Chapter 4: Supporting Information**

**Swelling and Shrinking Properties of**

**Thermo-responsive Polymeric Ionic Liquid**

**Hydrogels with Embedded Linear**

**pNIPAAm**

Simon Gallagher<sup>1</sup>, Larisa Florea<sup>2</sup>, Kevin J. Fraser<sup>2</sup> and Dermot Diamond<sup>1,2</sup>.

International Journal of Molecular Sciences, 5337-5349, **15**, 2014 DOI;

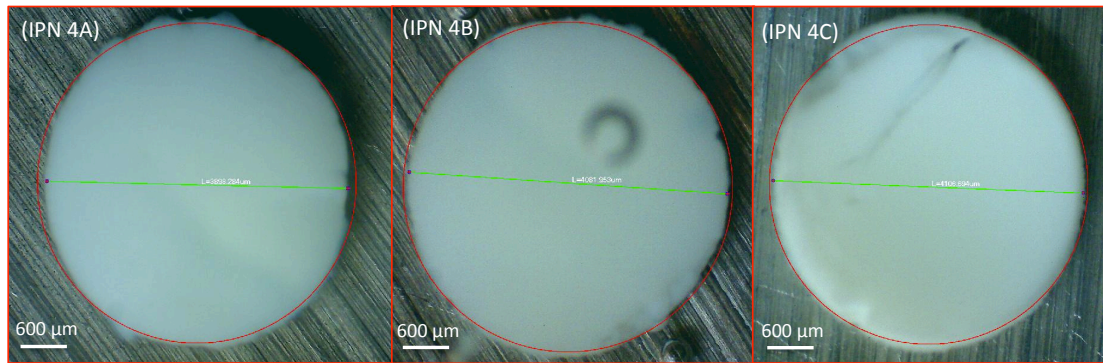
10.3390/ijms15045337

<sup>1</sup>CLARITY: Centre for Sensor Web Technologies, National Centre for Sensor  
Research, Dublin City University, Dublin 9, Ireland

<sup>2</sup> Insight Centre for Data Analytics, Dublin City University, Dublin, Ireland. Tel:

+353 1 700 5404

## Example of shrinking measurement



Sample	Microscope Diameter (mm)	MATLAB Circle Diameter (mm)
IPN 4A	3.898	4.123
IPN 4B	4.081	4.211
IPN 4C	4.106	4.258

**Figure 1.** Three examples of IPN 4 in deionized water at 40 °C captured with Aigo GE-5 microscope with a 60x objective lens and the diameter measured using Aigo ScopeImage 9.0 software. The measured diameters are then compared with a MATLAB R2010a program for validation purposes.

## Swelling and reswelling kinetics

The shrinking and reswelling kinetics were modeled using the Boltzmann sigmoidal function given below.

$$y = \frac{A_1 - A_2}{1 + e^{(x-x_0)/dx}} + A_2$$

where  $A_1$  is the low Y limit,  $A_2$  is

the high Y limit,  $x_0$  is the inflection (half amplitude) point and  $dx$  is the width.

For IPN1-4, the slope at  $x_0$  was calculated with the formula:  $\text{slope} = (A_2 - A_1)/4dx$ , according to the BOLTZMANN equation.

For P-SPA the slope was calculated graphically as the data does not show an inflection point.

Example of fitting of experimental data of shrinking kinetics using Boltzmann sigmoidal function;

**IPN 3:**

Adj. R-Square 0.9993

		Value	Standard Error
B	A1	1.00315	0.00333
B	A2	0.60235	0.00338
B	x0	47.67935	0.22474
B	dx	6.008	0.21836

**Slope calculated = -0.0166**

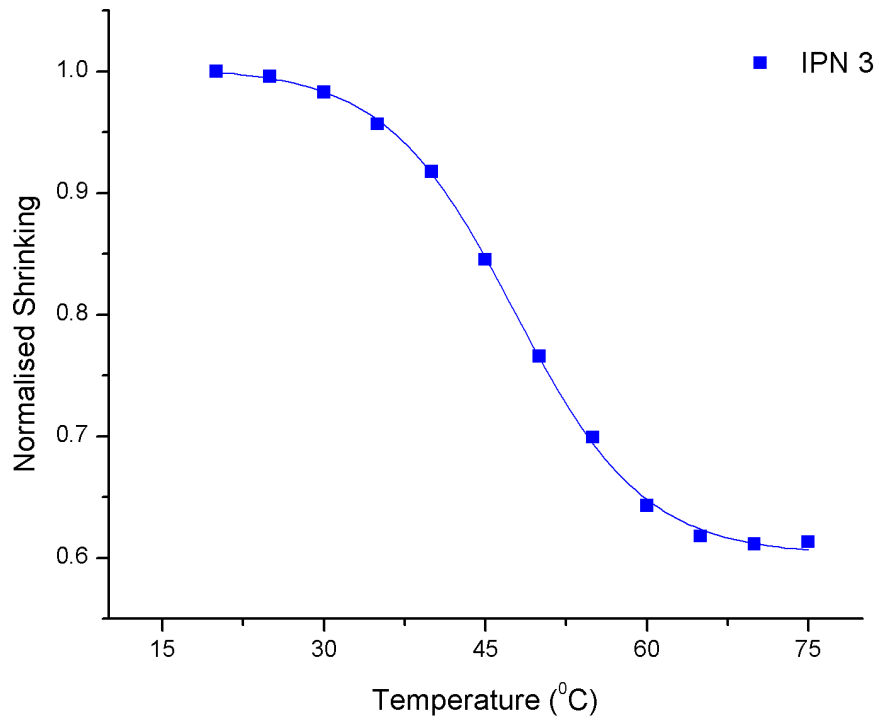


**Figure 2.** Shrinking data of IPN 3 fitted using Boltzmann sigmoidal function

# **Chapter 5: Synthesis and Characterisation of 1-Vinylimidazolium-based Polymeric Alkyl Sulphate Ionic Liquids**

Simon Gallagher<sup>1</sup>, Bartosz Ziolkowski<sup>1</sup>, Eoin Fox<sup>2</sup>, Kevin J. Fraser<sup>3</sup> and Dermot  
Diamond<sup>1, 3</sup>.

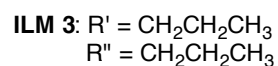
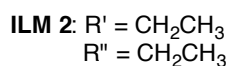
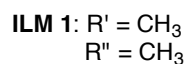
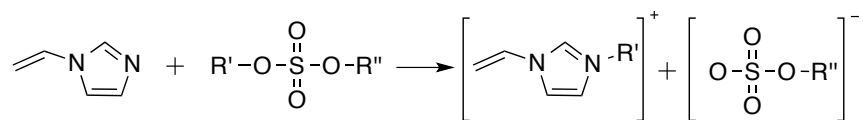
Macromolecular Chemistry and Physics 2014, Accepted

<sup>1</sup> CLARITY: Centre for Sensor Web Technologies, National Centre for Sensor  
Research, Dublin City University, Dublin 9, Ireland

<sup>2</sup> School of Chemistry, Dublin City University, Dublin 9, Ireland

<sup>3</sup> Insight Centre for Data Analytics, Dublin City University, Dublin, Ireland. Tel:  
+353 1 700 5404

For Supplementary Information see pg. 160



## Abstract

Three ionic monomers based on a 1-vinylimidazolium cation, 1-vinyl-3-methylimidazolium methyl sulphate, 1-vinyl-3-ethylimidazolium ethyl sulphate and 1-vinyl-3-propylimidazolium propyl sulphate have been synthesized and characterized by thermal and spectroscopic methods. The ionic liquid monomers (ILMs) were prepared using a halide-free route under ambient conditions by the quaternization reaction of 1-vinylimidazoles with alkyl sulphates. Through free-radical polymerization and rheology analysis, solid free-standing linear polymeric ionic liquid (PILs) films were obtained with a  $\tan\delta$  value as low as 0.180. After polymerization, thermal methods showed the linear PILs to possess a thermal stability of up to 340 °C, while rheology analysis revealed the films to have a storage moduli value as high as  $4.64 \times 10^6$  Pa.

## 5.1 Introduction

A progression in recent years from utilizing ILs in materials research has been the development of Polymeric Ionic Liquids (PILs). These are polymers that contain an ionic liquid species as part of their constitutional repeating monomer unit, which forms the solid, macromolecular structure.

Salamone *et al.* first published several vinylimidazolium-based ILs in the 1970s.<sup>1,2</sup> However, this did not receive much attention at the time. Since the end of the 1990s, Ohno and co-workers pioneered the polymerization of numerous types of IL monomers in pursuit of solid ion conductor materials,<sup>3-5</sup> producing imidazolium-based flexible polymers that exhibited ionic conductivity of up to  $1.88 \times 10^{-4} \text{ Scm}^{-1}$  at 30 °C.<sup>5</sup> Currently the area of PIL electrolytes has garnered plenty of interest<sup>6-11</sup> as they combine all the unique properties associated with ionic liquids (ILs), such as good ionic conductivity, thermal stability, non-volatility, and wide electrochemical stability, amongst others,<sup>12</sup> while also being able to form coatings, gels, films and membranes due to their polymeric nature.

Through variation of the cationic and/or anionic structures, PILs offer great flexibility for the regulation of their properties. This variation has led to the synthesis of novel PILs for utilization as a new class of polymers that combine the beneficial properties of ILs with those of classical polyelectrolytes.<sup>13, 14</sup> Potential applications of these new materials include lithium batteries,<sup>15</sup> solar cells,<sup>16</sup> biomedical<sup>17</sup> and electrochromic devices.<sup>18</sup> Therefore, the synthesis and characterization of novel PILs is of high scientific interest.

Solid polymer electrolytes based on imidazolium salts offer a number of advantages compared to other liquid electrolytes. They have a wide window of electrochemical stability<sup>12</sup> and do not decompose at temperatures of up to 350 °C. *N*-vinylimidazolium-based IL monomers are commonly prepared by quaternization reaction of a *N*-vinylimidazole with a halo-alkane compound. An attractive aspect of PILs derived from *N*-vinylimidazolium-based monomers is the potential to incorporate relatively high content of imidazolium cations by simply varying the alkyl chain length. Moreover, anion exchange can be performed by a simple metathesis reaction by replacing the halide with the desired anion, leading to modifications in properties such as thermal and ionic transport.<sup>19</sup>

For some anions, such as nitrate and dicyanamide, silver salts can assist the anion exchange process.<sup>20</sup> However, the complete removal of the by-product (silver halide) can be problematic.<sup>21</sup> The presence of halide contamination has also been shown to drastically alter physical properties, such as viscosity.<sup>22</sup> The use of volatile alkyl halides as alkylating agents, such as chloroethane, can also lead to preparative issues, which requires use of pressurized vessels in a laboratory.

Attempts have been previously reported in pursuit of a direct synthesis of *N*-vinylimidazolium-based ILs free of halides. Ohno and co-workers used the neutralization reaction of *N*-vinylimidazole with a corresponding acid in order to synthesize IL monomers in a single step.<sup>23</sup> Specifically, a non-halide tetrafluoroboric acid was reacted with *N*-vinylimidazole producing a monomer free of by-product and a halide anion. Zhang *et al.* also developed a halide-free process to produce a 1-vinyl-3-ethylimidazolium ethylsulphate monomer as a precursor for anion-exchange metathesis.<sup>24</sup>

In this work, 1-vinylimidazolium alkyl sulphate ILMs are synthesized using a direct, halide-free quaternization reaction under ambient conditions. The synthesis of the monomers is a simple one-pot reaction, with high-purity products obtained without time-consuming purification steps.

The polymerization behaviours of the ILMs are investigated using rheology, while the physicochemical and mechanical properties of the subsequent PILs are investigated and reported.

## 5.2 Experimental Section

### 5.2.1 Chemicals and Materials

1-vinylimidazole (Sigma-Aldrich, Ireland) was vacuum distilled at 75 °C, 0.1 Torr until a clear liquid was obtained. Dimethyl sulphate (99.8 %) (Sigma-Aldrich, Ireland) and diethyl sulphate (98 %) (Sigma-Aldrich, Ireland) were used as received, while dipropyl sulphate (TCI Chemicals, Ireland) was vacuum distilled as described above. 2-hydroxy-2-methylpropiophenone (HMPP) (Sigma-Aldrich, Ireland) (97 %) was used as received.

### 5.2.2 Characterization

$^1\text{H}$  and  $^{13}\text{C}$  NMR spectra were obtained with a Bruker 400 MHz spectrometer at 25 °C. ILM 1 was dissolved in deuterated DMSO, while ILM 2 and 3 were dissolved in deuterated chloroform. The spectra were analysed using Bruker TopSpin software.

Fourier transform Infrared spectra (FT-IR) were obtained with a Perkin Elmer Spectrum 100 instrument equipped with an attenuated total reflectance (ATR)

accessory, which was used in transmittance mode from 700 to 3200  $\text{cm}^{-1}$  with a resolution of 2  $\text{cm}^{-1}$ .

The thermal behaviour of the samples was determined using Q200 DSC and Q50 TGA instruments (TA Instruments). DSC scans were performed at a heating rate of 2  $^{\circ}\text{C min}^{-1}$  and TGA scans at a heating rate of 10  $^{\circ}\text{C min}^{-1}$ . Thermal scans below room temperature were calibrated with the cyclohexane solid-solid transition and melting point at  $-87.0^{\circ}\text{C}$  and  $6.5^{\circ}\text{C}$ , respectively. Thermal scans above room temperature were calibrated using indium, tin and zinc with melting points at 156.60, 231.93 and  $419.53^{\circ}\text{C}$ , respectively.

Viscosity measurements of the ILMs were carried out at 20  $^{\circ}\text{C}$  on an Anton Paar MCR301 rheometer equipped with a CP50 cone measuring tool, employed at a shear rate of up to 1000  $\text{s}^{-1}$ .

For the linear PILs, the evolution of the mechanical properties during polymerization was measured using the same rheometer and measuring cone. The rheometer had a bottom glass plate transparent to UV light. The polymerization mixture of 1.1 ml volume was placed on the glass plate and pressed with the 50 mm measurement tool with a gap of 208  $\mu\text{m}$ . A UV lamp with a peak emission wavelength of 365 nm was placed 40 mm under the glass plate. At the top of the rheometer plate where polymerization takes place, the light intensity of the UV lamp was measured with a Lutron UV-340A UV probe and found to be 950  $\mu\text{W/cm}^2$ . To monitor the polymerization and mechanical properties of PILs in real time, rheology measurements were taken over a period of 115 min. The UV light was switched on after 60 s. The storage and loss moduli were analysed at 0.1 % strain and 1 Hz oscillation frequency, and plotted against time. Data points were collected every 10 s.

For linear films, mechanical stability was measured using a PP15 cone, exerting 0.01-100 % strain on the polymer sample with an angular frequency ( $\omega$ ) of 10 rad/s. Data points were collected every 30 s. The values tabulated were when the polymer's storage modulus value decreases below 95 % as a function of stress.

Solubility of linear PILs was performed in a vial with a weight ratio of 1:1 PIL/solvent.

## 5.3 Experimental Section

### 5.3.1 1-vinyl-3-methylimidazolium methyl sulphate (ILM 1)

The *1-vinyl-3-methylimidazolium methyl sulphate* ionic liquid monomer was synthesized using a procedure similar to a previous approach.<sup>25</sup> In a three neck round-bottom flask, 1-vinylimidazole (10 g, 0.106 mole) was stirred in toluene (50 mL) and cooled in an ice-bath, under nitrogen. Cold diethyl sulphate (10.07 mL, 0.106 mole) was then added dropwise. It is important to maintain this reaction at a low temperature, as this reaction is highly exothermic. Formation of the IL product was immediate, causing the solution to turn opaque. Separation of the toluene solution and the denser IL phase was then carried out as follows: The reaction mixture was allowed to reach room temperature with constant stirring for 1 h. It is important not to allow the IL phase to crystallize as this makes removal of unreacted materials very difficult. The upper, organic phase was decanted, and the lower IL phase was washed with toluene (25 mL). The toluene phase was then reduced by rotary evaporation and

the residual liquid was dried at high vacuum 0.1 mBar for 24 h at room temperature.

A final colourless, crystallized product was obtained with a yield of 78 %.

$^1\text{H}$  NMR (400 MHz,  $\text{DMSO}_d$ ;  $\delta_{\text{H}}$ ): 3.39 (s, 3H,  $\text{NCH}_3$ ), 3.89 (s, 3H,  $\text{OCH}_3$ ), 5.45 (m, 1H,  $\text{NCH}=\text{CH}_2$ ,  $\text{H}^{\text{A}}$ ), 5.92 (m,  $\text{NCH}=\text{CH}_2$ ,  $\text{H}^{\text{B}}$ ), 7.27 (m, 1H,  $\text{NCH}=\text{CH}_2$ ), 7.84 (s, 1H, H5 (Im)), 8.17 (s, 1H, H4, (Im)), 9.40 (s, 1H, H2 (Im)) ppm (Figure SI4-3).

$^{13}\text{C}$  NMR (400 MHz,  $\text{DMSO}_d$ ;  $\delta_{\text{C}}$ ): 36.01 ( $\text{NCH}_3$ ), 52.79 ( $\text{OCH}_3$ ), 108.45 ( $\text{NCH}=\text{CH}_2$ ), 118.80 ( $\text{NCH}=\text{CH}_2$ ), 124.42 (C(5)H), 128.81 (C(4)H), 135.88 (C(2)H) ppm.

### 5.3.2 1-vinyl-3-ethylimidazolium ethyl sulphate (ILM 2)

Synthetic procedure was as indicated for *ILM 1* with diethyl sulphate used in place of dimethyl sulphate. Yield: 75 %, colourless, slightly viscous liquid.

$^1\text{H}$  NMR (400 MHz,  $\text{CDCl}_3$ ;  $\delta_{\text{H}}$ ): 1.29 (t, 3H,  $\text{NCH}_2\text{CH}_3$ ), 1.58 (t, 3H,  $\text{OCH}_2\text{CH}_3$ ), 4.10 (q, 2H,  $\text{OCH}_2\text{CH}_3$ ), 4.39 (q, 2H,  $\text{NCH}_2\text{CH}_3$ ), 5.34 (q, 1H,  $\text{NCH}=\text{CH}_2$ ,  $\text{H}^{\text{A}}$ ), 5.91 (d, 1H,  $\text{NCH}=\text{CH}_2$ ,  $\text{H}^{\text{B}}$ ), 7.32 (m, 1H,  $\text{NCH}=\text{CH}_2$ ), 7.62 (s, 1H, H5, (Im)), 7.81 (s, 1H, H4, (Im)), 9.86 (s, 1H, H2, (Im)) ppm (Figure SI4-2).

$^{13}\text{C}$  NMR (400 MHz,  $\text{CDCl}_3$ ;  $\delta_{\text{C}}$ ): 15.17 ( $\text{NCH}_2\text{CH}_3$ ), 15.39 ( $\text{OCH}_2\text{CH}_3$ ), 45.5 ( $\text{NCH}_2\text{CH}_3$ ), 63.49 ( $\text{OCH}_2\text{CH}_3$ ), 109.28 ( $\text{NCH}=\text{CH}_2$ ), 119.48 ( $\text{NCH}=\text{CH}_2$ ), 122.93 (C(5)H), 128.53 (C(4)H), 135.28 (C(2)H) ppm.

### 5.3.3 1-vinyl-3-propylimidazolium propyl sulphate (ILM 3)

Synthetic procedure was as indicated for *ILM 1* with dipropyl sulphate used in place of dimethyl sulphate. Yield: 72 %, colourless, viscous liquid.

$^1\text{H}$  NMR (400 MHz,  $\text{CDCl}_3$ ;  $\delta_{\text{H}}$ ): 0.94 (m, 6H,  $\text{NCH}_2\text{CH}_2\text{CH}_3$ ,  $\text{OCH}_2\text{CH}_2\text{CH}_3$ ) 1.67 (m, 2H,  $\text{OCH}_2\text{CH}_2\text{CH}_3$ ), 1.94, (m, 2H,  $\text{NCH}_2\text{CH}_2\text{CH}_3$ ), 3.98 (t, 2H,  $\text{OCH}_2\text{CH}_2$ ), 4.29 (t, 2H,  $\text{NCH}_2\text{CH}_2$ ), 5.33 (m, 1H,  $\text{NCH}=\text{CH}_2$ ,  $\text{H}^{\text{A}}$ ), 5.89 (m, 1H,  $\text{NCH}=\text{CH}_2$ ,  $\text{H}^{\text{B}}$ ), 7.31 (m, 1H,  $\text{NCH}=\text{CH}_2$ ), 7.60 (s, 1H, H5, (Im)), 7.86 (s, 1H, H4, (Im)), 9.89 (s, 1H, H2, (Im)) ppm (Figure SI4-3).

$^{13}\text{C}$  NMR (400 MHz,  $\text{DMSO}_d$ ;  $\delta_{\text{C}}$ ): 10.35 ( $\text{NCH}_2\text{CH}_2\text{CH}_3$ ), 10.60 ( $\text{OCH}_2\text{CH}_2\text{CH}_3$ ), 22.79 ( $\text{NCH}_2\text{CH}_2\text{CH}_3$ ), 23.49 ( $\text{OCH}_2\text{CH}_2\text{CH}_3$ ), 51.63 ( $\text{OCH}_2\text{CH}_2$ ), 69.15 ( $\text{NCH}_2\text{CH}_2$ ), 109.28 ( $\text{NCH}=\text{CH}_2$ ), 119.58 ( $\text{NCH}=\text{CH}_2$ ), 123.22 (C(5)H), 128.50 (C(4)H), 135.66 (C(2)H) ppm.

After drying under high vacuum, prior to being used, each ILM was stored in a refrigerator at 5 °C to avoid unwanted polymerization.

### 5.3.4 Free radical polymerization of ILMs

The following example describes the procedure used for the synthesis of all free-standing linear polymers obtained in this study. All linear polymers were synthesized according to this procedure, by varying the ratio of monomer to initiator. In a small vial, the ILM (0.3 g) was mixed with HMPP initiator (2 mol %). The solution was then transferred to a circular shaped PDMS (polydimethylsiloxane) mould 10 mm in diameter and 1 mm deep. The mould was then placed in a UV curing chamber ( $\lambda = 365$  nm,  $3.5$  mW/cm<sup>2</sup>) for 30 min. After polymerization, the free-standing linear films were dried in a vacuum oven for 24 h at 80 °C.

## 5.4 Results and Discussions

### 5.4.1 Synthesis

Our synthesis process is derived from a method reported by Rogers *et al.*, who prepared a series of 1,3-dialkylimidazolium alkyl sulphate ILs by the quaternization of 1-alkylimidazoles with alkyl sulphates.<sup>25</sup> In this study, 1-vinylimidazole is used instead of 1-alkylimidazoles, following the general reaction scheme shown in Figure 5.1, in order to produce the desired ILMs (Figure SI4-4).

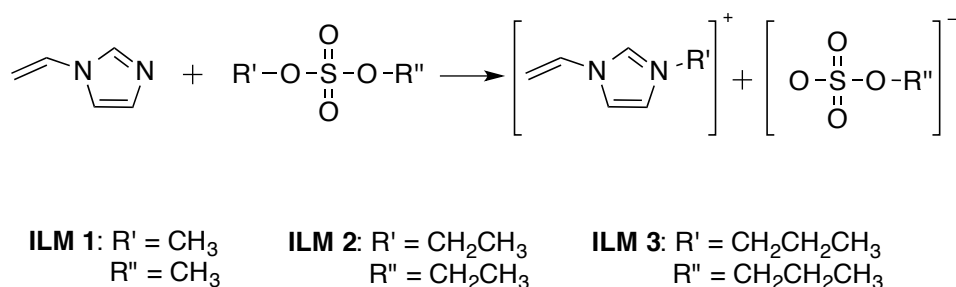


**Figure 5.1.** General preparative route to 1-vinylimidazolium ILMs.

The use of dialkyl sulphates over alkyl halides is preferable, as the alkylation rate of dimethyl sulphates is much faster.<sup>25</sup> As the quaternization reaction is very exothermic, toluene is used as a diluent to moderate and control the reactivity. Moreover, both reagents are soluble in toluene whereas the ILM products form a biphasic solution, thus facilitating simple isolation of the products. To the best of our knowledge, this is the first reported method synthesis of 1-vinyl-3-methylimidazolium methyl sulphate and 1-vinyl-3-propylimidazolium propyl sulphate.

The IR spectra show the presence of the vinyl group ( $\sim 3110\text{ cm}^{-1}$ ), the CH<sub>3</sub>(N) and CH<sub>2</sub>(N) stretch of the cation, and the C-O-SO<sub>3</sub> ( $\sim 1215\text{ cm}^{-1}$ ) asymmetrical,

symmetrical ( $\sim 1000\text{ cm}^{-1}$ ) stretch of the sulphate anion (Figure SI4-5, SI4-6 and SI4-7).

## 5.4.2 Physicochemical properties of ILMs

The thermal properties of the ILMs were evaluated by DSC scans, as shown in Table 5.1. ILM 1 did not display a  $T_g$  value, even at a slow heating rate of  $2\text{ }^\circ\text{C min}^{-1}$ . Its melting point and crystallization value was found to be  $25\text{ }^\circ\text{C}$  and  $-23\text{ }^\circ\text{C}$ , respectively (Figure SI4-8). ILM 2 and ILM 3 exhibited  $T_g$  values at  $-64\text{ }^\circ\text{C}$  and  $-61\text{ }^\circ\text{C}$  (Figure SI4-9), respectively. ILM 2 had a melting point at  $19\text{ }^\circ\text{C}$  and crystallization point at  $-14\text{ }^\circ\text{C}$ , while ILM 3 displayed no melting or crystallization processes within the scanning range (Figure SI4-10).

Viscosity values were obtained via rheology at a shear rate of  $1000\text{ s}^{-1}$  at  $20\text{ }^\circ\text{C}$  (Table 5.1, Figure SI4-11). ILM 1 was omitted from this measurement, as it was a crystalline solid at room temperature. For ILM 3, the viscosity value was  $0.372\text{ Pa}\cdot\text{s}$ , which was higher than ILM 2, and has a value of  $0.239\text{ Pa}\cdot\text{s}$ . This pattern is as expected as an increase in alkyl chain length on both the cation and the anion has been reported to increase the viscosity of imidazolium alkyl sulphate ILs in previous studies.<sup>26, 27</sup>

ILM	T <sub>g</sub> (°C) <sup>a</sup>	T <sub>m</sub> (°C) <sup>b</sup>	T <sub>cry</sub> (°C) <sup>c</sup>	η (Pa.s) <sup>d</sup>
1	-	25	-23	-
2	-64	19	-14	0.239
3	-61	-	-	0.372

**Table 5.1.** Thermal behaviour and viscosity of ionic liquid monomers **1-3** (figure 1). <sup>a</sup>T<sub>g</sub> - glass transition temperature measured by DSC. <sup>b</sup> T<sub>cry</sub>- crystallization temperature. <sup>c</sup> T<sub>m</sub> - melting point measured by DSC. <sup>d</sup> η - viscosity at shear rate 1000 s<sup>-1</sup>.

### 5.4.3 Polymerization properties of the ILMs

In a previous study, we monitored rheology changes during curing as the polymerization of pNIPAAm (poly(*N*-isopropylacrylamide) polymers proceeded in the presence of various ILs.<sup>28</sup> The same approach has been used here, as the rise in elastic moduli measured during polymerization gives some insight into the process of polymer network formation and mechanical properties. The polymerization properties of the PILs are presented in Figure 5.2 and Table 5.2. As ILM 1 is a solid, prior to this measurement it was stirred in a sealed vial with the required liquid photo-initiator for 10 min, which rendered a liquid that could be dispensed onto the rheometer plate.

ILM	$G_p$ (s) <sup>a</sup>	$G_0''$ (Pa) <sup>a</sup>	$G''$ (Pa) <sup>b</sup>	$G'$ (Pa) <sup>c</sup>	$\text{Tan}\delta^d$
1	32	14.4	$4.34 \times 10^5$	$2.36 \times 10^6$	0.180
2	57	14.7	$9.36 \times 10^5$	$3.81 \times 10^6$	0.239
3	284	44	$8.10 \times 10^5$	$3.96 \times 10^6$	0.203

**Table 5.2.** Polymerization and rheological properties of PILs. <sup>a</sup>  $G_0''$  - loss modulus before polymerization. <sup>b</sup>  $G''$ - loss modulus after 115 min of polymerization. <sup>c</sup>  $G'$ - storage modulus after 115 min of polymerization. <sup>d</sup>  $\text{tan}\delta$  -  $G''/G'$  after 115 min of polymerization.

During the rheology experiment, after the UV light was switched on, the storage modulus quickly overcame the loss modulus. The crossover of these two moduli can be taken as the gelpoint, i.e.; the point at which the samples show more elastic than viscous behaviour. In reaching this gelpoint, the PILs follow the trend; PIL 3 > PIL 2 > PIL 1 (Table 5.2).

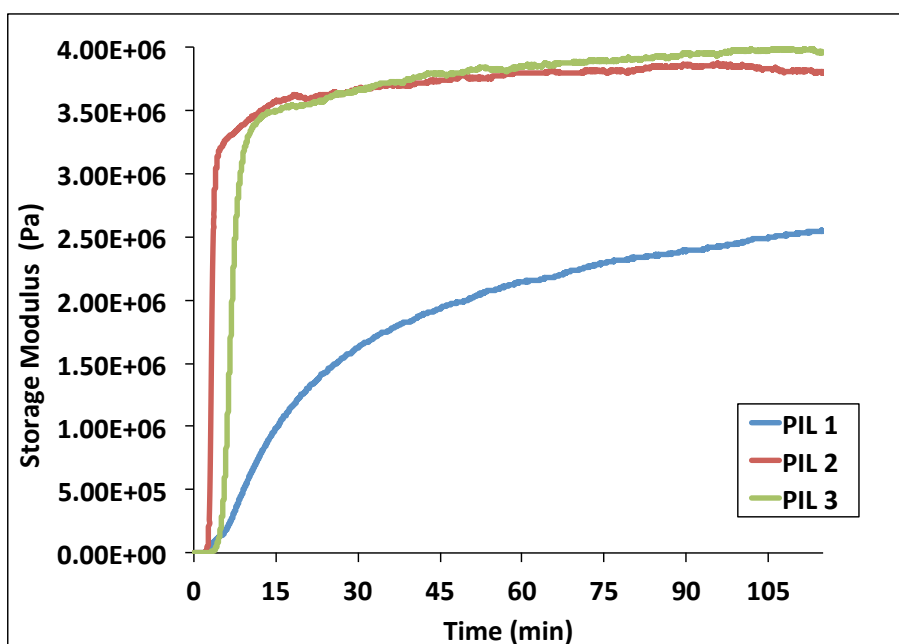


**Figure 5.2.** Storage moduli during UV polymerization of ILMs. UV polymerization was initiated after 60 s.

During UV polymerization (Figure 5.2), PIL 2 and PIL 3 were found to exhibit similar variations in storage moduli, while for PIL 1 the value was much lower, and increased at a much slower rate. In fact, over the course of the experiment (115 min), PIL 1 did not reach a steady-state, and was still increasing at 115 min. In contrast, with PIL 2 and PIL 3, the storage modulus rises very rapidly initially, but after a few minutes the rate of increase drops significantly, and thereafter it increases slowly up to ca. 40 minutes, after which no significant increase occurs.

For viscoelastic materials, a typical parameter characterizing the general mechanical properties is the ratio of the viscous (loss) to elastic (storage) moduli  $G''/G'$  ( $\tan\delta$ ). This number directly tells how rubbery/tacky the resulting PILs are after polymerization, which is important for handling purposes. If  $\tan\delta < 1$ , the material tends to be more solid in nature, but if  $\tan\delta = \infty$ , then it is a liquid.<sup>29</sup> Table 5.2 shows all PILs to have a  $\tan\delta$  value below 1, with the lowest being PIL 1 ( $\tan\delta = 0.180$ ), indicating that these ILMs, through free-radical polymerization, form solid, non-sticky films.

Figure 5.3 shows the ILMs polymerized in a UV curing chamber, as described in *Section 2.3*, using a greater UV intensity ( $3.5 \text{ mW/cm}^2$ ) than employed in the rheology study ( $950 \text{ }\mu\text{W/cm}^2$ ). Using this approach, solid, free-standing films are produced as shown in Figure 5.3.  $^1\text{H}$  NMR reveals complete loss of the vinyl group between 5.3-6.0 ppm for all PILs after 30 min polymerizing time in the UV chamber (Figure SI4-12), indicating complete polymerization with no evidence of unreacted monomer.

These results suggest that the PILs possess satisfactory gel formation behaviour and sufficient mechanical stability for further characterization. This is in contrast to

previous studies, which reported that free-standing polymeric ionic liquids are difficult to produce without the use of a crosslinker.<sup>30</sup>

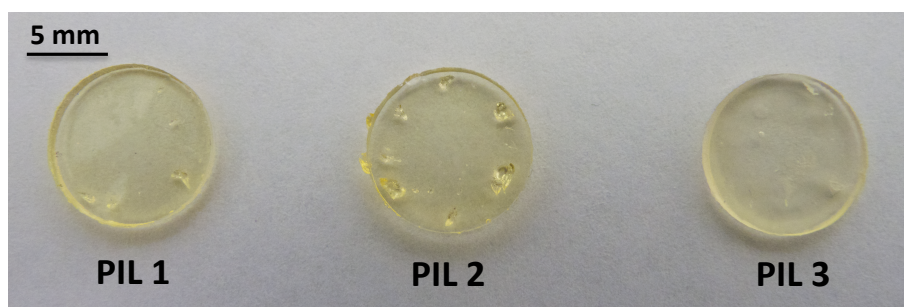


**Figure 5.3.** Appearance of polymerized PILs in 10 mm PDMS moulds after 30 min polymerization under 365 nm UV light at an intensity of 3.5 mW/cm<sup>2</sup>.

#### 5.4.4 Physicochemical properties of PILs

Table 5.3 summarizes the solubility of the PILs in various polar and non-polar solvents. All of the PILs were found to be completely soluble in water. Previous studies have shown that the presence of water can increase conductivity of PILs by up to two orders of magnitude.<sup>9, 14</sup> Therefore, as these PILs are water soluble it is recommended that future conductivity analysis of these materials be performed in an inert atmosphere.

Solubility was found to decrease for all three PILs as the solvent polarity decreased. For example, PIL 1 and PIL 2 required heat of 40 °C for 30 min before they dissolved in acetonitrile, and both were only partially soluble in ethanol. As might be expected (due to the more hydrophobic nature of the propyl groups), PIL 3 was soluble in methanol and ethanol, and was the only PIL to dissolve in acetone. None of the PILs were soluble in less polar solvents, such as tetrahydrofuran, ethyl acetate, toluene and hexane.

Previous studies have reported alteration of the solubility of polymeric ILs by simple anion exchange reactions.<sup>31</sup> This required synthesis of a halide-containing derivative before a metathesis reaction with the desired salt could be performed. In contrast, we have shown that the solubility of PILs can be varied using a much more simple approach based on varying the alkyl chain length of the anion and cation, i.e.; there is no need to use anion exchange or halide containing ILs.

Solvent	Dielectric Constant	Polymer		
		PIL 1	PIL 2	PIL 3
<b>Water</b>	<b>80</b>	+	+	+
<b>Acetonitrile</b>	<b>37.5</b>	+ <sup>t</sup>	+ <sup>t</sup>	±
<b>Methanol</b>	<b>33</b>	+ <sup>t</sup>	±	+
<b>Ethanol</b>	<b>24.5</b>	±	±	+
<b>Acetone</b>	<b>18</b>	-	-	+
<b>Isopropanol</b>	<b>21</b>	-	-	-
<b>Dichloromethane</b>	<b>9.1</b>	-	-	-
<b>Tetrahydrofuran</b>	<b>7.5</b>	-	-	-
<b>Ethyl Acetate</b>	<b>6</b>	-	-	-
<b>Diethyl Ether</b>	<b>4.3</b>	-	-	-
<b>Toluene</b>	<b>2.3</b>	-	-	-
<b>Hexane</b>	<b>1.8</b>	-	-	-

**Table 5.3.** Solubility of PILs. Solubility: (+) soluble at ambient temperature, (+<sup>t</sup>) soluble on heating, (±) partially soluble on heating, (-) insoluble even on heating.

The thermal stability and the mechanical properties of the free-standing PILs are summarised in Table 5.4. PIL 1 and PIL 2 were found to have glass transition temperatures ( $T_g$ ) of  $-69\text{ }^\circ\text{C}$  and  $-60\text{ }^\circ\text{C}$ , respectively (Figure SI4-13). PIL 3 did not exhibit  $T_g$  behaviour, despite the slow rate scan  $2\text{ }^\circ\text{C min}^{-1}$ . However, it did exhibit a  $T_{\text{cry}}$  crystallization point at  $-30\text{ }^\circ\text{C}$  (Figure SI4-14). Each PIL displayed excellent thermal stability, with onset loss temperatures ( $T_d$ ) at ca.  $330\text{ }^\circ\text{C}$  (Figure SI4-15). With respect to degradation temperatures, the following trend was observed  $\text{PIL 3} > \text{PIL 2} > \text{PIL 1}$ ; i.e. the thermal stability of the PILs was found to increase with increasing cation and anion alkyl chain length.

PIL	$T_g$ ( $^\circ\text{C}$ ) <sup>a</sup>	$T_{\text{cry}}$ ( $^\circ\text{C}$ ) <sup>b</sup>	$T_d$ ( $^\circ\text{C}$ ) <sup>c</sup>	$G'$ (Pa) <sup>d</sup>
1	-69	-	320	$6.21 \times 10^2$
2	-60	-	330	$5.41 \times 10^4$
3	-	-30	340	$4.64 \times 10^6$

**Table 5.4.** Thermal and mechanical properties of free-standing PILs. <sup>a</sup>  $T_g$  - glass transition temperature measured by DSC. <sup>b</sup>  $T_{\text{cry}}$  - crystallization temperature measured by DSC. <sup>c</sup>  $T_d$  - onset loss temperature according to TGA. <sup>d</sup>  $G'$  - Storage modulus of PIL gel obtained by rheology.

The mechanical characteristics of the linear PILs polymerized in a PDMS mold were analyzed via an amplitude sweep program with an angular frequency ( $\omega$ ) of  $10\text{ rad/s}$  and subjected to  $0.01\text{-}100\%$  strain with respect to the material. The storage modulus values tabulated in Table 5.4 are at the point where the polymer's storage modulus value decreases below  $95\%$  as a function of stress.

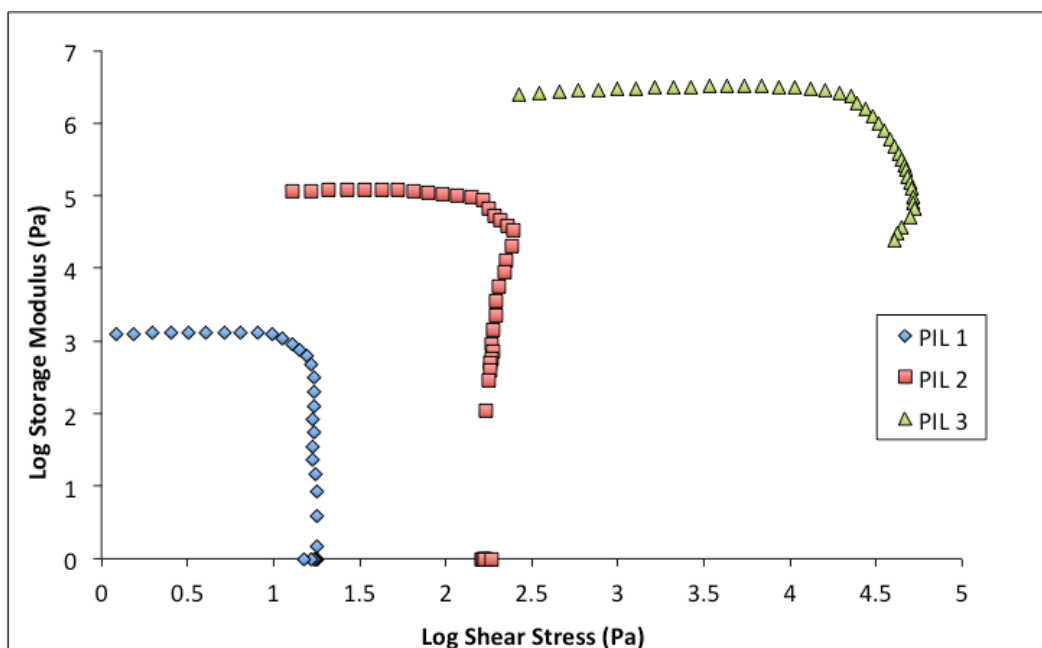


**Figure 5.4.** Amplitude sweep of linear PILs where storage modulus is measured as a function of strain subjected on the material.

The storage moduli of the PILs were found to decrease in the following order PIL 3 > PIL 2 > PIL 1 (Table 5.4 and Figure 5.4). PIL 3 was found to produce the largest storage moduli value ( $G' = 4.64 \times 10^6$ ). This trend is in accordance with the molecular weight of the ILMs. The increase in molecular weight of the ILMs is attributed to the increase of the alkyl chain of the anion and cation. In general, mechanical properties of polymers are found to increase as the molecular weight of the monomer increases.<sup>32, 33</sup> This, in turn, may be the reason for a higher storage moduli value for PIL 3, compared to PIL 1 and PIL 2.

## 5.5 Conclusions

New ionic liquid monomers have been prepared using a halide-free reaction between 1-vinylimidazolium and alkyl sulphates. The length of the alkyl chain of both the anion and cation of these monomers were found to affect their physicochemical and mechanical properties of their resulting polymer form. Through polymerization

analysis, the monomers were found to produce free-standing linear polymeric ionic liquid (PILs) films with a  $\tan\delta$  value as low as 0.180. The films maintained their thermal stability up to 340 °C and can produce a storage moduli value as high as  $4.64 \times 10^6$  Pa.

This use of a simple, halide-free synthesis and the satisfactory thermal and mechanical stability of the resulting solid polymer films make these materials interesting candidates for electrochemical analysis as robust, ion conductive polymer films.

## Acknowledgments

This publication has emanated from research conducted with the financial support of Science Foundation Ireland (SFI) under grants SFI/12/RC/2289 and 07/CE/I1147.

## 5.6 References

1. J. Salamone, S. Israel, P. Taylor and B. Snider, *Journal of Polymer Science Polymer Symposium*, 1974, **45**, 65-73.
2. J. Salamone, S. Israel, P. Taylor and B. Snider, *Polymer*, 1973, **12**, 639-644.
3. H. Ohno, *Electrochimica Acta*, 2001, **46**, 1407-1411.
4. H. Ohno, *Macromolecular Symposia*, 2007, **249-250**.
5. H. Ohno and K. Ito, *Chemistry Letters*, 1998, **27**, 751-752.
6. H. Ohno, M. Yoshizawa and W. Ogihara, *Electrochimica Acta*, 2004, **50**, 255–261.
7. A. S. Shaplov, D. O. Ponkratov, P. S. Vlasov, E. I. Lozinskaya, L. I. Komarova, I. A. Malyshkina, F. Vidal, G. T. M. Nguyen, M. Armand, C. Wandrey and S. V. Ya, *Polymer Science Series B*, 2013, **55**, 122-138.
8. C. Plesse, F. Vidal, H. Randriamahazaka, D. Teyssie and C. Chevrot, *Polymer*, 2005, **46**, 7777-7787.
9. J. Yuan and M. Antonietti, *Polymer*, 2011, **52**, 1469-1482.
10. J. Lu, F. Yan and J. Texter, *Progress in Polymer Science*, 2009, **34**, 431–448.
11. O. Green, S. Grubjesic, S. Lee and M. A. Firestone, *Polymer Reviews*, 2009, **49**, 339–360.
12. P. Wassersheid and T. Welton, *Wiley-VCH, Weinheim*, 2003.
13. H. Ohno, *Macromolecular Symposia*, 2007, **249-250**, 551–556.
14. D. Mecerreyes, *Progress in Polymer Science*, 2011, **36**, 1629-1648.
15. A.-L. Pont, R. Marcilla, I. De Meazza, H. Grande and D. Mecerreyes, *Power Sources*, 2009, **188**, 558.
16. K. Suzuki, M. Yamaguchi, S. Hotta, N. Tanabe and S. Yanagida, *Journal of Photochemistry and Photobiology A: Chemistry*, 2004, **164**, 81-85.
17. R. Marcilla, M. Sanchez-Paniagua, B. Lopez-Ruiz, E. Lopez-Cabarcos, E. Ochoteco, H. Grande and D. Mecerreyes, *Journal of Polymer Science Part A: Polymer Chemistry*, 2006, **44**, 299–304.
18. M. Kijima, K. Setoh and H. Shirakawa, *Chemistry Letters*, 2000, **29**, 936.
19. Y. S. Vygodskii, O. A. Mel'nik, E. I. Lozinskaya, A. S. Shaplov, I. A. Malyshkina, N. D. Gavrilova, K. A. Lyssenko, M. Yu. Antipin, D. G.

- Golovanov, A. A. Korlyukov, N. Ignat'ev and U. Welz-Biermann, *Polymer for Advanced Technologies*, 2006, **18**, 50-63.
20. P. Bonhote, A.-P. Dias, N. Papageorgiou, K. Kalyanasundaram and M. Gratzel, *Inorganic chemistry*, 1996, **35**, 1168-1178.
  21. J. Fuller and R. T. Carlin, *The 193rd Society Meeting of the Electrochemical Society*, 1998, **98-1**, 157.
  22. K. Seddon, A. Stark and M. Torres, *Pure and Applied Chemistry*, 2000, **72**, 2275-2287.
  23. M. Hirao, K. Ito and H. Ohno, *Electrochimica Acta*, 2000, **45**, 1291-1294.
  24. J. Gao, J. Cao, Z. Yin, X. Liu, H. Zhao, Y. Chu, X. Tan, X. Bian, F. Zhao and J. Zhang, *International Journal of Electrochemical Science*, 2013, **8**, 4914-4923.
  25. J. D. Holbrey, W. M. Reichert, R. P. Swatloski, G. A. Broker, W. R. Pitner, K. R. Seddon and R. D. Rogers, *Green Chemistry*, 2002, **4**, 407-413.
  26. F. M. Gacino , T. Regueira, L. Lugo, M. J. P. Comunas and J. Fernandez, *Journal of Chemical & Engineering Data*, 2011, **56**, 4984-4999.
  27. R. L. Gardas and J. A. P. Coutinho, *AIChE Journal*, 2009, **55**, 1274-1289.
  28. B. Ziolkowski, Z. Ates, S. Gallagher, R. Byrne, A. Heise, K. J. Fraser and D. Diamond, *Macromolecular Chemistry and Physics*, 2013, 787-796.
  29. J. M. G. Cowie, *Polymers: Chemistry & Physics of Modern Materials Cheltenham*, 1991.
  30. A. S. Shaplov, E. I. Lozinskaya, D. O. Ponkratov, I. A. Malyshkina, F. Vidal, P.-H. Aubert, O. g. V. Okatova, G. M. Pavlov, L. I. Komarova, C. Wandrey and Y. S. Vygodskii, *Electrochimica Acta*, 2011, **57**, 74-90.
  31. R. Marcilla, J. A. Blazquez, J. Rodriguez, J. Pomposo, A. and D. Mecerreyes, *Journal of Polymer Science Part A: Polymer Chemistry*, 2004, **42**, 208-212.
  32. R. W. Nunes, J. R. Martin and J. F. Johnson, *Polymer Engineering & Science*, 1982, **22**, 205-228.
  33. J. R. Martin, J. F. Johnson and A. R. Cooper, *Journal of Macromolecular Science, Part C: Polymer Reviews*, 1972, **8**.

# **Chapter 5: Supporting Information**

## **Synthesis and Characterization of 1-Vinylimidazolium Alkyl Sulphate Polymeric Ionic Liquids**

Simon Gallagher<sup>1</sup>, Bartosz Ziolkowski<sup>1</sup>, Eoin Fox<sup>2</sup>, Kevin J. Fraser<sup>3</sup> and Dermot Diamond<sup>1, 3</sup>.

Macromolecular Chemistry and Physics, 2014, Accepted

<sup>1</sup> CLARITY: Centre for Sensor Web Technologies, National Centre for Sensor Research, Dublin City University, Dublin 9, Ireland

<sup>2</sup> School of Chemistry, Dublin City University, Dublin 9, Ireland

<sup>3</sup> Insight Centre for Data Analytics, Dublin City University, Dublin, Ireland. Tel: +353 1 700 5404

# NMR Spectroscopy of Ionic Liquid Monomers

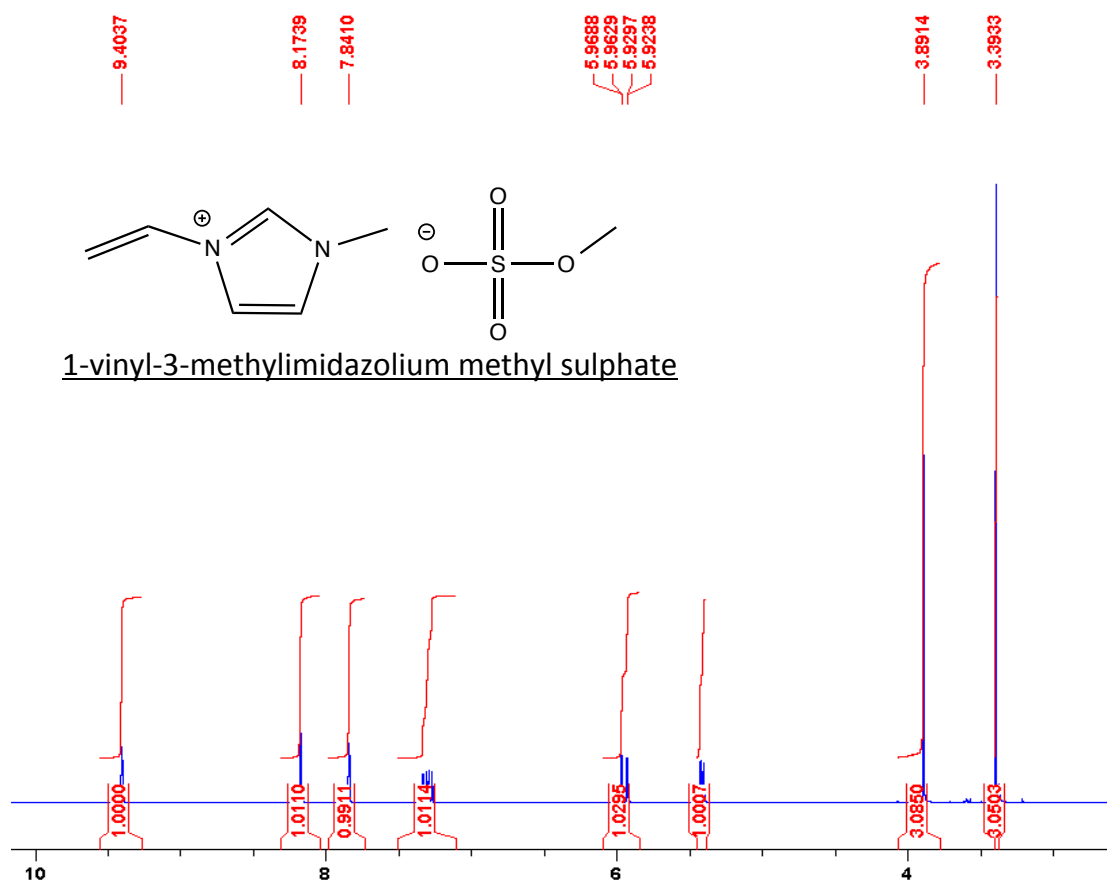
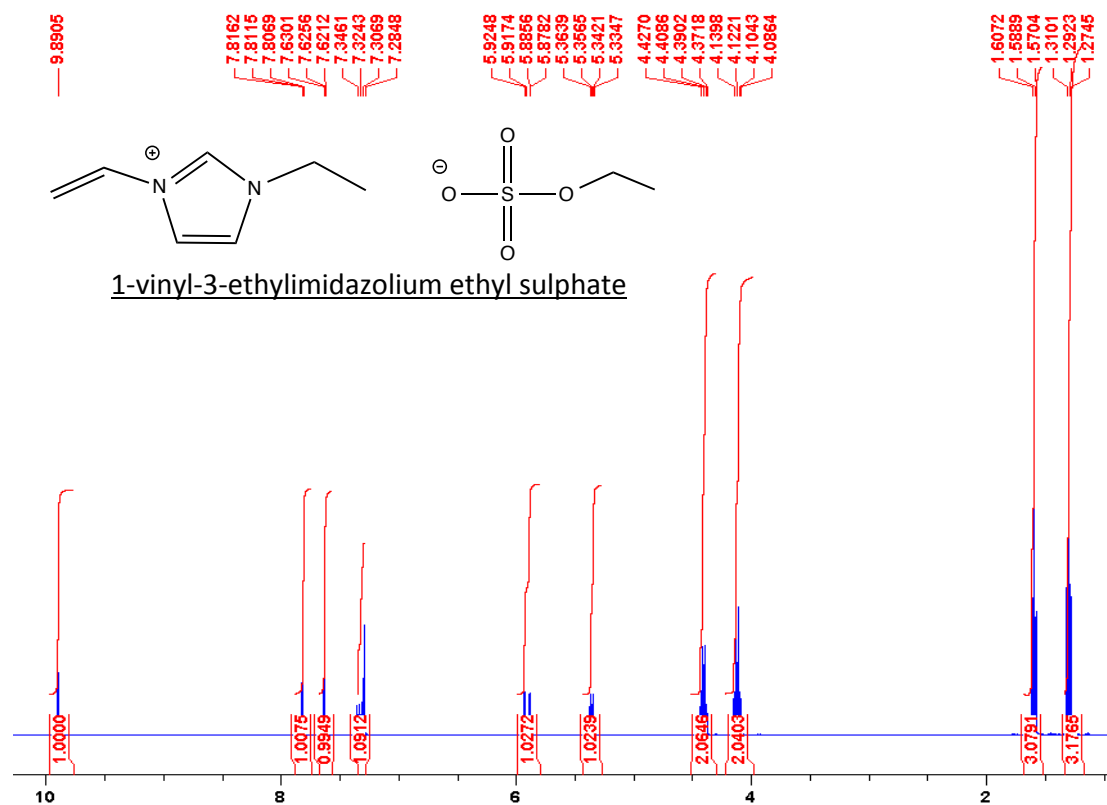


Figure 1.  $^1\text{H}$  NMR spectroscopy of 1-vinyl-3-methylimidazolium methyl sulphate.



**Figure 2.**  $^1\text{H}$  NMR spectroscopy of 1-vinyl-3-ethylimidazolium ethyl sulphate.

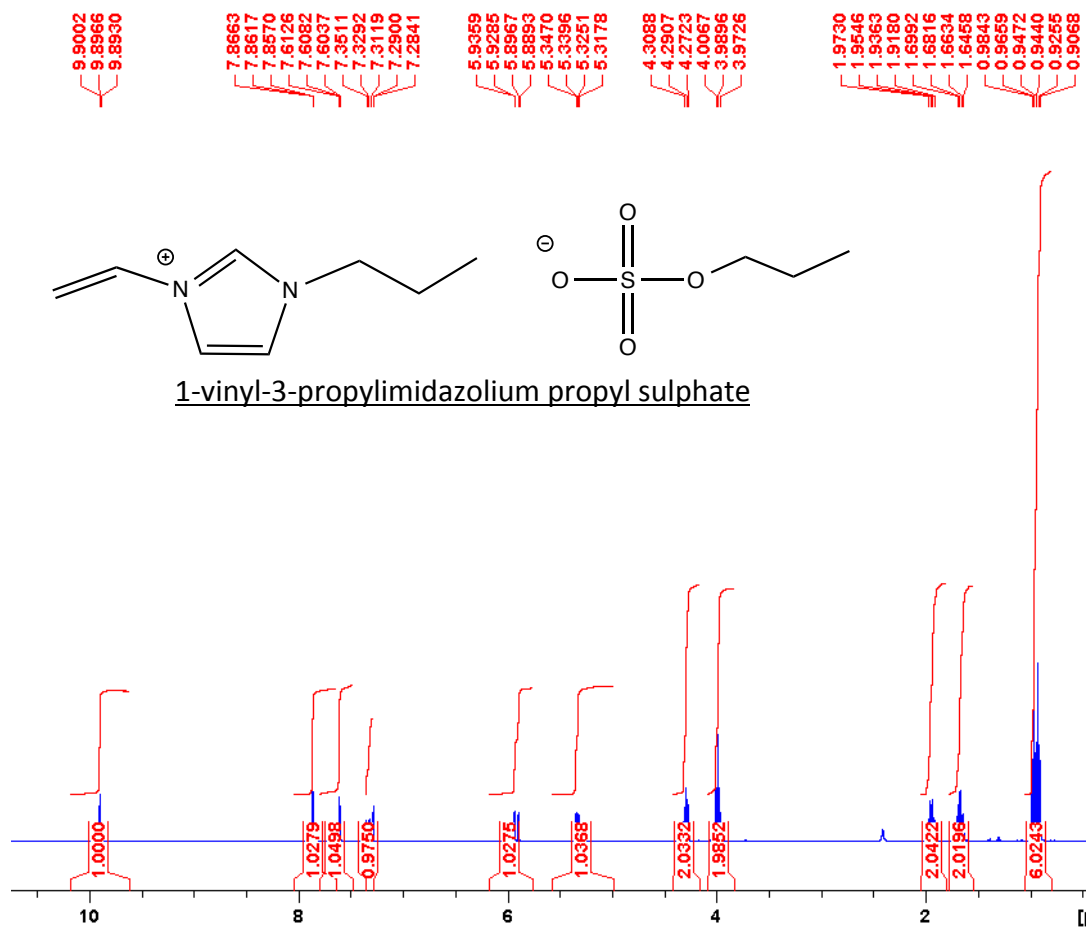


Figure 3. <sup>1</sup>H NMR spectroscopy of 1-vinyl-3-propylimidazolium propyl sulphate.

## 3-D Images of Ionic Liquid Monomers

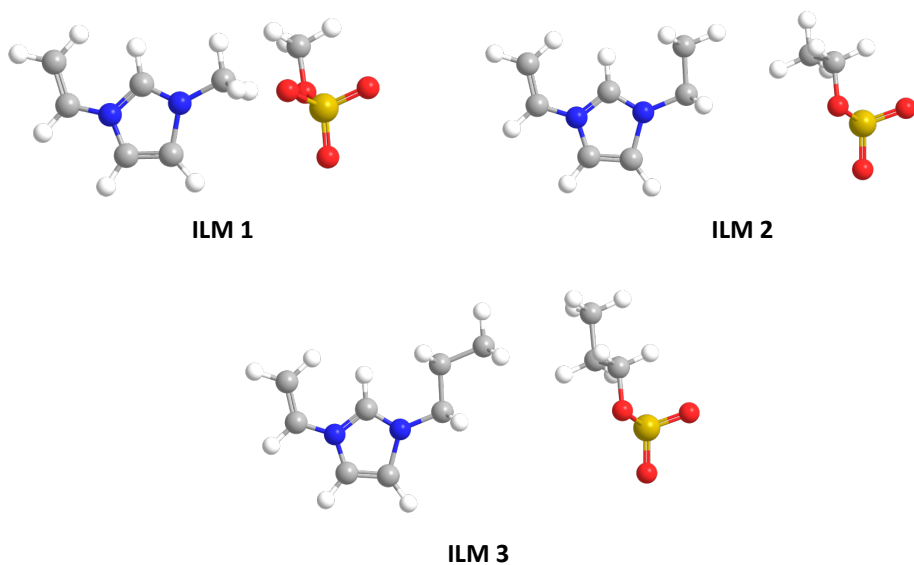
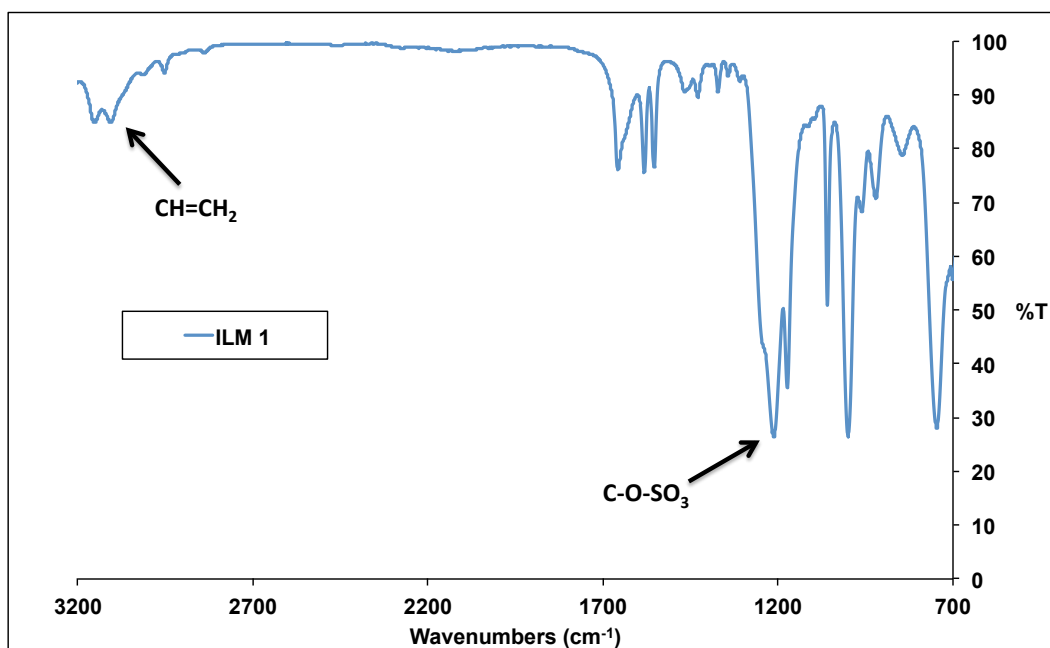


Figure 4. 3-D images of the synthesized Ionic Liquid monomers.

# Infra-red Spectroscopy of Ionic Liquid

## Monomers



**Figure 5.** Infrared spectrum of 1-vinyl-3-methyl-imidazolium methyl sulphate (ILM 1).

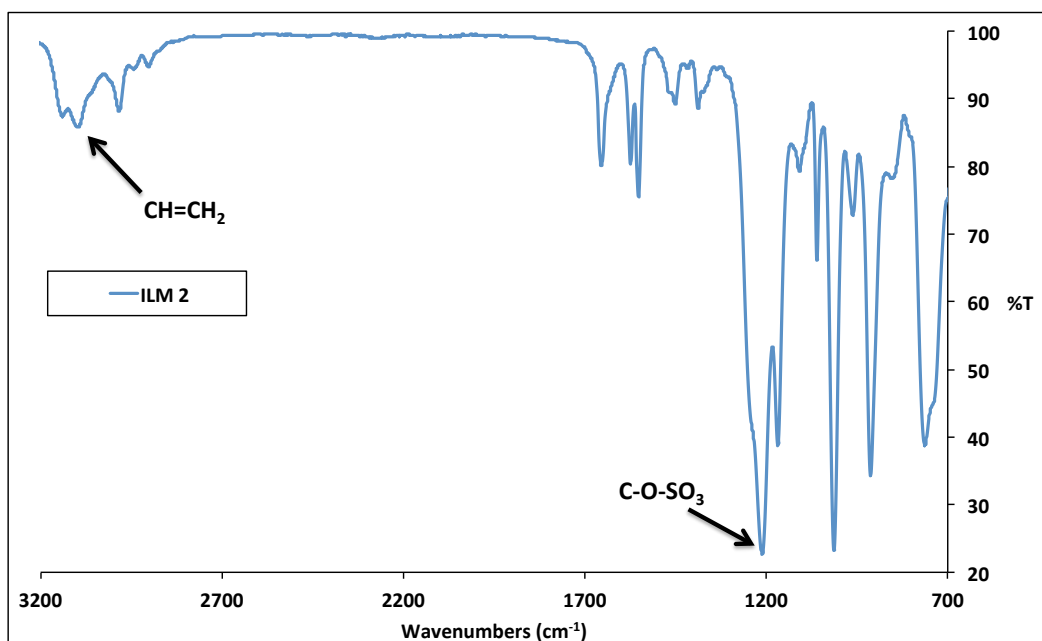


**Figure 6.** Infrared spectrum of 1-vinyl-3-ethyl-imidazolium ethyl sulphate (ILM 2).

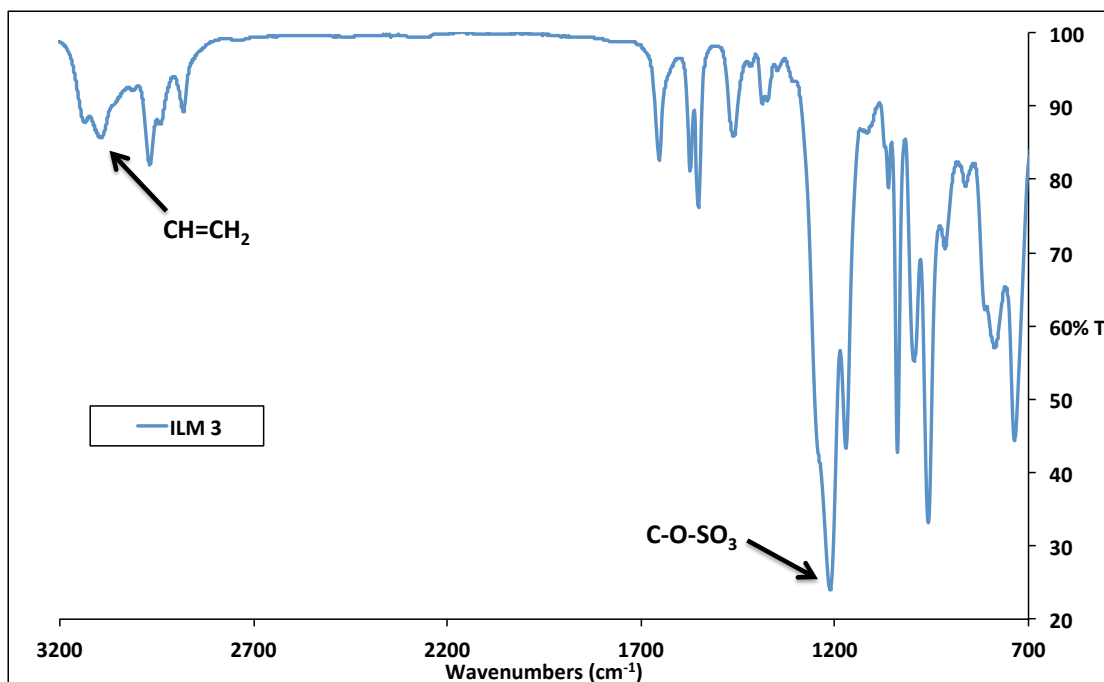


**Figure 7.** Infrared spectrum of 1-vinyl-3-propyl-imidazolium propyl sulphate (ILM 3).

## Thermal Behaviour of Ionic Liquid Monomers

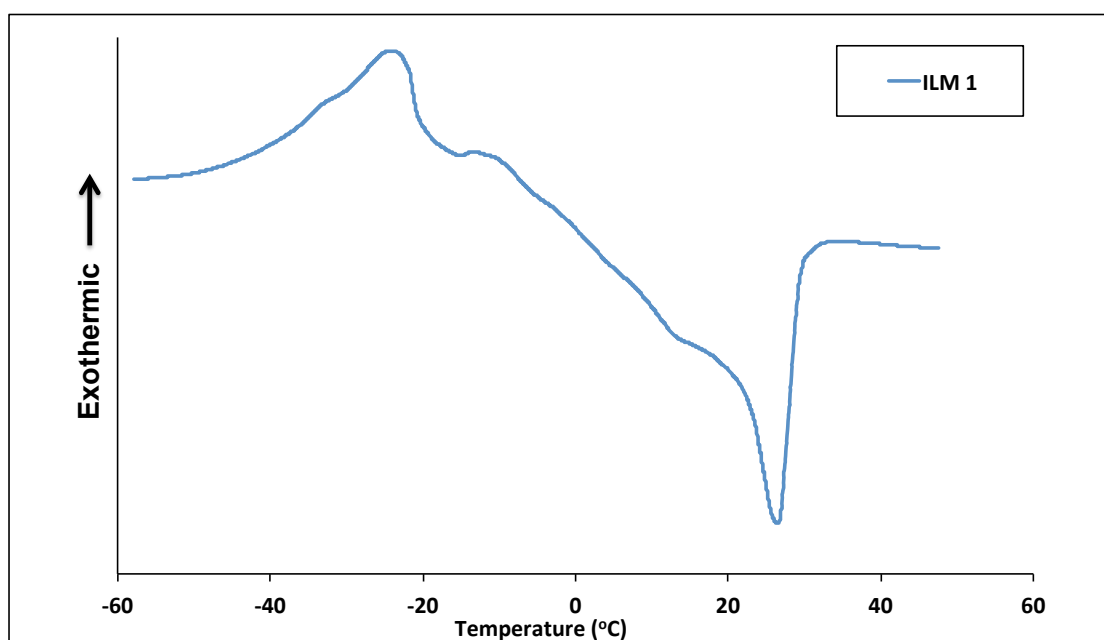


**Figure 8.** Melting  $T_m$  (25 °C) and crystallization  $T_{cry}$  (-23 °C) points of ILM 1.

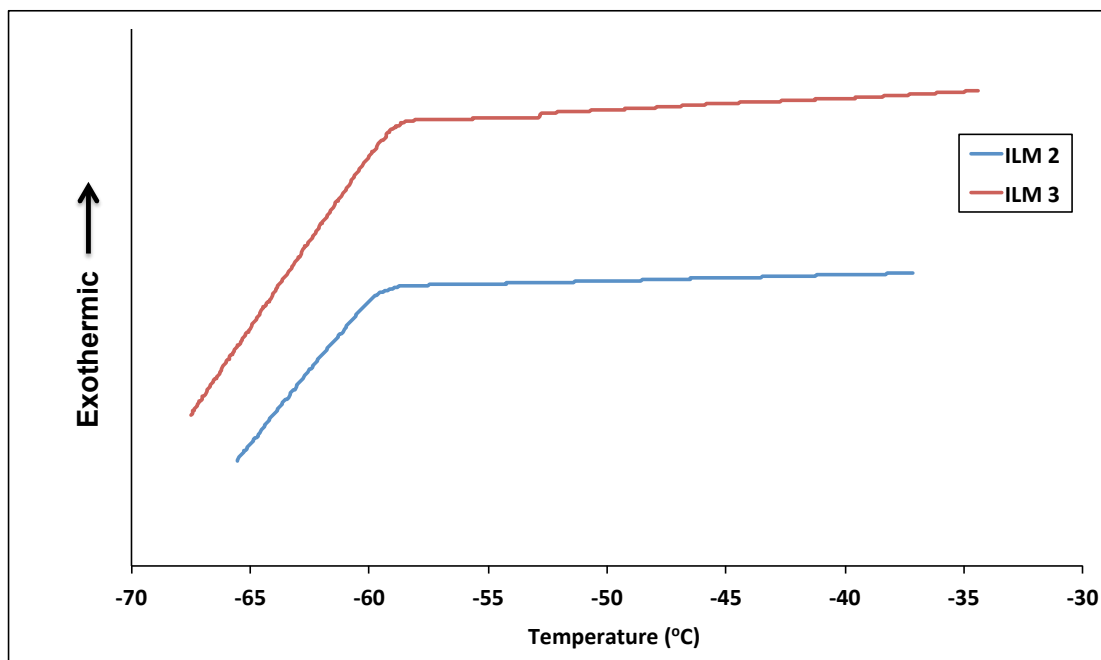


**Figure 9.** Glass transition temperatures  $T_g$  of ILM 2 (-64 °C) and 3 (-61 °C).

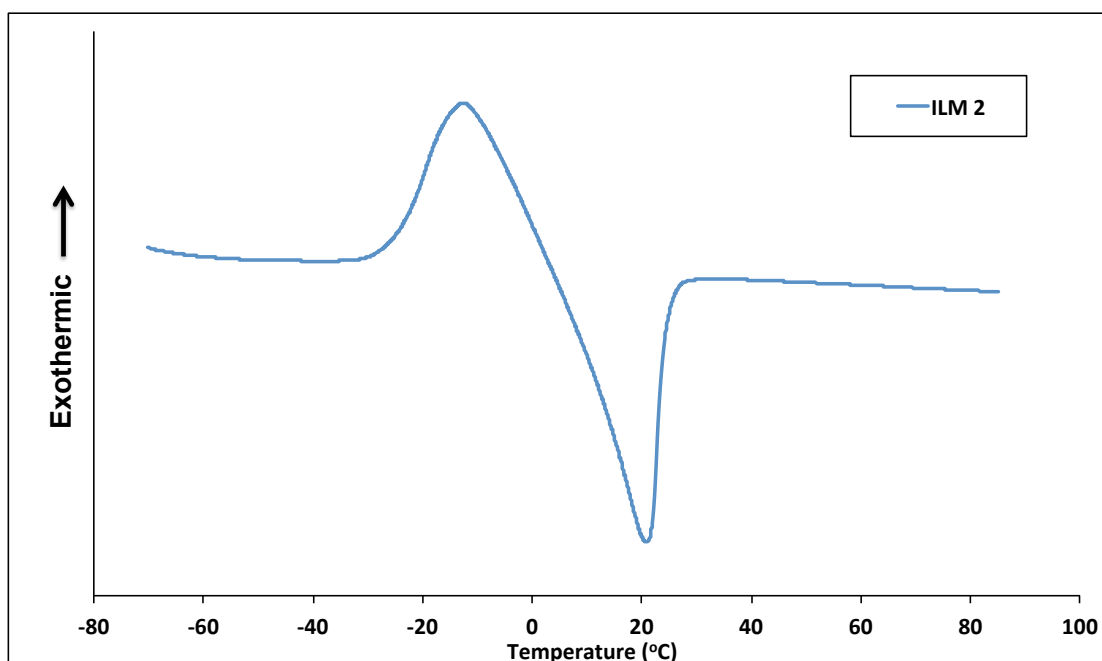


**Figure 10.** Melting  $T_m$  (19 °C) and crystallization  $T_{cry}$  (-14 °C) points of ILM 2.

# Viscosity of Ionic Liquid Monomers

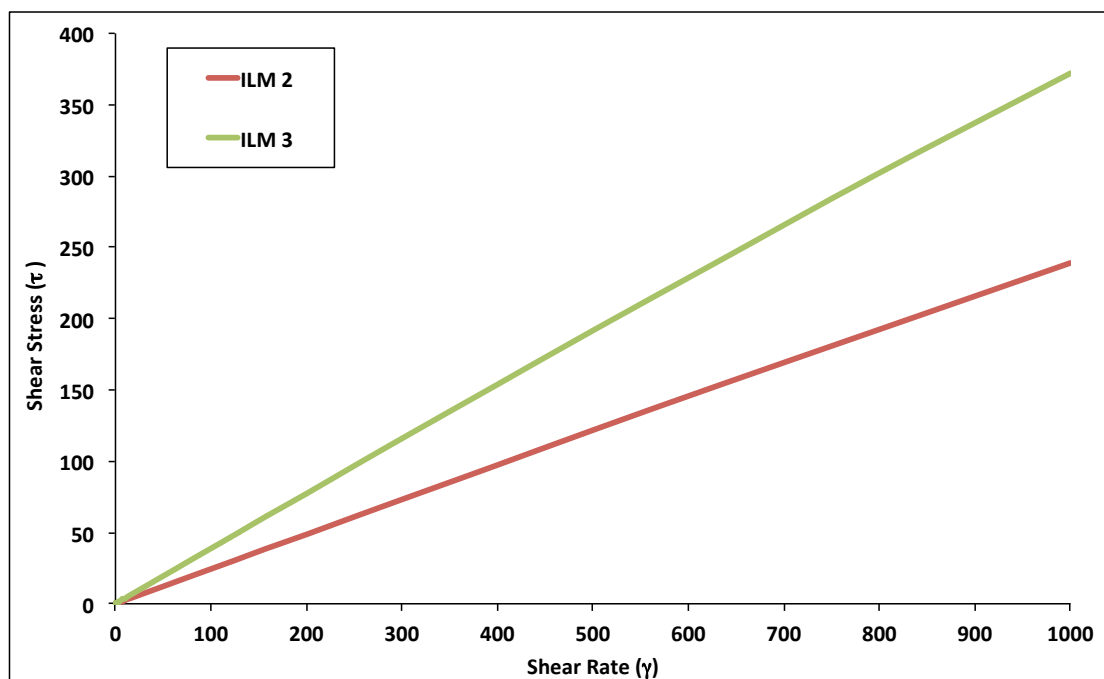


**Figure 11.** Viscosity analysis at 20 °C of ILM 2 (0.239 Pa.s) and 3 (0.372 Pa.s). Viscosity values are given at shear rate 1000 s<sup>-1</sup>.

# NMR of Polymeric Ionic Liquids

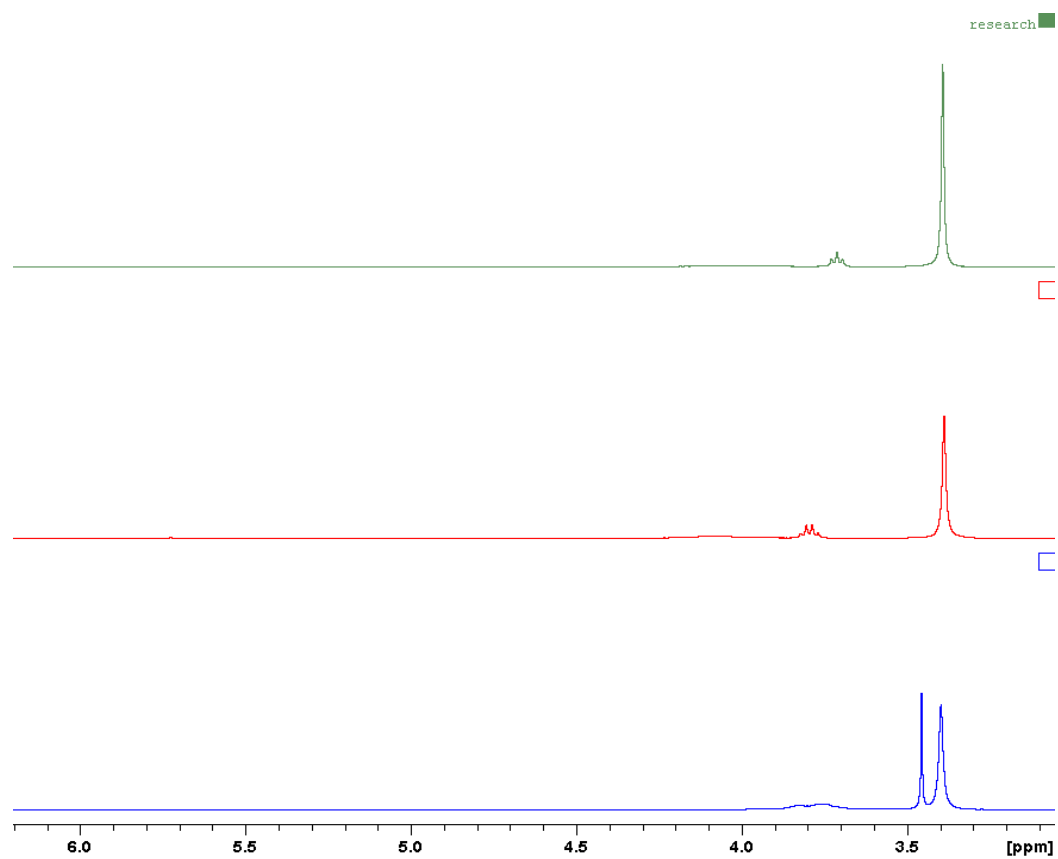


**Figure 12.**  $^1\text{H}$  NMR of PIL 1 (blue), 2 (red), and 3 (green) after 30 mins UV polymerization time.  $\text{NCH}=\text{CH}_2$  vinyl peaks that are normally located between 5.3 – 6 ppm as seen in Figure S1, do not appear.

# Thermal Behaviour of Linear Polymeric Ionic Liquids

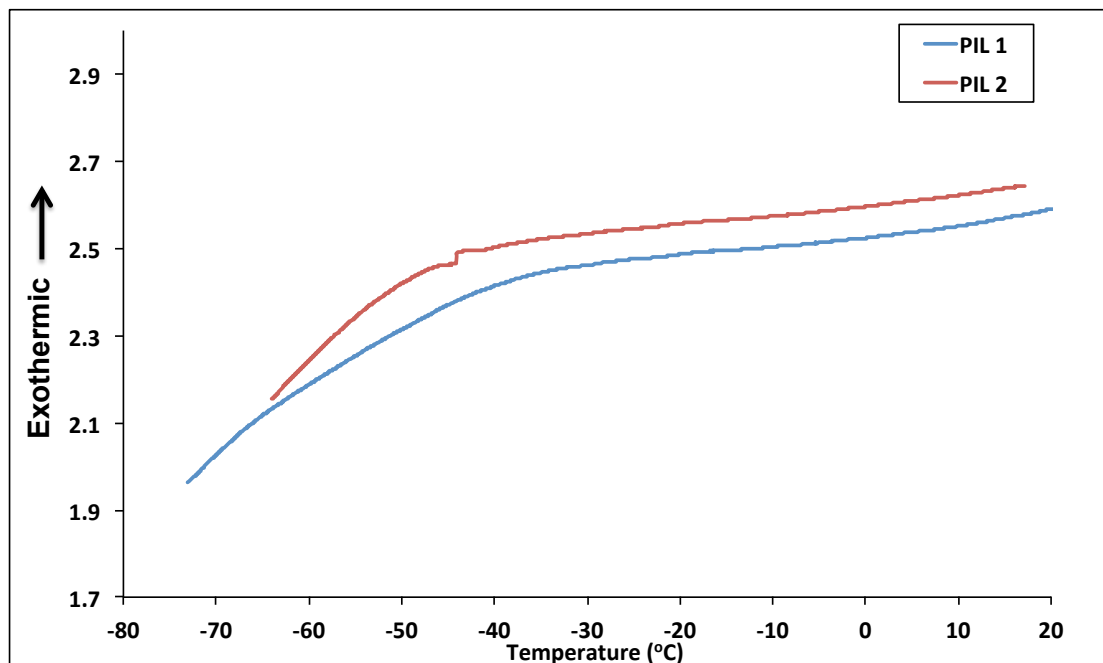


Figure 13. Glass transition temperatures  $T_g$  of PIL 1 (-69 °C) and 2 (-60 °C).

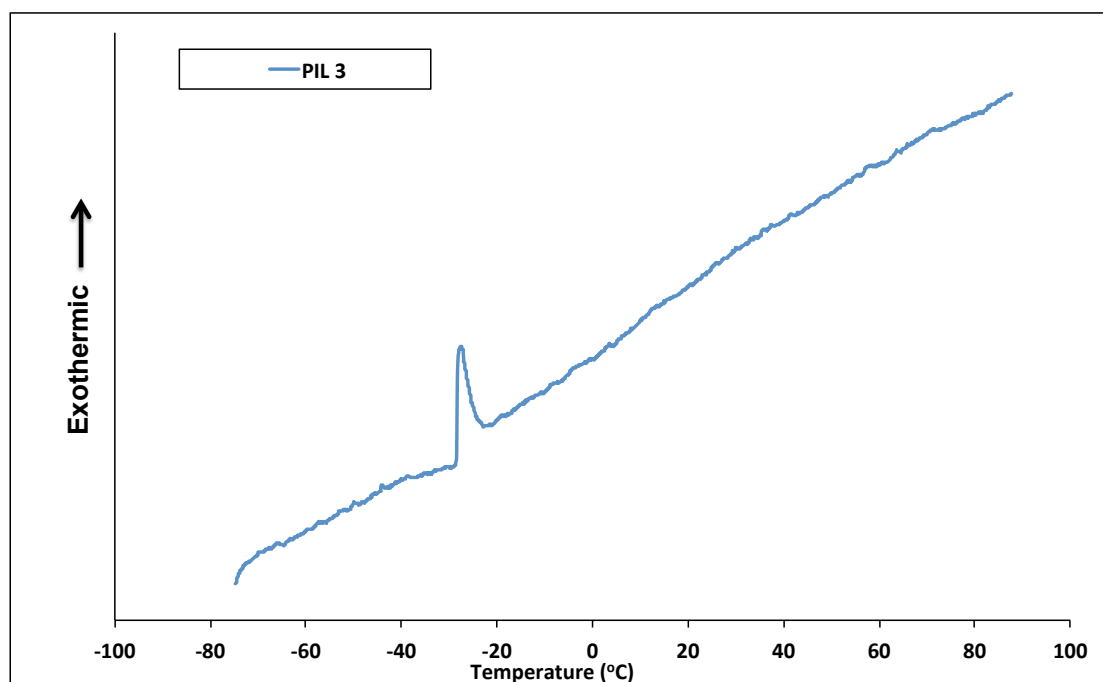
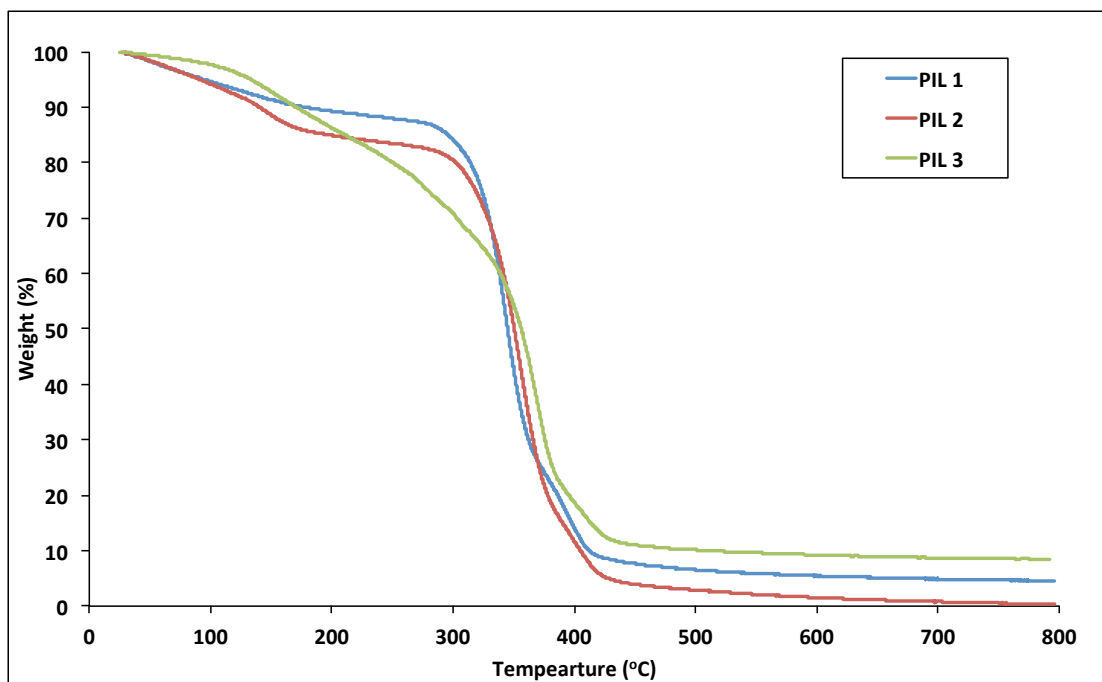


Figure 14. Melting  $T_m$  point of PIL 3 (-30 °C).



**Figure 15.** Thermogravimetric analysis with onset loss temperature of PIL 1 (320 °C), 2 (330 °C), and 3 (340 °C).

# **Chapter 6: Summary, conclusions and future perspectives**

## 6.1 Overall summary and conclusions

This thesis investigates the influence of ionic liquids on the behaviour of thermo-responsive polymers and their potential application to drug delivery and polymer actuation. These stimuli-responsive materials show enhanced properties compared to the standard hydrogel. Furthermore, a halide-free synthesis of polymeric ionic liquids has been presented as well as the characterization of their properties.

Research has been previously undertaken to improve the properties of pNIPAAm-based hydrogels. The viscoelastic properties of these gels, rigid LCST temperatures, and replacement of a volatile organic liquid phase have been addressed in recent years. The addition of ILs to the pNIPAAm network provides an opportunity to avoid these limitations. Therefore in Chapter 2, the thermo-responsive polymer pNIPAAm, was polymerized in the presence of various ionic liquids, which produced free-standing ionogels. A detailed study of interactions between the polymer network, and both independent liquid phases within the network (ILs and water) was presented. The LCST of the resulting ionogels were found to vary with respect to the IL used. The behaviour of swelling and shrinking of the ionogels were found to be greater than the standard hydrogel. For ionogels based on the [DCA]<sup>-</sup> anion an unexpected complete loss of the shrinking behaviour occurred. This was attributed to water interactions with the nitrile group of the [DCA]<sup>-</sup> anion. Scanning Electron Microscopy also revealed distinct morphological changes on the surface of the ionogels.

Due to the knowledge gained in the previous chapter, the pNIPAAm-based ionogel containing the IL [C<sub>2</sub>mIm][EtSO<sub>4</sub>] was recognized as the ionogel with the most appealing properties. Therefore in Chapter 3, this ionogel was selected for further characterization and compared to the equivalent hydrogel. The material was found to

display a lower, more hydrophilic LCST, which normally requires chemical modification of the polymer backbone. It exhibited enhanced viscoelasticity, enabling improved thermal actuation, mechanical stability and greater water uptake. Previous studies have polymerized pNIPAAm-based hydrogels containing dyes, such as Orange II, as drug mimics in order to showcase their drug delivery capabilities<sup>1</sup>. In this chapter, above its LCST, the ionogel was preloaded with Fluorescein, a fluorescent dye used for biomedical diagnostic purposes and, compared to the standard hydrogel, displayed accelerated dynamic release of showing different rates of release at different pH.

In recent years a subclass of ILs has been developed called Polymeric Ionic Liquids (PILs). From this area, PILs displaying thermo-responsive behaviour have been reported and recently our group established suitable cross-linkers in order to produce robust PIL hydrogels. In terms of applications such as microfluidics, these hydrogels displayed relatively slow response rate when subject to elevated temperatures compared with conventional thermo-responsive polymers like pNIPAAm. Previously, studies have made the use of semi-interpenetrating networks to improve the properties of hydrogels. Therefore in Chapter 4, semi-interpenetrating networks consisting of a crosslinked thermo-responsive polymeric ionic liquid and varying concentrations of linear pNIPAAm were produced and characterized. The semi-IPN hydrogels were found to have improved mechanical, shrinking and reswelling properties with respect to the standard polymeric ionic liquid hydrogel. At elevated temperatures, the enhancements in shrinking properties of the semi-IPNs were attributed to the presence of hydrophobic pNIPAAm. While water affinity for the hydrophilic pNIPAAm was found to increase reswelling of the semi-IPNs at room temperature. Although, these results optimize the thermo-responsive PIL hydrogels for applications such as

polymer-based microfluidic valves, there is still scope for further improvement in terms of actuation response.

PILs are primarily viewed as a subclass of polyelectrolytes and generally through their synthesis, complete removal of the silver-halide by-product can prove difficult. This is imperative for electrochemical applications and that's why in Chapter 5, a halide-free method was developed to produce PILs. Three ionic monomers based on a 1-vinylimidazolium cation were prepared using a halide-free route by quaternization reaction with alkyl sulphates. These monomers were characterized by thermal and rheology methods. Free-radical polymerization of the ionic liquid monomers produced free-standing polymeric ionic liquid films that displayed high thermal and mechanical stability.

## 6.2 Possible future applications and limitations

Having brought improvements to the properties of the materials presented there are still areas where further enhancements can be made. The following sections discuss some potential routes for further investigations of the materials so far.

This thesis has shown the synergistic properties of integrated PIL and pNIPAAm networks, but there have also recently been reports of other copolymers involving PILs and pNIPAAm. Yaun *et al.*<sup>2</sup> reported that the copolymer of pNIPAAm and poly(1-ethyl-3-vinylimidazolium bromide) exhibits dual stimuli-responsiveness in aqueous solution. This was due to an additive effect of the pNIPAAm fraction and the ionic strength of the PIL. The copolymer was found not to destabilize in aqueous solution without the addition of KBr salt or heat. This dual response was then used to

stabilize the solubility of carbon nanotubes over a wide temperature range and then destabilize these carbon nanotubes at a desired temperature or salt concentration (Figure 6.1). Due to the effect of the ionic strength of poly(1-ethyl-3-vinylimidazolium bromide) it would be interesting to vary the anion of the PIL and then copolymerize with pNIPAAm. Utilizing anions of different ionic strength in the copolymer such as iodide [I]<sup>-</sup>, chloride [Cl]<sup>-</sup>, dicyanamide [DCA]<sup>-</sup> and [NTf<sub>2</sub>]<sup>-</sup> would provide an interesting study to exhibit the effect on its phase transition properties in aqueous solution.

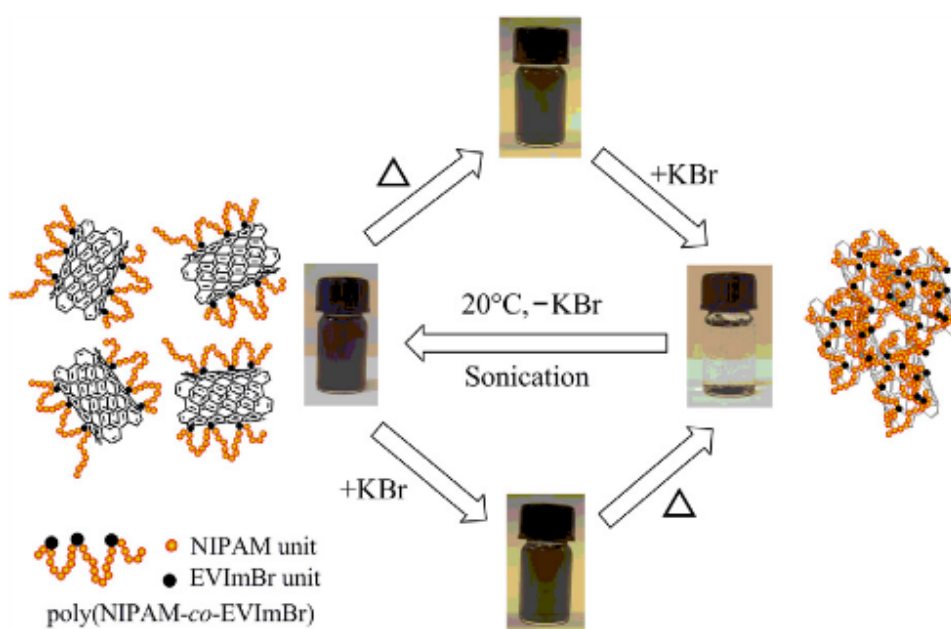


**Figure 6.1.** Schematic illustration of dual switching system to formulate a temperature- and ionic-strength responsive carbon nanotube dispersion using a pNIPAAm and pNIPAAm copolymer<sup>2</sup>.

The novel thermo-responsive semi-IPNs hydrogels presented in Chapter 4 provide an opportunity to develop different formulations of semi-IPNs containing pNIPAAm and various thermo-responsive PILs. The PIL used in the platform developed in Chapter 4 was tributylhexylphosphonium 3-sulfopropylacrylate, however there are many thermo-responsive PILs that have been synthesized recently (Figure 6.2)<sup>3-8</sup>, although

only some have undergone crosslinking to produce gels <sup>9</sup>. Generally, thermo-responsive PILs have been developed based on variations of phosphonium cations such as tetrabutyl or tributylhexyl, combined with anion derivatives based on benzenesulfonic acid <sup>3, 5, 6, 8</sup>.

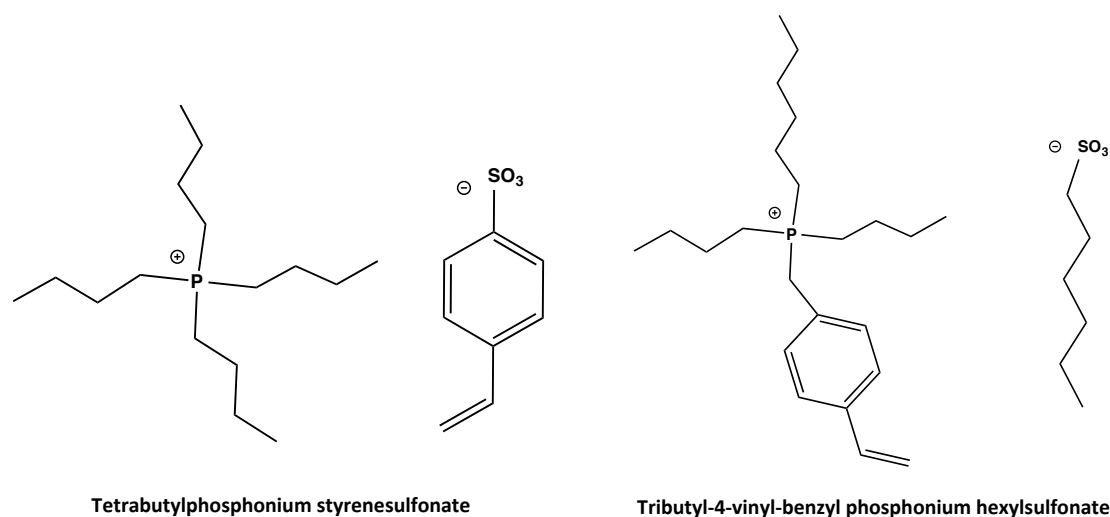


**Figure 6.2.** Examples of thermo-responsive polymeric ionic liquids <sup>4, 8</sup>.

As well as crosslinking these PILs, which would produce further novel thermo-responsive PIL hydrogels, they can also be integrated into the platform developed in Chapter 4. The creation of this semi-IPN platform also provides the opportunity to study other thermo-responsive polymers in place of the linear pNIPAAm. Research on other LCST-type polymers include; *N,N*-diethylacrylamide <sup>10</sup>, methylvinylether <sup>11</sup>, and *N*-vinylcaprolactum <sup>12</sup>. While maintaining a fully crosslinked thermo-responsive PIL, variation of the linear thermo-responsive polymer integrated into this network would make for an interesting characterization study in terms of swelling, shrinking, LCST threshold, mechanical stability, and actuation kinetics.

In previous studies, the photoresponsive spiropyran has been copolymerized with pNIPAAm in an IL medium to produce photoresponsive actuators <sup>13</sup>. In this study, upon the exposure of visible light, the merocyanine form of the spiropyran molecule

reverts to a more hydrophobic form, losing an acidic proton and producing a more hydrophobic environment in the ionogel. This, in turn, drives the expulsion of water from the ionogel, causing it to shrink. A drawback with this effect is that the gel has to undergo swelling in 0.1mM HCl prior to the photo-triggered contraction, which would be a limitation for certain applications.

Recently, our group has developed a hydrogel containing spiropyran copolymerized with pNIPAAm and acrylic acid. The presence of acrylic acid in the gel matrix provides an internal source of protons, allowing the protonation and deprotonation to occur internally within the gel, so there is no need for an external source of protons. Furthermore, the shrinking-expansion cycles of these gels in deionized water are repeatable (Figure 6.3), as protonation throughout the gel does not rely on movement of protons from an external acidic solution into bulk gel.

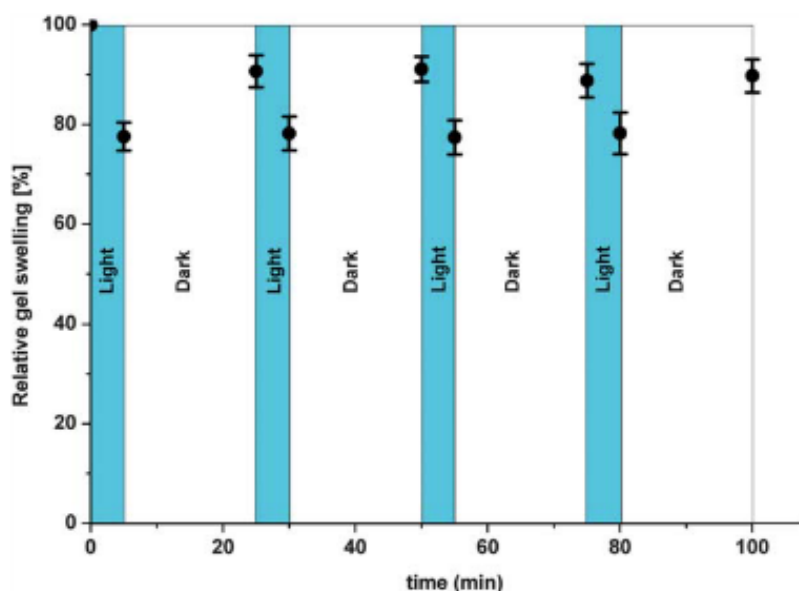


**Figure 6.4.** Alternating light and dark cycles for self-protonating spiropyran photoactuators <sup>14</sup>.

In the formulation of this gel, the components are polymerized in a mixture of 1,4-dioxane/water. It is proposed that this polymerization medium be replaced by a

thermo-responsive PIL. This, in turn, will provide an ever-present polymeric liquid phase that is hopefully capable of enhancing the shrinking/swelling properties of the hydrogel. Also, the presence of a PIL may produce a more robust gel, as shown in Chapter 2 and 3, ILs have been shown to improve the mechanical properties of pNIPAAm-based hydrogels.

In Chapter 3, a pNIPAAm-based ionogel is pre-loaded with fluorescein, acting as a drug mimic, and is shown to have improved dye release capabilities compared to a standard hydrogel. A well-known limitation of pNIPAAm is its poor mechanical behaviour in a swollen state when used as a drug delivery device. Because of its non-biodegradable nature, if the device were too soft and easily broken during handling, it would be difficult to be completely removed<sup>15</sup>.

As a result of these deficiencies, some modifications have been proposed, such as the copolymerization of pNIPAAm with hydrophobic monomers. However, this method would greatly weaken, even eliminate the thermal sensitivity of the pNIPAAm-based hydrogels due to the introducing of the thermosensitive moiety<sup>16,17</sup>.

In previous studies, Guilherme *et al.* have used pNIPAAm-based IPNs to demonstrate the release capabilities of dyes such as methylene blue and orange II<sup>1,18,19</sup>. These devices were shown to produce satisfactory release properties while maintaining satisfactory mechanical properties due to presence of a second polymer network. However, these pNIPAAm-IPNs are prepared using volatile organic solvents, which can be prone to solvent evaporation when subjected to shrinking/swelling cycles in open atmospheres<sup>20</sup>.

It is proposed that a dye be preloaded into a pNIPAAm-based IPN containing a thermo-responsive PIL as a second network. This will negate the need for an organic

solvent as the monomeric IL can act as the polymerization medium of the IPN. The dye will be used as a hydrophilic drug mimic and the proposed IPN will be characterized in terms of drug release capabilities when under stimulus.

The synthesis and characterization of novel PILs that exhibit high conductivity is of high scientific interest. In this respect, solid polymer electrolytes based on imidazolium salts offer a number of advantages compared to other liquid electrolytes. They have a wide window of electrochemical stability<sup>21</sup> and do not decompose at temperatures of up to 350 °C<sup>22</sup>. Moreover, a comprehensive report by Wassersheid *et al.* has shown that the overall trend in conductivity with respect to cation type follows the order imidazolium  $\geq$  ammonium  $\geq$  pyrrolidinium<sup>21</sup>.

In Chapter 5, three ionic monomers are synthesized using a halide-free route by a quaternization reaction of 1-vinylimidazoles with alkyl sulphates. Through free-radical polymerization, these monomers produced free-standing linear polymeric films. It is proposed that the ionic conductivity of these polymer films be investigated as potentially solid-state electrolytes. The author's study revealed that the films were soluble in water so it is recommended that conductivity measurements be performed in an inert atmosphere, as it has been found that the presence of water can increase conductivity of PILs of up to two orders of magnitude<sup>23</sup>.

In recent years, applications featuring ILs containing 1-allylimidazolium cations have generally involved the dissolution of certain polymers such as cellulose<sup>24</sup> and cytochrome c<sup>25</sup>. The development of green processing of biopolymers is urgent from viewpoints of sustainability and environmental protection. Rodgers *et al.* review on this subject outlines the anion and cation properties that should be present when considering ILs for dissolution and subsequent regeneration of biopolymers<sup>26</sup>. The

synthetic route developed in Chapter 5 opens an avenue for synthesis of other halide-free compounds by simply substituting the starting materials. It is proposed that 1-vinylimidazolium be replaced by 1-allylimidazolium in order to produce ILs through a halide-free quaternization reaction with alkyl sulphates as described in Figure 6.4.

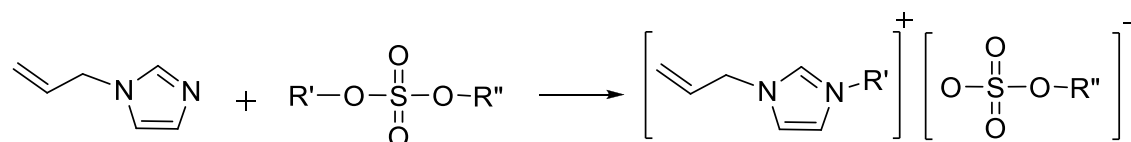


**Figure 6.4.** General preparative route to 1-allylimidazolium ILMs.

As in Chapter 5, hopefully this will produce halogen-free ILs under ambient conditions with varying alkyl chain lengths on both the anion and cation. It is generally put forward that imidazolium based ILs with anions that are good hydrogen bond acceptors are more effective in dissolving cellulose. As the proposed ILs put forward by the author contain an imidazolium cation and an anion with three accessible oxygen groups for hydrogen bonding, they would seem like appropriate solvent candidates for dissolution.

## 6.3 References

1. M. R. Guilherme, R. Silva, E. M. Giroto, A. F. Rubira and E. C. Muniz, *Polymer*, 2003, **44**, 4213-4219.
2. S. Soll, M. Antonietti and J. Yuan, *ACS Macro Letters*, 2012, **1**.
3. Y. Kohno, Y. Deguchi and H. Ohno, *Chemical Communications (Cambridge, England)*, 2012, **48**, 11883-11885.
4. Y. Kohno and H. Ohno, *Australian Journal of Chemistry*, 2011, **65**, 91-94.
5. Y. Kohno and H. Ohno, *Physical Chemistry Chemical Physics*, 2012, **14**, 5063-5070.
6. Y. Kohno and H. Ohno, *Chemical Communications (Cambridge, England)*, 2012, **48**, 7119-7130.

7. Y. Fukaya, K. Sekikawa, K. Murata, N. Nakamura and H. Ohno, *Chemical Communications (Cambridge, England)*, 2007, 3089-3091.
8. Y. Men, H. Schlaad and J. Yuan, *ACS Macro Letters*, 2013, **2**.
9. B. Ziolkowski and D. Diamond, *Chemical Communications*, 2013, **49**, 10308-10310.
10. I. Idziak, D. Avoce, D. Lessard, D. Gravel and X. X. Zhu, *Macromolecules*, 1999, **32**, 1260-1263.
11. R. Horne, J. Almeida, A. Day and N. Yu, *Journal of Colloid and Interface Science*, 1971, **35**, 77-84.
12. E. Makhaeva, H. Tenhu and A. Khokhlov, *Macromolecules*, 2002, 1870-1876.
13. F. Benito-Lopez, R. Byrne, A. M. Raduta, N. Vrana, G. McGuinness and D. Diamond, *Lab on a Chip*, 2010, **10**, 195-396.
14. B. Ziolkowski, L. Florea, J. Theobald, F. Benito-Lopez and D. Diamond, *Soft Matter*, 2013, **9**, 8754-8760.
15. X.-Z. Zhang, D.-Q. Wu and C.-C. Chu, *Biomaterials*, 2004, **25**, 3793-3805.
16. X.-Z. Zhang, X.-D. Xu, S.-X. Cheng and R.-X. Zhuo, *Soft Matter*, 2008, **4**, 385-391.
17. W. Xue and I. Hamley, *Polymer*, 2002, **43**, 3069-3077.
18. M. R. Guilherme, R. d. Silva, A. F. Rubira, G. Geuskens and E. C. Muniz, *Reactive and Functional Polymers*, 2004, **61**, 233-243.
19. M. R. Guilherme, E. A. Toledo, A. F. Rubira and E. C. Muniz, *Journal of Membrane Science*, 2002, **210**, 961-969.
20. T. Ueki and M. Watanabe, *Macromolecules*, 2008, **41**, 11.
21. P. Wassersheid and T. Welton, *Wiley-VCH, Weinheim*, 2003.
22. H. Ohno, *Electrochimica Acta*, 2001, **46**, 1407-1411.
23. J. Yuan and M. Antonietti, *Polymer*, 2011, **52**, 1471-1475.
24. H. Zhang, J. Wu, J. Zhang and J. He, *Macromolecules*, 2005, **38**, 8272-8277.
25. K. Tamura, N. Nakamura and H. Ohno, *Biotechnology and Bioengineering*, 2012, **109**, 729-735.
26. H. Wang, G. Gurau and R. Rogers, *Chemical Society Reviews*, 2012, **41**, 1519-1537.